DECLARATION

I, the undersigned declare that the dissertation, which I hereby submit for the degree Master of Science in Financial Engineering at the University of Pretoria, is my own independent work and has not previously been submitted by me or any other person for any degree at this or any other university.

SIGNATURE: .....

NAME: Francis Youbi

DATE: November 2016

Pricing Options under Lévy models using Spectral methods

by

Francis Youbi

supervised by

Dr Edson Pindza

and co-supervised by

Prof Eben Maré

in the

Department of Mathematics and Applied Mathematics

for the degree of

MSc Financial Engineering

Acknowledgement

I would like to firstly thank God for giving me the strength and time to achieve this work.

To my supervisor Dr Edson Pindza, thank you for giving me your time and attention throughout the completion of this dissertation. Your encouragement, support and inspiration has been a major tool to successfully completing this work.

To my co-supervisor Prof Eben Maré, I thank you for giving me the opportunity to register for this programme. Your tremendous amount of encouragement and guidance has been one of the main pillar of my success. Thank you for finding me a sponsor who assisted me with all my expenses throughout my study.

To Mr Brad Welch, I thank you for according me your financial support through the RidgeCape Capital company.

Last, but not least, it remains my pleasure to thank my close friends and family for their continued love and support. I particularly thank my wife Emily Youbi, my mother Mrs Odile Ndongo, my mother inlaw Mrs Linah Mafokwane, my sister Ms Clementine Manga and my brothers Mr Dieudonne Tonda, Mr Donatien Ndongo, Mr Jean Luc Ndongo, whom their prayers and emotional support has contributed to my well-being and courage to always work hard. I dedicate this dissertation to my wife and children Yann, Carliva and Adrien.

Abstract

Spectral methods have been actively developed in the last decades. The main advantage of these methods is to yield exponential order of accuracy when the function is smooth. However, for discontinuous functions, their accuracy deteriorates due to the Gibbs phenomenon. When functions are contaminated with the Gibbs phenomenon, proper workarounds can be applied to recover their accuracy. In this dissertation, we review the spectral methods and their convergence remedies such as grid stretching, discontinuity inclusion and domain decomposition methods in pricing options. The basic functions of Lévy processes models are also reviewed.

The main purpose of this dissertation is to show that high order of accuracy can be recovered from spectral approximations. We explored and designed numerical methods for solving PDEs and PIDEs that arise in finance. It is known that most standard numerical methods for solving financial PDEs and PIDEs are reduced to low order accurate results due to the discontinuity at strike prices in the initial condition.

Firstly the Black Scholes (BS) PDE was solved numerically. The computation of the PDE is done by using barycentric spectral methods. Three different payoffs call options are used as initial and boundaries conditions. It appears that the grid stretching, the discontinuity inclusion and the domain decomposition methods provide efficient ways to remove Gibbs phenomenon. On the other hand, these methods restore the high accuracy of spectral methods in pricing financial options. The spectral domain decomposition method appears to be the most accurate workaround when we solve a BS PDE in this dissertation.

Secondly, a financial PIDE was discretized and solved by using a barycen-

tric spectral domain decomposition method algorithm. The method is applied to two different options pricing problems under a class of infinite activity Lévy models. The use of barycentric spectral domain decomposition methods allows the computation of ODEs obtained from the discretization of the PIDE. The ODEs are solved by exponential time integration scheme. Several numerical tests for the pricing of European and butterfly options are given to illustrate the efficiency and accuracy of this algorithm. We also show that the option Greeks such as the Delta and Gamma sensitivity measures are computed with no spurious oscillation. The methods produce accurate results.

Contents

List of Figures

List of Tables

List of Symbols

- S : Stock price
- S_T : Stock price at time T
- K : Strike price
- T : Maturity time
- $V_c(S,T)$: Call option payoff at the expiration date T
- $V_p(S,T)$: Put option payoff at the expiration date T
- μ : The drift of the stock
- σ : The volatility of the stock
- $W(t)$: The standard Brownian motion

- N : Number of interpolation points
- T_n : Chebyshev polynomials
- $\sum_{n=0}^{N}$: Chebyshev partial sum
- $\Delta = [x_{min}, x_{max}]$: Interval from the minimum point to maximum point
- δ_{ij} : Kronecker δ-function
- $D^{(n)}$: nth order differential matrix
- $\mathcal{D}$: General domain
- $\mathcal{D}_1, ..., \mathcal{D}_M$: Sub-domains
- X_t : Stochastic process
- dS_t : Geometric Brownian motion
- $\mathcal{O}(N)$: Order of N

List of Terminology

- **An option:** A right (*but not the obligation*) to buy or sell a risky asset at a specific price after or within a specific time. It is a derivative contract between two parties, the writer and the holder

- **The writer:** Someone who fixes the terms of the contract and sell the option

- **The holder:** Someone who buys the option at the stock market by paying an option price

- **Put option:** Gives the holder the right to sell the underlying asset for an agreed price K (strike price) at the maturity time T

- **Call option:** Gives the holder the right to buy the underlying asset under the same conditions of the corresponding put option

- **Payoff or intrinsic value:** Value of the option at maturity

- **In-the-money:** When the payoff is positive

- **Out-the-money:** When the payoff is equal to zero

- **At-the-money:** When the strike price is equal or closer to the current asset price

- **European option:** An option that can only be exercised at the expiration date T

- **American option:** An option that can be exercised at any time up to the expiration date T

- **Bull spread option:** A neutral strategy that is a combination of two call option

- **Butterfly spread option:** A neutral strategy that is a combination of a bull spread option and a bear spread option

- **Vanilla option:** A financial instrument that gives the holder the right but not the obligation, to sell or buy an underlying asset, security or currency at a predetermined price within a given time frame.

It is a normal call or put that has no special or unusual features

- **Exotic option:** An option that differs in structure from common American or European options in term of the underlying asset, or the calculation of how or when the investor receives a certain payoff

- **Spectral method:** A computational method that uses basis functions which are non-zero over the whole domain

- **Chebyshev polynomials:** They are a sequence of orthogonal polynomials which are related to de Moivre's formula and which can be defined recursively

- **Calibration:** A process of determining the relationship between the readings obtained by a measuring instrument or system and the applicable units of some defined system of measurement

List of Abbreviation

- **BS:** Black-Scholes
- **BM:** Brownian Motion
- **ABM:** Arithmetic Brownian Motion
- **PDE:** Partial Differential Equation
- **GBM:** Geometric Brownian Motion
- **MCM:** Monte Carlo Method
- **PIDE:** Partial-Integro Differential Equation
- **PIDEs:** Partial-Integro Differential Equations

- **SCM:** Spectral Method
- **SDM:** Spectral Decomposition Method
- **DDM:** Domain Decomposition Method
- **SCDDM:** Spectral Domain Decomposition Method
- **CGL:** Chebyshev-Gauss-Lobatto
- **ODE:** Ordinary Differential Equation
- **ODEs:** Ordinary Differential Equations
- **DAEs:** Differential Algebric Equations
- **SDE:** Stochastic Differential Equation
- **GH:** Generalized Hyperbolic
- **NIG:** Normal Inverse Gaussian

- **CGMY:** Carr, German, Madan and Yor
- **ETI:** Exponential Time Integrator
- **ETD:** Exponential Time Difference
- **EPI:** Exponential Propagation Iterative
- **ETDRK:** Exponential Time Differencing Method of Runge-Kutta
- **RKEPI:** Runge-Kutta Exponential Propagation Iterative
- **SCGSM:** Spectral Grid Stretching Method
- **SCDIM:** Spectral Discontinuity Inclusion Method

List of Publications

Part of this dissertation has been submitted in the form of the following research papers submitted to international journals for publications.

1. F. Youbi, E. Pindza, E. Maré, A Comparative Study of Spectral Methods for Valuing Financial Options. Published in Applied Mathematics and Information Science, International Journal. Volume 3 (11), 939-950, (2017).

2. F. Youbi, E. Pindza, E. Maré, Barycentric spectral domain decomposition methods for valuing a class of infinite activity Lévy models, submitted for publication.

Chapter 1

Introduction

This chapter introduces the concept of option pricing theory and gives an overview of the objectives which has to be achieved in this thesis. A content of the dissertation marked the end of this chapter.

1.1 Background

Transactions in the market are characterized by the process of buying and selling. This is known as trading. To control this process, many studies have been done in finance and economy. Mathematical finance in particular, gives a better understanding of markets and tries to quantify it by using some mathematical techniques. The revolutionary paper of Black-Scholes (1973) and Merton (1973) gave the ground of the market's quantification. The paper makes some modelling assumptions in finance. The popular one (or delicate) is the one which states that the underlying asset

market (e.g., stock, futures, commodity, currency, index) is perfectly elastic so that the trading has no influence on its price. To have a fair possible price of the underlying asset in the market, many financial institutes resort to the modelling of its behaviour by looking for a stochastic process that will closely fit its returns distribution. This practice does not usually provide the origin of the important factors that affect the price of an asset during certain trades. Therefore some endogenous mechanisms are found to give better insight of how the market prices are formed (see the work done in the thesis of [74]).

In the next sections we introduce the basic idea and concept of the option pricing, its concepts and numerical methodologies, and outline the objectives of this thesis.

1.2 Option pricing theory

The field of Botany has been the catalyst of the option pricing. In 1828, Robert Brown (1773-1858), a Scottish botanist observed in his laboratory that plant pollen particles suspended in water have random motion [105]. This observation gave the young French employee of the financial institution, 'La Bourse de Paris', the idea of his doctoral research in option pricing model. In Louis Bachelier's (1870-1946) doctoral thesis (entitled *Théorie de la spéculation* [6]), that he successfully defended at 'La Sorbonne' in March 29, 1900, he made assumptions that the stock prices were having '*random walk*', which he referred to as the *Brownian motion* (or *arithmetic Brownian motion (ABM)*). He proved that stock prices can be modelled with a diffusion process or Brownian motion (BM). This revolutionary

work was published in the French scientific journal, *Annales Scientifiques de l'École Normale Supérieure* and was the origin of financial mathematics [31]. Five years later, Albert Einstein produced a well celebrated work of Brownian motions through the original study on 'random walk' [105]. This led to further studies made by Norbert Wiener (1894-1964) on BM in the 1920's.

To face the problem of 'random walk' of the stock prices, Kiyoshi Itô went on to develop the stochastic calculus in 1944. His work gave a strong ground of modelling stock prices successfully by using the BM and later became an important tool for modern finance. But in 1965, the economist Paul Samuelson re-introduced Bachelier's work into the economic sciences and advised that the Itô's geometric Brownian motion (GBM) model was a suitable model for stock price movements (see [135] and references within). His approach gave the way to his student Robert C. Merton and other researchers to develop various pricing formulas in finance. The famous one is the Black, Scholes and Merton equation for pricing a European call and put option. The formula was developed in 1973. It paved the way to the surviving members (Scholes and Merton) to receive the Nobel Prize for economics in 1997. This ground-breaking work introduced the concept of a strong hedging strategy in the market.

1.3 Option pricing concepts and numerical methods

Financial practice is developed by the assumption of the statistical behaviour of the market. To have a perfect reproduction of its behaviour,

we construct or produce mathematical models. These models are usually represented by Partial Differential Equations (PDEs). The popularity of options gives an importance of their studies. This attention is given by the fact that:

1. *Option are very attractive to investors, both for speculation and for hedging.*

2. *There is a systematic way to determine how much they are worth, hence they can be bought and sold with some confidence.*

From [33, 62, 112, 115], an option is defined as the right (*but not the obligation*) to buy or sell a risky asset at a specific price after or within a specific time. It is a derivative contract between two parties, the *writer* and the *holder*. The *writer* fixes the terms of the contract and sells the option. The *holder* buys the option at the stock market by paying an option price. To exercise this contract, rules are implemented in such a way that both parties have balanced 'rights'. For example, after maturity date T, the right of the *holder* expires and for later times the option becomes worthless. There are two types of option, the put and the call option. The put option gives the *holder* the right to sell the underlying asset for an agreed price K (strike price) at the maturity time T. The call option gives the right to the *holder* to buy the asset under the same conditions of the corresponding put option. The *holder* has a choice of exercising or not the option at time $t = T$ by checking the current price, $S = S_T$, of the underlying asset. In the case of a call option, the *holder* can buy the asset at costs K exercising the option or he can buy on the spot market for costs S. Hence the *holder* will exercise only when $S > K$, which makes a profit of $S - K$ per shares (with-

out transaction costs). This refers us to the intrinsic value of the option which is the value of the option at maturity. It is also called payoff. It is received when the underlying asset is at its current level (when the option expires) [115]. The payoff function is the value $V(S,T)$ of an option at the expiration date T. A call option payoff is given by:

$$V_c(S_T,T) = (S_T - K)^+ := \max(S_T - K, 0). \tag{1.1}$$

Similarly for a put, the payoff at expiration will be given by

$$V_p(S_T,T) = (K - S_T)^+ := \max(K - S_T, 0). \tag{1.2}$$

Figure 1.1 is the representation of a payoff for a European call and put options with $K = 50$. When the intrinsic value is positive, we say the option

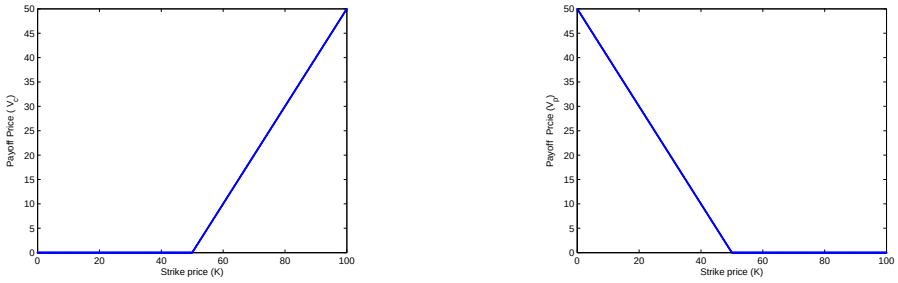

(a) European call option (b) European put option

Figure 1.1: Payoff of a European call and put options. $K = 50$.

is *in-the-money*. The option is said to be *out-of-the money*, if there is no intrinsic value and *at-the-money*, if the strike price is equal or closer to the current asset level [62].

There are different styles or families of options. The mostly used are European and American options. A European option can only be exercised at the expiration date T and a American option can be exercised

at any time up to the expiration date T. Options that are European and have a straightforward strike prices are often called vanilla options. Their opponents are called exotic options. These options have more complex contract details. For example, the Asian option has a payoff which depends on the average of the underlying price over adjusted period, and the barrier option has a value which depends on some combination of different assets price S_t by reaching the limited value of S during its life time [62].

To calculate or estimate a fair value of an option we use mathematical models. Under the assumption of GBM, the asset price is

$$\frac{dS(t)}{S(t)} = \mu dt + \sigma dW(t), \tag{1.3}$$

where μ is the drift of the stock, σ is the volatility and $W(t)$ is the standard BM (Wiener process). The parameters μ and σ can be deterministic or constant values. In this dissertation, we will use μ and σ as constant values in all numerical applications.

Definition 1. *[15] A standard Brownian (or a standard Wiener process) is a stochastic process* $\{W_t\}_{t\geq 0^+}$ *(that is, a family of random variable* W_t*, indexed by non-negative real numbers* t*), defined on a common probability space* $(\Omega, \mathcal{F}, \mathbb{P})$ *with the following properties:*

1. $W_0 = 0$.
2. *With probability* 1*, the function* $t \to W_t$ *is continuous in* t.
3. *The process* $\{W_t\}_{t\geq 0}$ *has stationary, independent increments.*
4. *The increment* $W_{t+s} - W_t$ *has the NORMAL* $(0, t)$ *distribution.*

In the above definition, the term independent increments means that for every choice of non-negative real numbers

$$0 \leq s_1 < t_1 \leq s_2 < t_2 \leq \ \leq s_n < t_n < \infty,$$

the increment random variables

$$W_{t_1} - W_{s_1}, W_{t_2} - W_{s_2}, ..., W_{t_n} - W_{s_n},$$

are jointly independent; the term stationary increments means that for any $0 < s, t < \infty$ the distribution of the increment $W_{t+s}W_s$ has the same distribution as $W_t W_0 = W_t$.

Equation (1.3) leads to the following partial differential equation (PDE) representing the standard Black-Scholes (BS) PDE [15],

$$\frac{1}{2}\sigma^2 S^2(t)\frac{\partial^2 V}{\partial S^2} + rS(t)\frac{\partial V}{\partial S} + \frac{\partial V}{\partial t} - rV = 0. \tag{1.4}$$

For a European option, its initial and boundary conditions are,

$$\begin{cases} V_c(0,t) &= 0 \ \text{ for all } \ t \geq 0, \\ V_c(S,t) &= S \ \text{ as } \ S \to \infty, \\ V_c(S,T) &= \max(S-K,0) \ \text{ for all } \ S \geq 0, \end{cases} \tag{1.5}$$

and

$$\begin{cases} V_p(0,t) &= Ke^{-rt} \ \text{ for all } \ t \geq 0, \\ V_p(S,t) &= 0 \ \text{ as } \ S \to \infty, \\ V_p(S,T) &= \max(K-S,0) \ \text{ for all } \ S \geq 0, \end{cases} \tag{1.6}$$

for respectively a European call and put. In (1.4) Π represents the call or put option price and the equation is valid if $S > 0$, $0 \leq t \leq T$. In both equations (1.3) and (1.4), σ is one of the most important parameters. It is a statistical measure of the market's behaviour or the guarantee for the

market to rise or fall within a period of time. It is usually measured by the standard deviation from the expectation. A high value of the volatility in the market means that prices change rapidly in a short period of time. This leads to a higher option prices often called the price of risk, which arise to a conclusion of "*the higher the risk, the higher the return*". We illustrate this theory in Table 1.1 by changing the values of σ. Considering an unchanged current price (S), strike (K) and risk-free rate (r) to be $100, 95$ and 10% respectively. Over a period of three months, we compute an European call and put option price of Equation (1.4). All results are recorded in Table 1.1. We observe that an increase of σ leads to an increase of the European call and put option price.

Volatility (σ) in %	Call price	Put price
10	7.50	0.13
20	8.60	1.23
30	10.20	2.81
40	11.90	4.55
50	13.70	6.35

Table 1.1: BS European Put and Call option with different values of σ.

Pricing options is very important when we try to adjust or calibrate models in finance. The challenge usually occurs when we want to price options that have different strike prices and dates of expiration at the same period. Thus fast and accurate models are needed for financial institutions. These models have become very important instruments for derivative pricing and for managing risk that could default any companies to produce positive returns at the end of any financial transactions.

In practice, analytical solutions can be difficult to find. Then to overcome this difficulty, the use of numerical methods has been a better choice to find solutions that will be accurate approximation to the analytical ones. The commonly used pricing methods in the financial world are the *binomial tree models*, which has been extended to the *trinomial tree model*. These two models are considered as *lattice methods* and were firstly used by Parkinson in 1977, then Cox *et al.* proceeded with the method in 1979 (see [135] and references within). Phelim P. Boyle also proposed in 1977 an alternative method, The *Monte Carlo method (MCM)*, which is also popular in finance. Paul Wilmott consider the method and its varieties to be an excellent solver for high dimensional problems and path-dependent options (see [135] and references within). It generates a massive number of sample paths to estimate the value of the option. We can easily used it but its computation is very expensive when we want to obtain a high accuracy.
Other alternative methods are:

- The finite difference method which was first implemented in pricing option by Brennan and Schwartz (see [135] and references within); discretize simultaneously the stock price and the time line to give an approximation of the price option in forms of discrete points.
- The partial-integro differential equation (PIDE) methods, which will be a subject of one application in this dissertation, use numerical schemes to solve partial-integro differential equations (PIDEs) directly.
- The Spectral method (SCM), which is reviewed in Chapter 2.

- The numerical integration methods model the option price in a form of discounted expected value of the payoff at maturity. These methods are very attractive due to the fact that they have a fast computational speed, particularly on the plain vanilla option.

A variety of other methods on pricing the option are found in many journals of finance and economics [14, 33, 58, 86].

1.4 Numerical approach of pricing options under spectral methods

A function that has continuous derivatives up to some desired order over some domain is said to be smooth. Smooth functions are often approximated by using Chebyshev polynomial interpolations since they provide a strong and rapid convergence. However, Chebyshev interpolants are enable to produce a high accuracy for functions having discontinuities in the domain of interest [101]. In the presence of such phenomena, the accuracy of high order methods deteriorates. This is due to the well known Gibbs phenomenon. The phenomenon became famous in 1898 when Albert Michelson observed it through a mechanical graphing machine used to compute and re-synthesize the Fourier series of a square wave. It is only after the publication of J. Willard Gibbs's paper that a detailed mathematical description of the phenomenon was given and named after Gibbs in 1906 [128].

Jump discontinuities produce pointwise convergence almost everywhere. Hence, in this case there is no uniform convergence. The Gibbs phe-

nomenon states that, the pointwise convergence of an approximation of discontinuous functions is at most first order [83, 108]. Since the Gibbs phenomenon local effect is found in oscillations near the jumps, discontinuous functions cannot have a uniform convergence. The same happen when the Gibbs phenomenon effect is global. Although the error in this case decay away from the jumps, the decay rate is only first order. Hence, the rate of convergence over the whole domain will slow down in the existence of one or more discontinuities. To reduce the Gibbs phenomenon on a piecewise smooth function, a projection of each smooth sub-interval on another basis can be done. Then, these parts can be combine to one another to restore the function on the whole interval [52].

Spectral methods are often perceived to be too sensitive and lack robustness to allow the modelling of problems of realistic complexity which, by their very nature, most often are non-smooth. It is well-known that option prices and their derivatives usually change dramatically near slope discontinuities of the payoff functions, hence oscillations due to Gibbs phenomena arise. The phenomenon affects the convergence and solution of financial PDEs. This explains why the application of spectral methods in the field of computational finance is still limited. Several workarounds exist and are commonly used to suppress or avoid this phenomenon. The use of these workarounds restores the exponential accuracy of these methods [108]. They include, filtering [127], Gegenbauer reconstruction [51], grid stretching [12] and domain decomposition [95, 134] methods. The method which is mostly accurate should have the exact location of all discontinuities. Recently, these workarounds have regained robustness and have received considerable attention in the field of finance. This is due to their effectiveness [102]. Among the suggested methods which reduce or

eliminate the problem of jumps discontinuities, the spectral domain decomposition method (SCDDM) appear to be the most efficient [108].

Option prices and their derivatives are modelled in a form of ordinary or partial differential equations (ODEs or PDEs). These equations do not often have a closed form solutions. Hence their computations can only be done by approximation. One of the methods to solve ODEs and PDEs in finance is the SCDDM. To obtain an accurate approximation solution of these equations, one has to solve the ODEs or PDEs under Lévy processes model using the SCDDM. But the commonly used numerical method in finance is the fully implicit second-order accurate Crank-Nicolson method. The method becomes computationally inefficient for large system of ODEs. Such problems of ODEs can be solve by using the exponential integrators. Some examples can be found in the publication of [71], where they used ETI together with Galerkin methods for spatial discretization. Using the ETI in their work, helped them to prove strong error estimates when a general semi-linear stochastic equation is estimated. One can further consult the publication of [118]. They discuss European, barrier and butterfly spread options for BS GBM model and Merton's jump diffusion model with constant coefficients. In their work, the ETI scheme was used to develop a more stable integrator than the one commonly used in the Crank-Nicolson method.

Time-stepping is the common practice for temporal integration of PIDE. But Tangman *et al.* [118] applied an ETI scheme to solve the PIDE. The scheme uses a 'one step' formula to tackle the time direction of PIDE which eliminate the use of discretization in time. By combining the ETI scheme with the SCM based on Chebyshev nodes for spatial discretization to price different options [118], numerical results show that the applica-

tion is exact in time and approximately achieves the fourth-order accuracy.

More applications of the ETI in finance can be found in the publication of Pang and Sun [92]. The references within also provide an extension of needed knowledge on the method in a financial point of view.

1.5 Overview of the objectives

The dissertation focuses on the study of pricing options under Lévy models using spectral methods. We will study the solution of PDE and PIDE arising in finance as a consequence of the so-called Lévy processes applied to the pricing of contingent claims using spectral methods. The aim of this research is to explore and design numerical methods for solving financial PDEs and PIDEs. Most standard numerical methods for solving PDEs and PIDEs in finance are reduced to low order accuracy results. This is due to the discontinuity at the strike price in the initial condition. We use the Lévy processes model in the spectral methods to restore the accuracy of the PIDE solutions.

1.6 Contents of the dissertation

In the second chapter, we present the spectral methods with their basic properties and define SCDDM with examples. We give an historical development of the spectral methods and we discuss about their foundations, construction and implementation in mathematics. We close the chapter

by reviewing the background of SCDDM and its basic definition. In the third chapter, we present the Lévy processes models. A formulation of the BS model is firstly presented. From this presentation its limitations are pointed out. We then explain from a statistical point of view how the hypothesis of log-normal returns defined by the BS model goes wrong in describing market returns. Hence, the discussion about the importance of the Lévy processes models in finance. To understand the benefit of using the Lévy processes models in finance, we review some basic definitions of these models and present their major mathematical properties. Therefore, a description of the Lévy jump-diffusion processes, its application in finance, and some popular models used in finances is made. The last part of the chapter is dedicated to the presentation of the PIDE approach under Lévy models and the mode of its resolution. We then present, to close the chapter, the calibration of an exponential Lévy models with a simulation in finance.

The fourth and fifth chapters are the implementation of the spectral methods and Lévy process. The chapters outline the resolution of a PDE and PIDE arising from a financial problem. The main purpose of the chapter is to show that high order accuracy can be recovered from spectral approximation contaminated with the Gibbs phenomenon when proper workaround are applied. We then close the dissertation with chapter five which is a general conclusion of this study.

Chapter 2

Spectral methods approach

The complexity of some PDEs or ODEs and their initial boundary condition in Finance, Mathematics, Physic, etc., has been a challenge of researchers to find accurate solutions for these equations. Hence the use of SCM to solve the problem of accuracy from each field of study. This chapter introduces the spectral methods with their basic properties and the definition of the SCDDM with examples.

2.1 Historical development of the method

The resolution of partial or differential equations has been an important and attractive area of research in the field of Mathematics, Physics, Finance, etc. Therefore, methods have been developed to obtain accurate results. One class of methods to get numerical solutions of these different equations is spectral methods. Their popularities began in the 1970s

through the work of Orszag [91]. Basic concepts of spectral methods, such as interpolation and expansion were introduced long before the 1970s by meteorologists [64]. The progress made in 1970s and 1980s on these methods gave the opportunity to other researchers to improve these methods. For example, the symposium proceedings by Voigt, Gottlieb and Hussaini [129] published in 1984, and the first edition of the book by Canuto, Hussaini, Quarteroni, and Zang [18] published in 1988 are one of the innovation of the spectral methods. An overview of spectral methods introduction can be found in the books written by Fornberg [44] and Trefethen [123]. The application and the investigation of spectral methods in interpolation and approximation theory [22, 36, 84], numerical integration [34, 37, 117], special function theory [99], computational fluid dynamics, etc., are important in the study of orthogonal polynomial sequences. They are powerful tools to estimate functions that are difficult to compute and form part of the essential elements of numerical integration and approximation of solutions in differential, integral equations [130]. The spectral methods domains are not very flexible, but their convergence are exponential when the solutions of the studied functions are smooth. In the case of discontinuities like shocks or problems in complex geometries (problems with coordinate singularities, discontinuous coefficients or solution), the convergence of the method is spoiled and the technique cannot give accurate results [72].

The difference between the spectral methods and the finite difference methods is that, the first one uses basis functions that are non-zero over the whole domain, while second one uses basis functions that are non-zero only on small sub-domains. In other words, spectral methods take on a global approach while finite element methods use a local approach [19].

The following study of the spectral methods basic properties demonstrates its importance in the approximation of smooth functions solution.

2.2 Basic properties of spectral methods

2.2.1 Foundation of the method based on Gauss quadratures

In [53], the mathematical foundation of spectral methods was introduced by firstly explaining the basic function of an orthogonal projection. To give an overview of an orthogonal projection, we consider an interval $\Delta = [x_{min}, x_{max}]$ and if we want to talk about basis, we shall first define a scalar product on Δ. The scalar product of two functions h and l with respect to the measure v can be defined as

$$v(h,l) = \int_{\Delta} h(x)l(x)v(x)dx, \tag{2.1}$$

with v representing a positive function on Δ. By using equation (2.1), we can find a set of orthogonal polynomials q_n of degree n. The composition of those polynomials up to a given degree N forms a set which represents the basis $\mathbb{Q}_N$ [53]. A projection of any u function on Δ can be obtained by the use of the polynomials q_n. Hence the projection of u is defined by

$$Q_N u = \sum_{n=0}^{N} k_n q_n(x), \tag{2.2}$$

where $k_n = \frac{(u,q_n)}{(q_n,q_n)}$ represents the coefficients of the projections. The truncation error is the difference between u and its projection. It approaches 0

when N increases; i.e.

$$\| u - Q_n u \| \longrightarrow 0, \text{ when } N \longrightarrow \infty. \tag{2.3}$$

Equation (2.3) is very interesting, but does not solve the problem of finding k by computing integrals of the form $\int_\Delta h(x)l(x)v(x)dx$. Hence the use of the Gauss quadratures is very important if one wants to determine the value of u at many points. The following theorem from [53] illustrates the importance of Gauss quadratures when we want to use the projections of any functions.

Theorem 1. *[53] There exist $N+1$ real positive v_n and $N+1$ real x_n in Δ such that:*

$$\forall\ h \in \mathbb{Q}_{2N+\epsilon}, \quad \int_\Delta h(x)v(x)dx = \sum_{n=0}^{N} h(x_n)v_n.$$

The weights are represented by v_n and the collocations points by x_n . The choice of the exact degree will depend on the quadrature. The usual choices are [53]:

- Gauss: $\epsilon = 1$
- Gauss-Radau: $\epsilon = 0$ and $x_0 = x_{min}$
- Gauss-Labatto: $\epsilon = -1$ and $x_0 = x_{min}$ and $x_N = x_{max}$

The above mentioned quadratures are the most used and suitable for any projection computation.
The application of the Gauss quadratures to approximate the coefficient of the expansion produces the following result

$$\alpha_n = \frac{1}{\beta}\sum_{j=0}^{N} u(x_j)q_n(x_j)v_j \quad \text{with} \quad \beta_n = \sum_{j=0}^{N} q_n^2(x_j)v_j. \tag{2.4}$$

This can't be exact since $k_n \neq \alpha_n$ and to compute α_n we only need to evaluate u at the $N+1$ collocation points. Therefore, to interpolate u we need to use the following polynomial

$$I_N u = \sum_{n=0}^{N} \alpha_n q_n(x), \tag{2.5}$$

and the difference between $I_n u$ and $Q_n u$ is called the aliasing error. $I_n u$ is the spectral approximation of u and it is the only polynomial of degree N that will match with u at every collocation point such that:

$$[I_n u](x_i) = u(x_i) \quad \forall i \leq N. \tag{2.6}$$

A detailed application of (2.6) is done by [53]. On its page 1 to 3, the publication demonstrates the validity of Equation (2.6) on a given function and its projection. Furthermore, it shows how the error decreases exponentially when we compute the maximum difference between $I_N u$ and u. This demonstrates that the spectral methods have a very fast convergence compared to other methods such as finite differences where the error only follows a power-law in term of N. More details on how the Gauss quadratures are implemented and constructed can be found in [135]. The choice of quadrature is not the only factor that can be considered. To obtain an accurate solution when using projection computation, one has to follow the rules of choosing the basis functions.

2.2.2 Choice of basis functions

The simple rule to apply when comes to the choice of the basis functions is that:

- When the solution of the PDEs or ODEs is periodic, we use the Fourier series.
- When the solution is not periodic and the domain is square or a cube, we use the Chebyshev polynomials along each dimensions.
- When the domain is spherical, we use the spherical harmonics basis.

In this dissertation, we will use the SCM on non periodic functions such as, the payoff of an option. The usual polynomials used in non periodic problems are the Legendre and Chebyshev polynomials. One can consult [53] on page 5 to see the basic properties of Legendre polynomial, since it is not the objective of our study. We are interested in approximating the payoff of some vanilla and exotic option by using the Chebyshev basis. But the solution of these functions are not smooth, thus the interpolation technique will be the suitable candidate to resolve our problem. How to construct these interpolations?

2.2.3 Construction of the Chebyshev polynomials and its interpolation

From [16], $P_{N-1}(x)$ is an interpolating expression to the functions $f(x)$. Usually $P_{N-1}(x)$ is an ordinary or trigonometric polynomial. Its N degrees of freedom are determined by the requirement that the interpolants agree with $f(x)$ at each of a set of N interpolation points:

$$P_{N_i}(x_i) = f(x_i), \qquad i = 1, 2, ..., N. \tag{2.7}$$

The polynomial interpolation is defined as a method used before the calculator era. The tables of mathematical functions were used to evaluate

functions at certain given points. If the value of those points were not listed on the table, then the interpolation method was applied. To achieve that, a linear interpolation was done by drawing a straight line between the two points in the table that contains the desired x. Therefore, the linear function at x was approximated by $f(x)$, such that:

$$f(x) \approx \frac{(x-x_1)}{(x_0-x_1)} f(x_0) + \frac{(x-x_0)}{(x_1-x_0)} f(x_1). \tag{2.8}$$

Equation (2.8) is known as linear interpolation. It can be defined as $P_1(x)$ being that unique linear polynomial which satisfies the two interpolation conditions

$$P_1(x_0) = f(x_0), \quad P_1(x_1) = f(x_1). \tag{2.9}$$

But to have the accuracy of the function using the linear interpolation, the tabulated points must be very close to each other. This idea can be extended to higher order. An example will be the one of a parabola where the approximation of $f(x)$ is done by the quadratic polynomial $P_2(x)$ satisfying the three interpolation conditions [16]

$$P_2(x_0) = f(x_0) \quad ; \quad P_2(x_1) = f(x_1) \quad ; \quad P_2(x_2) = f(x_2), \tag{2.10}$$

such as

$$P_2(x) \equiv C_0(x) f(x_0) + C_1(x) f(x_1) + C_2(x) f(x_2), \tag{2.11}$$

where

$$\begin{cases} C_0(x) &= \frac{(x-x_1)(x-x_2)}{(x_0-x_1)(x_0-x_2)}, \\ C_1(x) &= \frac{(x-x_0)(x-x_2)}{(x_1-x_0)(x_1-x_2)}, \\ C_2(x) &= \frac{(x-x_0)(x-x_1)}{(x_2-x_0)(x_2-x_1)}. \end{cases} \tag{2.12}$$

Therefore, we can fit any $N+1$ points by a polynomial of N^{th} degree

$$P_N(x) \equiv \sum_{i=0}^{N} f(x_i) C_i(x), \tag{2.13}$$

which is known as Lagrange interpolation function. In Equation (2.13), the expressions $C_i(x)$ defined by

$$C_i(x) = \prod_{j=0, j\neq i}^{N} \frac{x - x_j}{x_i - x_j}, \tag{2.14}$$

are cardinal functions which are polynomials of degree N. The N factors of $(x - x_j)$ insure that $C_i(x)$ will vanished at all the interpolation points except x_i. The denominator forces $C_i(x)$ to take the value 1 at interpolation points $x = x_i$. Therefore every factors in the product will be $\frac{(x_i - x_j)}{(x_i - x_j)} = 1$, at that point. Furthermore, Equation (2.14) satisfy the conditions

$$C_i(x_j) = \delta_{ij}, \tag{2.15}$$

where the expression δ_{ij} is known as the Kronecker δ-function which is a function of two variables with positive integers such that

$$\delta_{ij} = \begin{cases} 0 & \text{if} \quad i \neq j, \\ 1 & \text{if} \quad i = j. \end{cases}$$

This polynomial interpolation is the basic foundation of the Chebyshev and Legendre polynomials. In Section 2 of [53], some basic properties of the Chebyshev and Legendre polynomials are detailed. We will only focus on the Chebyshev polynomials since they will be the ones applied in our study.

The Chebyshev polynomials T_n are an orthogonal set on the interval [-1, 1] with respect to the weight $w(x) = \frac{1}{\sqrt{1-x^2}}$, i.e we have,

$$\int_{-1}^{1} \frac{T_n T_m}{\sqrt{1 - x^2}} dx = \begin{cases} 0 & \text{if} \quad n \neq m, \\ \pi & \text{if} \quad n = m = 0, \\ \frac{\pi}{2} & \text{if} \quad n = m \neq 0. \end{cases} \tag{2.16}$$

They can be computed by using the recurrence relation [107]

$$\begin{cases} T_0(x) &= 1, \\ T_1(x) &= x, \\ T_{n+1}(x) &= 2xT_n(x) - T_{n-1}(x). \end{cases} \tag{2.17}$$

Figure 2.1 represents the five first polynomials computed from Equation (2.17). The Chebyshev interpolation method is used to approximate the

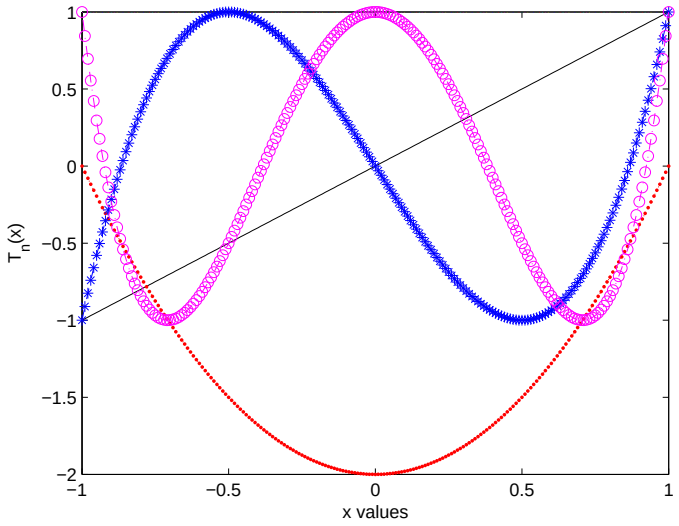

Figure 2.1: The first five Chebyshev polynomials, from T_0 to T_4. T_0 is represented by the point $(0;1)$. T_1 is the straight line. T_2 is the red dotted square function graph. T_3 is the blue graph and T_4 is the red graph with circle points.

solutions of differential equation. This is done by a polynomial which interpolates data u_k at the Chebyshev points $x_k = cos(\frac{k\pi}{N})$, $k = 0, 1, 2, ..., N$. The data u_k must be determined by the polynomial interpolants that satisfy the differential equation exactly at the points x_k. Depending on the smoothness of the solution, the error will decline at different rate as N

increases [121]. A general solution, u, of an unknown PDE will be represented by the global interpolation of the Chebyshev partial sum [107],

$$u_N(x) = \sum_{n=0}^{N} a_n T_n(x), \tag{2.18}$$

where the discrete coefficients, a_n, are defined by

$$a_n = \frac{2}{N}\frac{1}{c_n}\sum_{n=0}^{N}\frac{u(x_j)T_n(x_j)}{c_j}, \tag{2.19}$$

with

$$c_j = \begin{cases} 2 & \text{when} \quad j = 0, N, \\ 1 & \text{otherwise.} \end{cases}$$

2.2.4 Computation of the discrete (expansion) coefficients

The choice of the tests functions and spectral basis allows to develop many type of spectral solvers. To solve a_n in equation (2.18), we mostly use the Tau methods, the collocation method and the Galerkin method. The Memoir of Lanczos introduced the tau method [41], using Chebyshev polynomials. This was connected to the solution of linear differential equation which has polynomial coefficients. More details of this method are given in [41]. The main idea of the Galerkin method is to expand the solution in terms of a linear combination of polynomials that satisfy the boundary conditions. In that method, the usual orthogonal polynomials can't be expanded. Hence we talk about the Galerkin basis which is often apply when we want to solve a PDE. The book of [114] on the spectral methods, from page 6 to page 15, gives more properties and applications of the Galerkin method.

We will apply the collocation or pseudo-spectral method in this dissertation. The method does not use the spectral coefficients but works with the values of the solution at the spacial grid points associated with the basis functions, usually the Gaussian quadrature points. Those points are called collocation points. Hence we talk about working with the solutions in the physical space instead of the ones in spectral space. Refer to [114] for more applications and analysis on the collocation method.

2.3 Representation of spectral and barycentric methods

This section gives an introduction to a barycentric interpolation methods used in this thesis. We first detail the interpolation process, then its differentiation and its integral processes.

2.3.1 Interpolation process

We know that polynomial interpolants can be represented in Lagrange's form and Newton's divided difference [2]. But the knowledge of representing the polynomial interpolation in the barycentric form was made by Taylor [120].
The Section 2.1 of [69] gives more historical details on the barycentric interpolation and refers readers to references that gives the reasons why it took so long for its benefits to become known to the numerical analysis community.

Let consider an example of a rational function ϕ of type (N,N) that interpolates a function f at $N+1$ distinct points $x_0, x_1, ..., x_N$, assuming that these points are ordered monotonically, in an interval $[-1,1]$. Firstly, we recall the Lagrange form of $\phi_N(x)$ as

$$\phi_N(x) = \sum_{j=0}^{N} f(x_i)L_j(x), \quad L_j(x) = \prod_{k=0,k\neq j}^{N} \frac{x-x_k}{x_j-x_k}, \tag{2.20}$$

where the Lagrange polynomial L_j corresponding to the node x_j has the property

$$L_j(x_k) = \begin{cases} 1, & j=k, \\ 0, & \text{otherwise.} \end{cases} \tag{2.21}$$

Then we state the following theorem with proof to define the interpolation of a rational function ϕ.

Theorem 2. *[59] The barycentric form of the rational function ϕ_N is represented by*

$$\phi(x) = \frac{\sum_{k=0}^{N} \frac{v_k}{x-x_k} f(x_k)}{\sum_{k=0}^{N} \frac{v_k}{x-x_k}}, \tag{2.22}$$

with $v_0, v_1, ..., v_N$ being non-zero numbers known as barycentric weights.

Proof. [59] A rational function of type (m,n) is written as a polynomial of degree at most m divided by a polynomial of degree at most n. We can represented ϕ as

$$\phi(x) = \frac{g(x)}{p(x)}, \tag{2.23}$$

where g and p are polynomials of degrees at most N. The barycentric form (2.22) is related to its representation in (2.23). We can show this relation by letting the polynomials in (2.23) to be represented as $g(x_k) = g_k$ and

$p(x_k) = p_k$, with $k = 0, 1, ..., N$. The interpolation property of ϕ implies that $g_k = p_k f(x_k)$, $p_k \neq 0$, $k = 0, 1, ..., N$. The following equation represents g and p as polynomial interpolants in Lagrange's form,

$$\phi(x) = \frac{\sum_{k=0}^{N} \prod_{j=0, j\neq k}^{N} \frac{(x - x_j)}{(x_k - x_j)} p_k f(x_k)}{\sum_{k=0}^{N} \prod_{j=0, j\neq k}^{N} \frac{(x - x_j)}{(x_k - x_j)} p_k}. \tag{2.24}$$

By rewriting the numerator and denominator of equation (2.24), with the assumption that, $x \neq x_k$, we obtain

$$\phi(x) = \frac{\prod_{j=0}^{N}(x - x_j) \sum_{k=0}^{N} \prod_{j=0, j\neq k}^{N} \frac{p_k}{(x_k - x_j)} \frac{1}{x - x_k} f(x_k)}{\prod_{j=0}^{N}(x - x_j) \sum_{k=0}^{N} \prod_{j=0, j\neq k}^{N} \frac{p_k}{(x_k - x_j)} \frac{1}{x - x_k}}, \tag{2.25}$$

and when we cancel the common factors in the numerator and denominator of equation (2.25), we obtain an expression of the form (2.22). □

This can been also shown by using the following proof:

Proof. [12] We define $\ell(x)$ the numerator of L_j in (2.20) as

$$\ell(x) = \frac{1}{x - x_j} \prod_{k=0}^{N}(x - x_k). \tag{2.26}$$

In addition, if we define the barycentric weight by

$$v_k = \frac{1}{\prod_{k=0, k\neq j}^{N} (x_j - x_k)}, \quad k = 0 \ldots N, \tag{2.27}$$

i.e., $v_j = 1/\ell'(x_k)$, then L_j in (2.20) becomes

$$L_j(x) = \ell(x)\frac{v_k}{x - x_k}. \tag{2.28}$$

Consequently, the Lagrange formula (2.20) becomes

$$\phi_N(x) = \ell(x)\sum_{k=0}^{N}\frac{v_k}{x - x_k}f_{(x_k)}. \tag{2.29}$$

The formula (2.29) can be written in a more elegant way. If we represent the constant function $f(x) = 1$, we obtain

$$1 = \sum_{j=0}^{N} L_j(x) = \ell(x)\sum_{k=0}^{N}\frac{v_k}{x - x_k}. \tag{2.30}$$

Dividing (2.29) by (2.30), we get the barycentric formula for ϕ_N

$$\phi_N(x) = \frac{\displaystyle\sum_{k=0}^{N}\frac{v_k}{x - x_k}f_{x_k}}{\displaystyle\sum_{k=0}^{N}\frac{v_k}{x - x_k}}. \tag{2.31}$$

□

The appearance in the numerator and denominator of the barycentric weights of ϕ in equation (2.22) allows one to multiply these weights by an arbitrary non-zero constant without changing ϕ. Since these constants have no effect on the interpolation property of ϕ, they can be chosen to enforce additional constraints on ϕ.

The formula (2.22) discussed by Berrut and Trefethen [12] is the most used form of Lagrange interpolation in practice. It admits $\mathcal{O}(N)$ operations as opposed to the formula (2.20) which requires $\mathcal{O}(N^2)$ [56, 132] additions and multiplications for each evaluation of $\phi_N(x)$. Hence, every time a node

x_j is modified or added, all Lagrange fundamental polynomials have to be recalculated. There is a significant advantage of the spectral collocation method based on the modified barycentric Lagrange interpolation. This is due to the fact that after the transformation, the derivatives in the underlying differential equation do not have to be transformed correspondingly. But in other spectral collocation methods, the transformation is usually needed. More details regarding the convergence and stability properties of the modified Lagrange formula are extensively discuss in [12, 59, 131].

2.3.2 Differentiation process in the barycentric interpolation

The rational function ϕ_N in (2.30) can be differentiate by using nth order differential matrix $D^{(n)}$. The matrix will have entries related to the differential of ϕ by

$$\begin{aligned}\phi^{(n)}(x_j) &= \sum_{k=0}^{N} \frac{d^n}{dx^n}\left(\frac{\frac{v_k}{x-x_k}}{\sum_{\ell=0}^{N}\frac{v_\ell}{x-x_\ell}}\right)\Bigg|_{x=x_j} f_{(x_k)}, \quad j=0,1,.....,N,\\ &\equiv \sum_{k=0}^{N} D_{jk}^{(n)} f_{(x_k)}, \; j=0,1,.....,N.\end{aligned}$$

The computation of $D^{(n)}$ for random values of n has an importance in practical use of barycentric interpolation. This will allow to:

1. Compute the derivatives $\phi^{(n)}(x_0), \phi^{(n)}(x_1), ..., \phi^{(n)}(x_N)$ by multiplying $D^{(n)}$ to the function value's vector provided that the values of

$f(x_0), f(x_1), ..., f(x_N)$ are known.

2. Compute the unknown function values $f(x_0), f(x_1), ..., f(x_N)$ when we know that ϕ satisfy nth order linear differential equation. The process is done by solving a system of linear equations which has coefficients matrix depending on $D^{(n)}$.

When ϕ is a polynomial interpolants, there is numerous formulae that can be used to compute $D^{(n)}$ [7]. For the case where ϕ is a rational polynomial function, the only available formulae are those for $D^{(1)}$ and $D^{(2)}$ [11]. The computation of the first and second order differentiation matrices associated with the barycentric interpolants ϕ_N represented by (2.30) are matrices whose entries are related to the derivatives of ϕ_N. They are obtained from Lemma 1.

Lemma 1. *[11] Let $\ell_j'(x_i) = D_{ij}^{(1)}$ and $\ell_j''(x_i) = D_{ij}^{(2)}$, we have*

$$D_{ij}^{(1)} = \begin{cases} \dfrac{\lambda_j/\lambda_i}{x_i - x_j} & \text{if } i \neq j, \\ -\displaystyle\sum_{i \neq j}^{N} D_{ij}^{(1)}, & \text{if } i = j, \end{cases} \tag{2.32}$$

$$D_{ij}^{(2)} = \begin{cases} -2\dfrac{\lambda_j/\lambda_i}{x_i - x_j}\left(\displaystyle\sum_{k=0, k\neq i}^{N} \frac{\lambda_k/\lambda_i}{x_i - x_k} - \frac{1}{x_i - x_j}\right) & \text{if } i \neq j, \\ -\displaystyle\sum_{i \neq j}^{N} D_{ij}^{(2)}, & \text{if } i = j, \end{cases} \tag{2.33}$$

where $i, j = 0, 1, \ldots, N$.

Proof. [11] Suppose that Lagrange form of a rational function ϕ is repre-

sented by

$$\phi(x) = \sum_{j=0}^{N} \phi_j \ell_j(x), \tag{2.34}$$

then the first and the second order derivatives of u are given by

$$\phi'(x) = \sum_{j=0}^{N} \phi_j \ell_j'(x), \quad \phi''(x) = \sum_{j=0}^{N} \phi_j \ell_j''(x). \tag{2.35}$$

Also the barycentric formula of ℓ_j is

$$\ell_j(x) = \frac{\dfrac{w_j}{x - x_j}}{\displaystyle\sum_{k=0}^{N} \frac{w_k}{x - x_k}}. \tag{2.36}$$

Multiplying both sides of (2.36) by $x - x_i$ and simplifying we get

$$\ell_j(x) \sum_{k=0}^{N} w_k \frac{x - x_i}{x - x_k} = w_j \frac{x - x_i}{x - x_j}. \tag{2.37}$$

Furthermore, we let

$$s(x) = \sum_{k=0}^{N} w_k \frac{x - x_i}{x - x_k}, \tag{2.38}$$

then the first and the second order differentiations of (2.37) yields the following equations

$$\ell_j'(x)s(x) + \ell_j(x)s'(x) = w_j \left(\frac{x - x_i}{x - x_j} \right)', \tag{2.39}$$

and

$$\ell_j''(x)s(x) + 2\ell_j'(x)s'(x) + \ell_j(x)s''(x) = w_j \left(\frac{x - x_i}{x - x_j} \right)''. \tag{2.40}$$

To find the entries of the first and second differentiation matrices, we solve (2.39) and (2.40) at $x = x_i$. This gives

$$s(x_i) = w_i, \; s'(x_i) = \sum_{k=0, k\neq i}^{N} w_k/(x_i - x_k), \; s''(x_i) = -2 \sum_{k=0, k\neq i}^{N} w_k/(x_i - x_k)^2. \tag{2.41}$$

When $i \neq j$:

$$\ell_j(x_i) = 0,\ \ell_j'(x_i) = \frac{w_j/w_i}{x_i - x_j},\ \ell_j''(x_i) = -2\frac{w_j/w_i}{x_i - x_j}\left[\sum_{k=0,k\neq i}^{N} \frac{w_k/w_i}{x_i - x_k} - \frac{1}{x_i - x_j}\right]. \quad (2.42)$$

When $i = j$:

$$\ell_j'(x_j) = -\sum_{i\neq j}^{N} \ell_j'(x_i),\ \ \ell_j''(x_j) = -\sum_{i\neq j}^{N} \ell_j''(x_i). \quad (2.43)$$

□

2.3.3 Integration process in the barycentric interpolation

The discretization of the integral is realized by the barycentric quadrature formula described below

$$\int_a^b u(x)dx = \int_a^b \phi_N(x)dx = \int_a^b \frac{\sum_{j=0}^{N} \frac{v_j}{x-x_j} f_j}{\sum_{j=0}^{N} \frac{v_j}{x-x_j}} dx = \sum_{j=0}^{N} \omega_j f_j, \quad (2.44)$$

where

$$\omega_j = \int_a^b \frac{\frac{v_j}{x-x_j}}{\sum_{j=0}^{N} \frac{v_j}{x-x_j}} dx, \quad (2.45)$$

is the integral of the j^{th} Lagrange fundamental rational function. In this dissertation, we consider Chebyshev-Gauss-Lobatto (CGL) points given by $z_j = \cos(\pi j/N)$ and the weights v_j defined by $v_0 = 1/2$, $v_j = (-1)^j$ for $j = 1,\ldots,N-1$, and $v_N = (-1)^N/2$ (see [12]). The interpolation points x_j are obtained from the CGL points using the relation $x_j = \frac{1}{2}(b-a)z_j + \frac{1}{2}(b+a)$. The integrals (2.44) are then computed numerically with Clenshaw-Curtis rules [24] to achieve the desired accuracy. The method is based on a function that can be represented by its expansion in the Chebyshev polynomials which produce an easily integrable series.

In general, if $f(x)$ is continuous and of bounded variation in (a,b), then it can be expanded in the form

$$f(x) = F(t) = \frac{1}{2}a_0 + a_1\beta_1(t) + a_2\beta_2(t) + ..., \quad a \leq x \leq b, \tag{2.46}$$

where

$$\beta_r(t) = \cos(r\cos^{-1} t), \quad t = \frac{2x-(b+a)}{b-a}.$$

The integration of Equation (2.46) gives [23]

$$\frac{2}{b-a}\int_{-1}^{x} f(x)dx = \int_{-1}^{t} F(t)dt = \frac{1}{2}b_0 + b_1\beta_1(t) + b_2\beta_2(t) + ..., \tag{2.47}$$

with

$$b_r = \frac{a_{r-1} - a_{r+1}}{2r}, \quad r = 1, 2, 3, ...$$

We determine the value of b_0 by using the lower limit of integration, therefore

$$b_0 = 2b_1 + 2b_2 + 2b_3 + 2b_4 + ...$$

Hence Equation (2.47) becomes

$$\begin{aligned}\frac{2}{b-a}\int_{a}^{b} f(x)dx &= \int_{-1}^{1} F(t)dt = \frac{1}{2}b_0 + b_1 + b_2 + ... \\ &= 2(b_1 + b_3 + b_5 + ...).\end{aligned}$$

To compute the coefficients in Equation (2.46), one must first observe that any polynomial of degree N in x can be written in the form

$$f(x) = F(t) = \frac{1}{2}a_0 + a_1\beta_1(t) + a_2\beta_2(t) + ... + \psi, \tag{2.48}$$

with

$$\psi = a_{N-1}\beta_{N-1}(t) + \frac{1}{2}a_{N+1}\beta_{N+1}(t).$$

This leads to the expression

$$f(x) = F(t) = \left(\sum_{r=0}^{N}\right)'' a_r \beta_r(t), \quad -1 \le t \le 1. \tag{2.49}$$

The expression $\left(\sum_{r=0}^{N}\right)''$ denotes a finite sum whose first and last terms have to be halved. Thus, the coefficients in Equation (2.48) are determined by

$$a_r = \frac{2}{N}\left(\sum_{s=0}^{N}\right)'' F_s \cos\frac{\pi rs}{N},$$

where

$$F_s = F\left(\cos\frac{\pi s}{N}\right).$$

This is due to the orthogonality of the cosine function with respect to the point $t_s = \cos\frac{\pi s}{N}$, defined by the equation

$$\left(\sum_{r=0}^{N}\right)'' \cos\frac{\pi is}{N}\cos\frac{\pi js}{N} = \begin{cases} 0 & \text{if} \quad i \neq j, \\ N & \text{if} \quad i = j = 0 \text{ or } N, \\ \frac{1}{2}N & \text{if} \quad i = j \neq 0 \text{ or } N. \end{cases} \tag{2.50}$$

The next section is an example of a SCM (SCDDM) used to accurately approximate the solution of a PDE or ordinary differential equation (ODE).

2.4 Spectral domain decomposition method

Challenges arise when we want to approximate a function with a jump discontinuity by using a high order spectral methods or finite difference. More often, the jumps and derivatives at discontinuity points of a function are known and the derivatives can be easily computed. Meanwhile, it is

difficult to accurately approximate a jump discontinuity in a function or its derivatives when we use a single polynomial. This is the case in option pricing problems. To alleviate the problem of jump discontinuity in a function, a use of some methods comes with a cost in accuracy near the discontinuities or in the computational cost, or in the implementation of the method. Nevertheless, a simple approach such as the SCDDM can be used to recover the accuracy at discontinuity points [83].

2.4.1 Background and definition of the domain decomposition method

PDEs are commonly solved by using basic approaches such as finite difference, finite elements and spectral methods. Among these methods, finite difference method appears to be the easiest to code. Since the method converges only algebraically, a large number of grid points and memory are needed. The other two approaches expand the solution of PDEs in basis functions. Meanwhile, the difference is that finite elements methods uses many sub-domains and expand the solution to low order in each sub-domain. On the other hand, to obtain a solution of a PDE, spectral methods use few sub-domains with high expansion orders compare to the finite elements approach. The method offers a fast convergence and accurate solution.

The work done by the German mathematician Hermann Schwarz (see [134] and references within) has pioneered the Domain Decomposition Method (DDM). It was first designed to solve PDEs on parallel computers. The method solves boundary value problems by dividing the interval

into smaller boundaries called sub-domains and recapitulates the solution between adjacent sub-domains. DDM offers several advantages in mathematics as mention in [134]. Orszag [91] introduced the DDM in SCM. His work produced the multi-domain SCM which consists of matching the solution across different sub-domain. The application is often done when the basis function is not continuous on the domain $\mathcal{D}$ [95]. DDM can be defined as an interval $\mathcal{D} = [a, b]$ broken into M sub-domains such as

$$\mathcal{D}_1 = (x^{(0)}, x^{(1)}), \mathcal{D}_2 = (x^{(1)}, x^{(2)}), ..., \mathcal{D}_M = (x^{(M-1)}, x^{(M)}),$$

with $x^{(0)} = a, x^{(M)} = b$. In general, $\mathcal{D}$ is covered by $N_{\mathcal{D}}$ sub-domains as

$$\mathcal{D} = \bigcup_{\mu=1}^{N_{\mathcal{D}}} \mathcal{D}_\mu, \tag{2.51}$$

where each sub-domains has its own set of basis functions and expansion coefficients

$$u^{(\mu)}(x) = \sum_{k=0}^{N_\mu} \tilde{u}_k^{(\mu)} \phi_k^{(\mu)}(x), \quad x \in \mathcal{D}_\mu, \quad \mu = 1, ...N_{\mathcal{D}}. \tag{2.52}$$

The notation $u^{(\mu)}$ represents the approximation in the μth domain, and the different sub-domains $\mathcal{D}_\mu$ can touch or overlap each other. For example, to solve a second order non-linear elliptic PDE or system of equation,

$$(\mathcal{N}u)(x) = 0, \quad x \in \mathcal{D}, \tag{2.53}$$

in some domain $\mathcal{D} \subset \mathbb{R}^d$ with boundary conditions

$$g(u)(x) = 0 \quad x \in \partial\mathcal{D},$$

where $\mathcal{N}$ and d, respectively, denote the elliptic operator and mappings, the matching conditions must be satisfy. Hence, each functions $u^{(\mu)}$ defined only on the single sub-domain $\mathcal{D}_\mu$ must fit together to form a smooth

solution of (2.53) over the full domain $\mathcal{D}$. For infinite resolution, the following conditions at the limit must hold [95]:

1. When two sub-domains, $\mathcal{D}_\mu$ and $\mathcal{D}_\nu$, touch each other on their intersection surface, the function and its derivative must be smooth, hence
$$\begin{cases} u^\mu(x) &= u^\nu(x), \\ \frac{\partial u^\mu}{\partial n}(x) &= -\frac{\partial u^\nu}{\partial n}(x), \\ x &\in \partial\mathcal{D}_\mu \cap \partial\mathcal{D}_\nu. \end{cases} \tag{2.54}$$
2. When two sub-domains, $\mathcal{D}_\mu$ and $\mathcal{D}_\nu$, overlap each other, the functions $u^{(\mu)}$ and $u^{(\nu)}$ must be identical in $\mathcal{D}_\mu \cap \mathcal{D}_\nu$. Since the solution of a PDE is unique, we must prove that, at boundary of the overlapping domain,
$$u^{(\mu)}(x) = u^{(\nu)}(x), \quad x \in \partial(\mathcal{D}_\mu \cap \mathcal{D}_\nu). \tag{2.55}$$

A description of this spectral method is given in the following section.

2.4.2 Implementation of the spectral domain decomposition method

For simplicity, we will take an example of one dimensional mappings done by [16, 68] and compare it to the one done by [95]. One can consult [95] in its Section 3.2 for the basic functions and mapping in higher order dimensions when using the SCDDM. In one dimensional mapping, [16, 68] first define the Chebyshev polynomials for $X \in [-1, 1]$ and in general, define the differential equations on a different interval $x \in [a, b]$. Then, to use the

Chebyshev polynomial, they introduced a mapping

$$X : [a,b] \rightarrow [-1,1], \quad x \rightarrow X = X(x), \tag{2.56}$$

which represents the mapping of the physical coordinate x onto the collocation coordinate X. Under the mapping, the application of the chain rule result in the transformation of the original PDE defined on [a,b] into a new PDE, involving the Jacobian of the mapping, defined on [-1, 1]. As an example, consider the differential equation

$$\epsilon \frac{\partial^2 u}{\partial x^2} + x\frac{\partial u}{\partial x} = -\epsilon\pi^2 \cos(\pi x) - \pi\ x\ \sin(\pi x), \quad x \in [a,b],\ \epsilon = 10^{-5}, \tag{2.57}$$

with $a = -1$ and $b = 1$. The transformation (2.57) leads to,

$$X'^2 \frac{\partial^2 u}{\partial X^2} + X'' \frac{\partial u}{\partial X} + XX' \frac{\partial u}{\partial X} = \mathcal{M}, \quad X \in [-1,1], \tag{2.58}$$

with $\mathcal{M} = -\epsilon\pi^2 \cos(\pi X) - \pi X \sin(\pi X)$, $X' = \partial X/\partial x$ and $X'' = \partial^2 X/\partial x^2$. One can expand $u(X)$ in Chebyshev polynomials and compute the derivative $\partial/\partial X$ by using the recurrence relation of the spectral coefficient of the derivative given in Equation (14) of Section 2.1 in [95]. Then proceed to code Equation (2.58) in term of $\partial u/\partial X$. But this approach is viewed by [95] to have several disadvantages which he enumerates in his Section 3.1. A different approach is then proposed by [95]. The method consists of using the expansion of Chebyshev polynomials on $X \in [-1,1]$ to obtain the physical solution. They mapped $X(x)$ as

$$u(x) = \sum_{k=0}^{N} \tilde{u}_k T_K(X(x)), \tag{2.59}$$

then computed $\partial u(X)/\partial X$ and $\partial^2 u(X)/\partial X^2$ by using the same recurrence of Equation (14) Section 2.1 in [95]. However, they did not substitute

$\partial u(X)/\partial X$ and $\partial^2 u(X)/\partial X^2$ into Equation (2.58). They computed numerically

$$\frac{\partial u(x)}{\partial x} = X' \frac{\partial u(X)}{\partial X}, \tag{2.60}$$

$$\frac{\partial^2 u(x)}{\partial x^2} = X'^2 \frac{\partial^2 u(X)}{\partial X^2} + X'' \frac{\partial u(X)}{\partial X}, \tag{2.61}$$

and then substituted these values into Equation (2.57). This translate to the mapping of the collocation points to the physical coordinates

$$x_i = X^{-1}(X_i).$$

Figure 2.2 represents the errors between the numerical and the exact so-

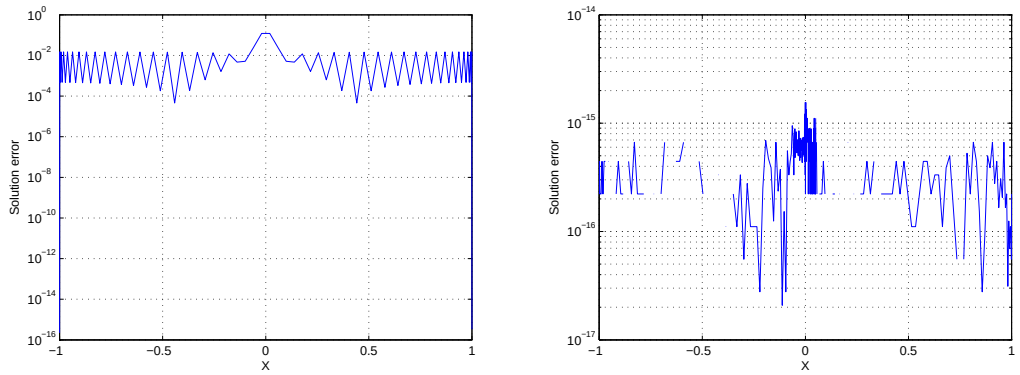

(a) Spectral method (b) spectral decomposition method

Figure 2.2: Graphic representation of the error between the numerical solution and the exact solution.

lution of (2.57). It shows that, the error between the exact solution and the SCM solution (Figure 2.2(a)) of (2.57) is less accurate than the one in Figure 2.2(b) (errors between the numerical and the exact solution of spectral decomposition method (SDM)) . This is described by the numbers recorded in Table 2. One can see that, with the increase of the interpolation points (N), we have a absolute accuracy of 1.6×10^{-15} for $N = 80$ when

SDM is used to solve the differential equation. Meanwhile, SCM has a less significant error value (1.2×10^{-1}) at the same interpolation point. Therefore, SDM can be regarded as a best solver for PDEs or ODEs compare to SCM. The efficiency of SDM is due to the fact that, when the domain is de-

N	SCM Error	SDM Error
10	1.2×10^{-1}	7.2×10^{-1}
20	6.5×10^{-2}	3.5×10^{-3}
40	9.9×10^{-2}	4.7×10^{-9}
80	1.2×10^{-1}	1.6×10^{-15}

Table 2.1: Comparison of the error between the numerical solution and the exact solution for different N when using SCM or SDM.

composed into more sub-intervals we obtain a diagonal segments from the matrix forms of (2.57). Figure 2.4.3 shows that a non decomposed domain gives a non reduced matrix and the more we decomposed the domain in many sub-intervals , the more we obtain a reduced matrix form of the PDE or ODE. This approach allows one to easily compute the differential equation. Figure 2.4.4 represents the grid points used in each domain. In (a), the line representing the grid points is thin compare to the one in (b) and (c). This is due to the fact that in (a) there is less grid points used compare to the one used in (b) and (c). Hence a better accuracy can be achieved when more grid points are used in each domain.

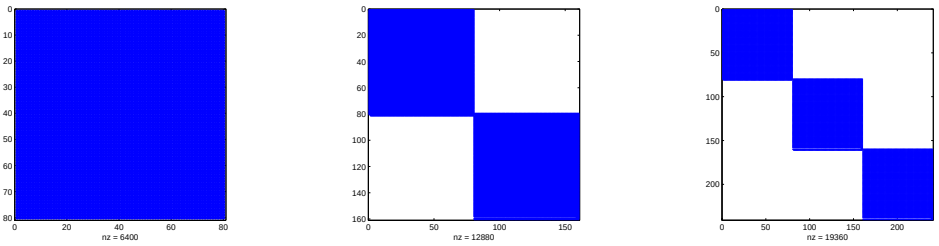

(a) None decomposed domain

(b) Decomposed domain into two sub-intervals

(c) Decomposed domain into three sub-intervals

Figure 2.4.3: Matrix representation of a none decomposed domain and two different decomposed domains.

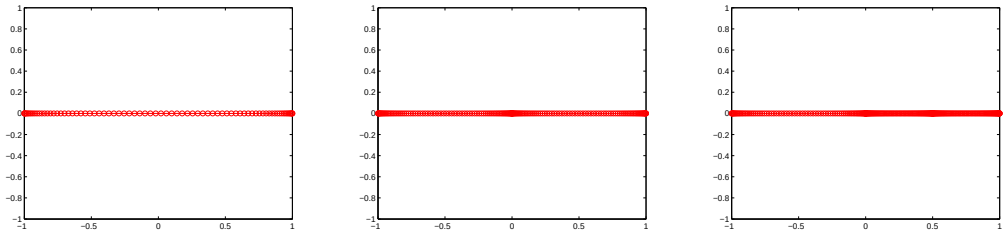

(a) Grid point representation of domain (a)

(b) Grid point representation of domain (b)

(c) Grid point representation of domain (c)

Figure 2.4.4: Grid points representation of different decomposed domains.

2.5 A summary of this chapter

Spectral methods have been actively developed in the last decades. The main advantage of these methods is that they yield exponential order of accuracy if the function is smooth enough. However, for discontinuous functions, their accuracy deteriorates to low accuracy due to the Gibbs phenomenon. To recover the high order accuracy from the spectral approximation contaminated with the Gibbs phenomenon, one can apply

some workarounds such as SCDDM. SCDDM in general, does not produce accurate results when it is directly used to solve an PDE. Hence we make use of the Lévy models to obtain better results when we use the SCDDM in the resolution of financial PDEs. In the next section we define and give some examples of the Lévy processes models used in the field of finance.

Chapter 3

Lévy processes models

Option pricing problems are often modelled by stochastic processes. Such problems were initially introduced in financial institutions in the late 1960s. The famous stochastic model for the equilibrium condition between the expected return on the option, the expected return on the stock and the risk-less interest rate is the celebrated BS equation which was discovered by Black and Scholes in 1973 [14]. However, it is well known that constant volatility BS model is not consistent with market prices. Therefore, more general models for stochastic dynamics of the risky assets have been developed. We can mention, stochastic volatility models [58, 63], deterministic local volatility functions [25, 38], jump-diffusion models [73, 85], Lévy models [81].

This chapter reviews the formulation of the BS equation and gives the importance of the Lévy model in finance. Its also introduces the basic definitions of the Lévy processes and describes its jump-diffusion.

3.1 Formulation of the Black and Scholes model

In the model of BS [14], it is assumed that log-increments of the stock prices are Gaussian (the prices follow a normal distribution). However many classical methods have been introduced as an alternative to the BS approach. One of the most important and efficient of such model is that of the Lévy process model. This types of process have been fitting many empirically observed properties of real world data much better than the BS model.

Louis Bachelier in his work [6] proposed the following model to describe the price, S, of an asset

$$S_t = S_0 + \sigma W_t, \tag{3.1}$$

where W_t is a BM. The model faced numerous difficulties, such includes the failure to account for negative stock prices. Hence Paul Samuelson in 1965 [106] suggested a model to overcome some of the imperfections of Bachelier's model. He proposed that log-prices of an asset follows a BM. To also improve the trading methods, Black and Scholes proved from Samuelson model that one can price a European call option. They used some conditions which state firstly that no transaction costs or taxes and trading takes place continuously in time. Secondly, borrowing and short selling are allowed. Hence in the BS world, the stock price, S, follows a GBM [14]

$$dS_t = \mu S_t dt + \sigma S_t dW_t, \tag{3.2}$$

where μ and σ are known constants and W_t is a standard BM. Equation (3.2) is a stochastic differential equation which has a solution

$$S_t = S_0 e^{(\mu - \frac{1}{2}\sigma^2)t + \sigma W_t}. \tag{3.3}$$

Furthermore, Figure (3.1.1) represents a simple path of a GBM of an asset with $\mu = 0.30$ and $\sigma = 0.20$. The important argument in BS approach is the

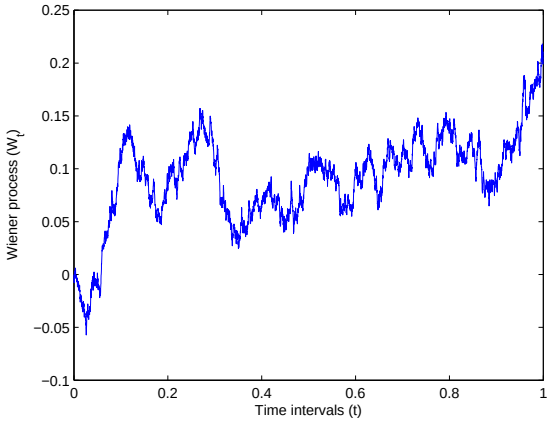

Figure 3.1.1: Simple path of a geometric Brownian motion of an asset price.

construction of a risk-less portfolio which is represented by the BS PDE for a call option:

$$\frac{\partial C}{\partial t} + rS\frac{\partial t}{\partial S} + \frac{1}{2}\sigma^2 S^2 \frac{\partial^2 C^2}{\partial S^2} = rC. \tag{3.4}$$

The stochastic behaviour of the market has driven the attention of researchers in mathematical finance to model it. Equation (3.4) is powerful and simple to use when pricing stock option but fails when some phenomenon such as volatility smile or skew arises. Hence, recently, a multitude of models are available to alleviate the stochastic phenomenon. Some of the most popular and still manageable models are the Lévy models. These models also play an important role in many field of science, such as physics, economics, actuarial science, etc..

Many authors give an overview of the Lévy processes application in different fields [9, 76, 77, 97]. One can refer to the introduction done by [93] in his lecture notes and the references cited therein.

In the next section, we review the basic definitions of the Lévy model and outline its importance in finance.

3.2 Importance of the Lévy models in finance

The use of the Lévy processes in finance has been and still is advantageous to describe the observed reality of financial markets. This observation is done in a more accurate way compare to the models based on BM. During the stock exchange processes, jumps and spikes are commonly observed as the asset prices changes over time.

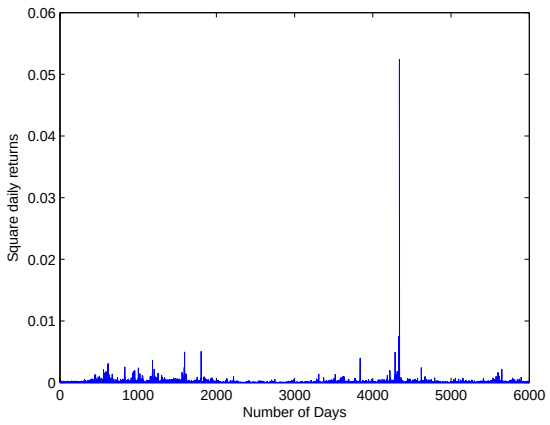

Figure 3.2.1: Square of daily log returns prices of Standard and Poors (S&P) 500 from 1981 to 2004.

Figure 3.2.1, which represents the square of daily log returns of S&P from 01 January 1981 to 31 December 2004, shows a classical example of spikes and jumps observed in stock exchange processes. Furthermore, the asset returns displays fat tails and skewness when represented by the empirical distribution graph. Figure 3.2.2 is an example of a nor-

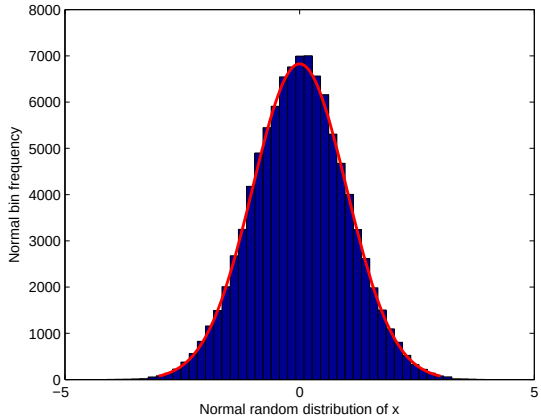

Figure 3.2.2: Normal distribution simulation histograms with $N = 100000$.

mally distributed random values of x with $N = 100000$. Hence, if the asset return empirical distribution graph has the same form with Figure 3.2.2, then the return distribution can be accurately estimated . On Figure 3.2.3,

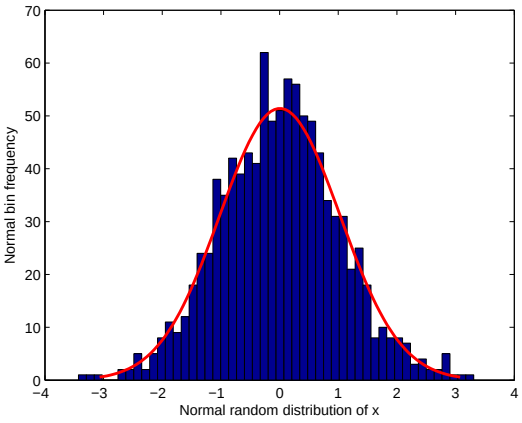

Figure 3.2.3: Normal distribution simulation histograms with $N = 1000$.

with $N = 1000$, the random values of x are not normally distributed. The right and left tails are not equally shaped. Therefore, if we have a return empirical distribution graph with the same results as depicted in Figure

3.2.3, the normality will not be respected and we will need to implement models that will accurately fit the return distribution in order to estimate the profit and loss distributions. Likewise, in the 'risk-neutral ' world, the BS model theory is not respected, since the implied volatilities are not constant across strike nor across maturities. Thus, to minimize the risk in trading, a model is needed to capture the behaviour of the implied volatility smiles in a accurate fashion. In the 'real' and 'risk-neutral' world scenario that we mention above, Lévy processes is the appropriate method to accurately and consistently report all these observations [93].
In all the following sections, the lecture notes of [93] will be the main reference. One can also, for further reading consult [30, 39, 48, 49, 113].

3.3 Basic definition of Lévy processes

For a better understanding of the basic definition of Lévy processes, we define some basic term such as σ-algebra, probability measure, a filtration, an 'usual conditions' and càdlàg function.

Definition 2. *An algebra $\mathcal{F}$ of subset Ω is called σ-algebra on Ω if for any sequence $(A_n)_{n\in\mathbb{N}} \in \mathcal{F}$, we have*

$$\bigcup_{n=1}^{\infty} A_n \in \mathcal{F}.$$

Such a pair $(\Omega, \mathcal{F})$ is called a measurable space.

Definition 3. *A filtration (or information flow) on $(\Omega, \mathcal{F}, \mathbb{P})$ is an increasing family of σ-algebra $(\mathcal{F})_{t\in[0,T]}$:*
$\mathcal{F}_s \subset \mathcal{F}_t \subset \mathcal{F}_T \subset \mathcal{F}$ *for* $0 \leq s < t \leq T$.

Definition 4. *Let Ω be a non-empty set, and let $\mathcal{F}$ be a σ-algebra of the subset Ω. A probability measure $\mathbb{P}$ is a function that, to every set $A \in \mathcal{F}$ assigns a number in $[0,1]$, called probability of A and written $\mathbb{P}(A)$. We require*

1. $\mathbb{P}(\Omega) = 1$ *and*
2. *whenever $\mathcal{A}_1, \mathcal{A}_1 \ldots$ is a sequence of disjoint sets in $\mathcal{F}$, then*

$$\mathbb{P}\left(\bigcup_{n=1}^{\infty} A_n\right) = \sum_{n=1}^{\infty} \mathbb{P}(A_n).$$

The triplet $(\Omega, \mathcal{F}, \mathbb{P})$ is called a probability space.

Definition 5. *We say that a filtered probability space $(\Omega, \mathcal{F}, \mathbb{P}, \mathbf{F})$, with $\mathbf{F} = (\mathcal{F})_{t\in[0,T]}$, satisfies the 'usual condition' if :*

1. *$\mathcal{F}$ is $\mathbb{P}$-complete.*
2. *$\mathcal{F}_0$ contain all $\mathbb{P}$-null set of Ω. This means intuitively that we know which events are possible and which are not.*
3. *$\mathbf{F}$ is right-continuous, i.e. $\mathcal{F}_t = \mathcal{F}_{t+} := \bigcup_{s>t} \mathcal{F}_s$.*

Definition 6. *A function $f : [0,T] \to \mathbb{R}^d$ is said to be càdlàg if it is right continuous with left limits. If the process is càdlàg (left continuous), one should be able to predict the value at t-'see it coming'-knowing the value before t.*

A stochastic process X_t with stationary independent increments which is continuous in probability is called a Lévy process. More precisely, the process can be define as follow:
Suppose $(\Omega, \mathrm{F}, \mathbf{F}, P)$ is a filtered probability space, with $\mathcal{F} = \mathcal{F}_T$ and the filtration $\mathbf{F} = (\mathcal{F})_{t\in[0,T]}$ satisfies the usual conditions. Suppose $T \in [0,\infty]$ denotes the time horizon which, in general, can be infinite.

Definition 7. *A càdlàg, adapted, real valued stochastic process* $X = (X)_{0\leq t\leq T}$ *with* $X_0 = 0$ *almost surely (a.s.) is called a Lévy process if the following condition are met:*

$(\mathbf{X_1})$: *X has independent increments, i.e.* $X_t - X_s$ *is independent of* $\mathcal{F}_s$ *for any* $0 \leq s < t \leq T$.

$(\mathbf{X_2})$: *X has stationary increments, i.e. for any* $0 \leq s, t \leq T$ *the distribution of* $X_{t+s} - X_t$ *does not depend on t.*

$(\mathbf{X_3})$: *X is stochastically continuous, i.e for any* $0 \leq t \leq T$ *and* $\epsilon > 0$*:* $\lim_{s\to t} P(|$ $X_t - X_s$ $|> \epsilon) = 0$.

Among the Lévy processes, the deterministic process (linear drift) appear to be the simplest process. While the BM is the only (non-deterministic) Lévy process having continuous paths. Jumps of size one are Poisson process and those of random size are compound Poisson process. The compound Poisson and the Poisson processes are part of the class of Lévy processes. We shall notice that the combination of compound Poisson and the BM is a Lévy process and is often called a 'jump-diffusion' process [93]. To avoid confusion of terms, we will always refer the jump diffusion in this dissertation as a 'Lévy jump-diffusion' process since there are jump-diffusion processes which are not Lévy processes.

3.4 Description of the Lévy jump-diffusion processes

This section reviews some basic definitions and theorem of the Lévy jump-diffusion processes. Let $X = (X_t)_{0\leq t\leq T}$ be a jump-diffusion composed by

the BM and a reduced compound Poisson process, modelled by the following stochastic differential equation (SDE)

$$X_t = \alpha t + \sigma W_t + \left(\sum_{k=1}^{N_t} G_k - t\lambda\theta \right), \tag{3.5}$$

where the parameters $\alpha \in \mathbb{R}, \sigma \in \mathbb{R} \geq 0$ and $W = (W_t)_{0 \leq t \leq T}$ is the standard BM. $W = (W_t)_{0 \leq t \leq T}$ represents the Poisson process with parameter λ ($\mathbb{E}[W_t] = \lambda t$). $G = (G_k)_{k \geq 1}$ is an independent and identically distributed sequence of random variables with probability distribution F and $\mathbb{E}[G] = \theta < \infty$. Therefore, the distribution of jumps arriving is described by F according to the theory of the Poisson process. Every randomness sources are mutually independent [30, 39, 93].

Definition 8. *A càdlàg stochastic process $X = (X)_{t \in [0,T]}$ is a martingale relative to $(\mathbb{P}, \mathcal{F}_t)$ if*

1. *X is $\mathcal{F}_t$-adapted,*
2. *$\mathbf{E}[\mid X_t \mid] < \infty$ for any $t \in [0, T]$,*
3. *$\forall\ s < t,\ \mathbf{E}[X_t \mid \mathcal{F}_s] = X_s$.*

A BM is known to be a martingale from literatures, hence the reduced Poisson process is also a martingale. So, $X = (X_t)_{0 \leq t \leq T}$ is a martingale if and only if $\alpha = 0$.
The property of the function X_t is

$$\begin{aligned} \mathbb{E}[e^{iuX_t}] &= \mathbb{E}\left[\exp(iu(\alpha t + \sigma W_t + \sum_{k=1}^{N_t} G_k - t\lambda\theta)) \right], \\ &= \exp[iu\alpha t]\mathbb{E}\left[\exp(iu\sigma W_t) \exp(iu(\sum_{k=1}^{N_t} G_k - t\lambda\theta)) \right], \end{aligned}$$

because all sources of randomness are independent, we get

$$\mathbb{E}[e^{iuX_t}] = \exp[iu\alpha t]\mathbb{E}[\exp(iu\sigma W_t)]\mathbb{E}\left[\exp(iu(\sum_{k=1}^{N_t} G_k - iut\lambda\theta))\right].$$

Theorem 3. *[93] The characteristic function of X_t is represented by the following equation which is a special case of the Lévy-Khintchine formula*

$$\mathbb{E}[e^{iuX_t}] = \exp\left[t\left(iu\alpha - \frac{u^2\sigma^2}{2} + \int_{-\infty}^{\infty}(e^{iux} - 1 - iux)\lambda F(x)\right)\right]. \tag{3.6}$$

Proof. [93] If we consider

$$\mathbb{E}[e^{iu\sigma W_t}] = e^{-\frac{1}{2}\sigma^2u^2t}, \quad W_t \sim \text{Normal}(0,t),$$

$$\mathbb{E}[e^{iu\sum_{k=1}^{N_t} G_k}] = e^{\lambda t(\mathbb{E}[e^{iuG}-1])}, \quad N_t \sim \text{Poisson}(\lambda t),$$

we get

$$\mathbb{E}[e^{iu\sum_{k=1}^{N_t} G_k}] = \exp[iu\alpha t]\exp\left[-\frac{1}{2}u^2\sigma^2t\right]\exp\left[\lambda t(\mathbb{E}[e^{iuG} - 1] - iu\mathbb{E}[G])\right],$$

$$= \exp[iu\alpha t]\exp\left[-\frac{1}{2}u^2\sigma^2t\right]\exp\left[\lambda t(\mathbb{E}[e^{iuG} - 1 - iuG])\right],$$

since F is the distribution of G, then we get

$$\mathbb{E}[e^{iu\sum_{k=1}^{N_t} G_k}] = \exp[iu\alpha t]\exp\left[-\frac{1}{2}u^2\sigma^2t\right]\exp\left[\lambda t\int_{-\infty}^{\infty}(e^{iux} - 1 - iux)F(x)\right].$$

Now, since t is a common factor, we re-write the above equation to obtain the desirable result. □

More literatures and examples on the jump-diffusion are given by Bertoin [13], Raible [98] and Sato [109]. One can also, refer to [93] from page 8 to 16 Sections 4, 5, 6, and 7. These sections give more details on the relation between the Lévy process and the infinity divisible distribution, the analysis of jumps and Poisson random measures, the Lévy-Itô decomposition and the Lévy measure, path and moment properties.

Definition 9. *The distribution of a real-valued random variable X is infinitely divisible if for every $n \in \mathbb{N}_+$, there exists a sequence of independent, identically distributed variables $(X_1, X_2, ..., X_n)$ such that $X_1 + X_2 + ... + X_n$ has a same distribution as X.*

Definition 10. *If the distribution of X is stable then the distribution is infinitely divisible.*

There is an important link between the Lévy processes and infinitely divisible distribution. If $(X(t))_{t\geq 0}$ is a Lévy process, therefore all process values $X(t)$ are infinitely divisible. More theorems, examples and applications can be found in [93, 109] and references within to understand their connection.

3.5 Application of Lévy processes in Finance

The Finance industry widely used BS model to price option. This is due to the fact that many options can be priced explicitly. They also use efficient computational methods such as the MCM to price more complicated derivatives and high number of options. The BS model in particular has a poor model fit and some price obtained from the model has to be adjusted to be realistic [112]. However, many model based on Lévy processes, which has a very wide modelling freedom, can correct this poor fitting [133].
In the following Subsections, we describe an asset price model driven by a Lévy process under the real and risk-neutral measure.

3.5.1 Market driven by the real-world measure

Two modelling approaches are used to price an option in the real world measure. The first approach is based on the exponential Lévy process and the second approach is based on the application of Itô's formula. Under the real world-measure, the following equation is used to model the asset price process as the exponential of a Lévy process.

$$S_t = S_0 \exp(X_t), \quad 0 \leq t \leq T, \tag{3.7}$$

with, X being the Lévy process of an infinitely divisible distribution estimated from available data set of a particular asset. Therefore, the stationary and independent increments will be produced by the log-returns. They will be distributed across time intervals of specific length. Clearly, the process X carries its path properties over S, i.e., when X is a pure-jump process then S will also be in the same process. This approach gives an opportunity to record the price fluctuations of the asset at the micro structure level, even in a daily time scale. Figure 3.5.1 is a simulation of a simple path of Equation (3.7) with $S_0 = 50, T = 1, r = 0.05$ and $\sigma = 0.20$.

The second approach is given by the application of Itô's formula which yields that $S = (S_t)_{0 \leq t \leq T}$ is the solution of the SDE

$$dS_t = S_t - \left(dX_t + \frac{c}{2} dt + \int_{\mathbb{R}} (e^x - 1 - x) \mu^X (dt, dx) \right). \tag{3.8}$$

The solution S can also be specify when we replaced the BM in the BS SDE by a Lévy process, i.e. via

$$dS_t = S_t - dX_t, \tag{3.9}$$

which has a stochastic exponential solution

$$S_t = S_0 \xi(X_t). \tag{3.10}$$

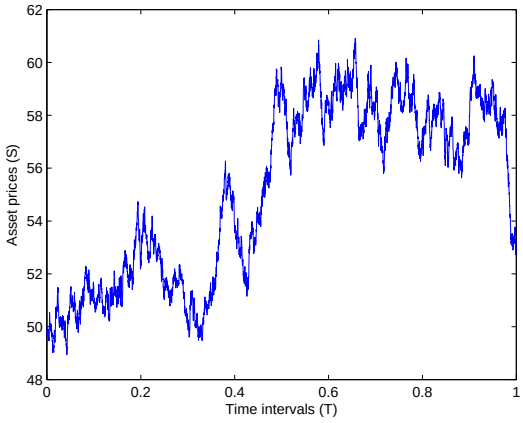

Figure 3.5.1: Simple path of the exponential Lévy process of an asset price.

But this approach will not be favourable to the financial applications, since a negative value can be produced by the asset price, unless we restrict jumps to be above -1 by taking the measure (ν) as $\sup(\nu) \subset [-1, \infty)$. Also the approach does not give the distribution of the log-returns [93]. Since one approach is appropriate to study the distribution properties of the price process and the other for probing the martingale properties. Then the two models can be closely related or complementary to each other [49]. In general, the market is regarded to be incomplete, because the price process is driven by the Lévy process. The exception is made when the market is driven by the Normal (BS model) and Poisson distribution [93, 112, 133]. If we use a particular asset, such as moment derivatives, variance swaps, then the market driven by the Lévy process can be complete. There will exist a unique martingale measure; see [93] at page 31 for a given example.

3.5.2 Market driven by the risk-neutral measure

In financial mathematics, a risk neutral measure is a probability measure such that each share price is exactly equal to the discounted expectation of the share price under this measure [112]. Hence to describe a price of an asset under a risk neutral measure, we make the following two assumptions:

- The Lévy process X has first exponential moment, such that

$$\mathbb{E}[e^{X_t}] < \infty.$$

- The Lévy process has finite first moment if and only if $\int_{|x|\geq 1} \mid x \mid \nu(dx) < \infty$.

Then under the risk neutral measure ($\bar{R}$), the asset price can be modelled as an exponential Lévy process

$$S_t = S_0 \exp(X_t),$$

where X has the triplet $(\bar{\alpha}, \bar{c}, \bar{\nu})$ and satisfies the above two mentioned assumptions [112, 133]. The process X has the unique decomposition represented by

$$X_t = \bar{\alpha} t + \sqrt{\bar{c}} \bar{W}_t + \int_0^t \int_{\mathbb{R}} x(\mu^X - \bar{\nu}^X)(ds, dx)$$

where $\bar{W}_t$ is a $\bar{R}$-BM and $\bar{\nu}^X$ is the $\bar{R}$-compensator of the jump measure μ^X [93]. By making the assumption that $\bar{R}$ is the risk neutral measure, then the asset price will have a rate of return $\mu = r - \delta$ and a martingale in a form of the re-invested process $(e^{(r-\delta)t} S_t)_{0\leq t\leq T}$ under $\bar{R}$. The two parameters r

and δ represent respectively, the risk free interest rate and the continuous dividend yield of an asset. Hence the drift $\bar{\alpha}$ has a form

$$\bar{\alpha} = r - \delta - \frac{\bar{c}}{2} - \int_{\mathbb{R}} (e^x - 1 - x)\bar{\nu}(dx),$$

where $r \geq 0$ and $\delta \geq 0$. More details are given by Goll [49], Shoutens [112], Papapantoleon [93] and Winkel [133].

3.6 Some popular models of Lévy processes used in the mathematical finance

In this section, we review the most popular models used in mathematical finance from the point of view of Lévy process. These models are tools to solve different cases of financial problem.

- The **BS model** has been the most famous asset price model based on the Lévy process. Its log-return is normally distributed with mean μ and variance σ^2. This is summarized as, $X_t \sim$ Normal (μ, σ^2) and density, $f_{X_t}(x) = \frac{1}{\sigma\sqrt{2\pi}} \exp\left[-\frac{(x-\mu)^2}{2\sigma^2}\right]$. Therefore, the characteristic function is represented by, $\varphi_{X_t}(u) = \exp\left[i\mu u - \frac{\sigma^2 u^2}{2}\right]$, $i = 1, ..., n$; The first and second moments are $\mathbf{E}[X_t] = \mu$, $\text{Var}[X_t] = \sigma^2$ and the skewness of X_t is 1, the kurtosis is equal to 3. The canonical decomposition of X_t is represented by, $X_t = \mu t + \sigma W_t$ and the Lévy triplet is $(\mu, \sigma^2, 0)$ [62].

- The **Merton** model has been the first to use a discontinuous price process to model asset returns. The model is represented by the

canonical decomposition,

$$X_t = \mu t + \sigma W_t + \sum_{k=1}^{N_t} J_k,$$

with $J_k \sim \text{Normal}(\mu_J, \sigma_J^2), k = 1, 2, 3, ...$, and the jump size of the distribution has density, $f_J(x) = \frac{1}{\sigma_J\sqrt{2\pi}}\exp\left[-\frac{(x-\mu_J)^2}{2\sigma_J^2}\right]$. Hence, the characteristic function of X_t is

$$\varphi_{X_t}(u) = \exp\left[i\mu u - \frac{\sigma^2 u^2}{2} + \lambda(e^{i\mu_J u - \sigma_J^2 u^2/2} - 1)\right],$$

and the Lévy triplet is $(\mu, \sigma^2, \lambda f_J)$ [49, 133].

- The **Kou** model is a jump-diffusion model that is similar to Merton's model. The difference is observed at the jump size which is double-exponentially distributed ($\sim Db\exp$). Hence the canonical decomposition of the driving process is

$$X_t = \mu t + \sigma W_t + \sum_{k=1}^{N_t} J_k,$$

with $J_k \sim Db\exp(p, \theta_1, \theta_2), k = 1, 2, 3, ...$, and the jump size has density

$$f_J(x) = p\theta_1 e^{\theta_1 x} 1_{\{x<0\}} + (1-p)\theta_2 e^{\theta_2 x}\mathbf{1}_{\{x>0\}}.$$

The characteristic function of X_1 is represented by

$$\varphi_{X_t}(u) = \exp\left[i\mu u - \frac{\sigma^2 u^2}{2} + \lambda\left(\frac{p\theta_1}{\theta_1 - iu} - \frac{(1-p)\theta_2}{\theta_2 + iu} - 1\right)\right],$$

and the Lévy triplet is $(\mu, \sigma^2, \lambda f_J)$ [93].

- **The Generalized Hyperbolic (GH)** model has increments of time length 1 which follow a **GH** distribution ($\sim$ **GH**) with parameters

$\alpha, \beta, \delta, \mu, \lambda$, which indicate that $X_t \sim \mathbf{GH}(\alpha, \beta, \delta, \mu, \lambda)$. The density of the **GH** model is defined as

$$f_{GH}(x) = c(\lambda, \alpha, \beta, \delta)\left(\delta^2 + (x-\mu)^2\right)^{\frac{(\lambda-\frac{1}{2})}{2}} \Gamma,$$

Where

$$\Gamma = \mathrm{K}_{\lambda-\frac{1}{2}}\left(\alpha\sqrt{\delta^2 + (x-\mu)^2}\right)\exp(\beta(x-\mu)),$$

and

$$c(\lambda, \alpha, \beta, \delta) = \frac{(\alpha^2-\beta^2)^{\lambda/2}}{\sqrt{2\pi}\alpha^{\lambda-\frac{1}{2}}\mathrm{K}_\lambda\left(\delta\sqrt{\alpha^2-\beta^2}\right)}.$$

In the density function $f_{\mathbf{GH}}(x)$, K_λ represents the Bessel function of the third kind with index λ (see [1] for more details), the parameter $\alpha > 0$ determines the shape, $0 \leq |\beta| < \alpha$ determines the skewness, $\mu \in \mathbb{R}$ the location and $\delta > 0$ represents the scaling parameter. The heaviness of the tail is affected by $\lambda \in \mathbb{R}$ and this allows to go through different subclasses such as the hyperbolic distribution ($\lambda = 1$) or the normal inverse Gaussian ($\lambda = \frac{1}{2}$).

The distribution of **GH** has the characteristic function

$$\varphi_{\mathbf{GH}}(u) = e^{iu\mu}\left(\frac{\alpha^2-\beta^2}{\alpha^2-(\beta+iu)^2}\right)^{\frac{\lambda}{2}} \frac{\mathrm{K}_\lambda\left(\delta\sqrt{\alpha^2-(\beta-iu)^2}\right)}{\mathrm{K}_\lambda\left(\delta\sqrt{\alpha^2-\beta^2}\right)}.$$

The canonical decomposition of the Lévy process driven by a **GH** distribution is

$$X_t = t\mathbf{E}[X_1] + \int_0^t \int_{\mathbb{R}} x\left(\mu - \nu^{\mathbf{GH}}\right)(ds, dx),$$

where the Lévy measure $\nu^{\mathbf{GH}}$ has the form

$$\nu^{\mathbf{GH}}(dx) = \frac{e^{\beta x}}{|x|}\left(\int_0^\infty \frac{\exp(-\sqrt{2y+\alpha^2}|x|)}{\pi^2 y(J^2_{|\lambda|}(\delta\sqrt{2y}) + Y^2_{|\lambda|}(\delta\sqrt{2y})}dy + \lambda e^{-\alpha|x|}\mathbf{1}_{\{x\geq 0\}}\right),$$

and J_λ, Y_λ denote respectively the Bessel function of first and second kind with index λ. The Lévy triplet of model is $(\mathbf{E}[X_1], 0, \nu^{\mathbf{GH}})$ [93].

- **The Normal Inverse Gaussian (NIG)** model is a particular case of the **GH** model for $\lambda = \frac{1}{2}$. The density of the model is represented by

$$f_{\mathbf{NIG}}(x) = \frac{\alpha}{\pi}\exp\left(\delta\sqrt{\alpha^2-\beta^2}+\beta(x-\mu)\right)\frac{\mathrm{K}_1\left(\alpha\delta\sqrt{1+(\frac{x-\mu}{\delta})^2}\right)}{\sqrt{1+(\frac{x-\mu}{\delta})^2}}.$$

  The characteristic function of the model has the modified form

$$\varphi_{\mathbf{NIG}}(u) = e^{iu\mu}\frac{\exp\left(\delta\sqrt{\alpha^2-\beta^2}\right)}{\exp\left(\delta\sqrt{\alpha^2-(\beta+iu)^2}\right)},$$

  while the canonical decomposition is

$$X_t = t\mathbf{E}[X_1] + \int_0^t\int_{\mathbb{R}} x\left(\mu - \nu^{\mathbf{NIG}}\right)(ds,dx),$$

  with the Lévy measure [93]

$$\nu^{\mathbf{NIG}}(dx) = e^{\beta x}\frac{\alpha\delta}{\pi|x|}\mathrm{K}_1(\alpha|x|)\,dx.$$

- **The Meixner process** is constructed from the following assumption. We let $X = (X_t)_{0\le t\le T}$ be a Meixner process with Law $(H_1|P) = \mathbf{Meixner}(\alpha,\beta,\delta), \alpha > 0, -\pi < \beta < \pi, \delta > 0$, therefore the density of the model is

$$f_{\mathbf{Meixner}}(x) = \frac{\left(2\cos\frac{\beta}{2}\right)^{2\delta}}{2\pi\alpha\Gamma(2\delta)}\exp(\frac{\beta x}{\alpha})\left|\Gamma\left(\delta+\frac{ix}{\alpha}\right)\right|^2,$$

  and the characteristic function of the model is

$$\varphi_{X_t}(u) = \left(\frac{\cos\frac{\beta}{2}}{\cosh\frac{\alpha u - i\beta}{2}}\right)^{2\delta t},$$

  where $t \in [0,T]$. The Meixner process is a pure jump Lévy process with a measure represented by

$$\nu^{\mathbf{Meixner}}(dx) = \frac{\delta\exp\left(\frac{\beta}{\alpha}x\right)}{x\sinh\left(\frac{\pi x}{\alpha}\right)}$$

and the canonical decomposition represented by

$$X_t = t\mathbf{E}[X_1] + \int_0^t \int_{\mathbb{R}} x\left(\mu^X - \nu^{\mathbf{Meixner}}\right)(ds, dx).$$

The Lévy triplet of the model is $(\mathbf{E}[X_1], 0, \nu^{\mathbf{Meixner}})$ [49, 112].

- **The Carr, German, Madan, and Yor (CGMY)**
  Lévy process is closely related to stable processes when additional exponential factors are involved. In close forms, its density is not known [93]. The characteristic function $X_t, t \in [0, T]$ is represented by

$$\varphi_{X_t}(u) = \exp\left(t\mathbf{C}\Gamma(-\mathbf{Y})[(\mathbf{M} - iu)^{\mathbf{Y}} + (\mathbf{G} + iu)^{\mathbf{Y}} - \mathbf{M}^{\mathbf{Y}} - \mathbf{G}^{\mathbf{Y}}]\right),$$

and the Lévy measure of the process is represented by

$$\nu^{\mathbf{CGMY}}(dx) = \mathbf{C}\frac{e^{-\mathbf{M}x}}{x^{1+\mathbf{Y}}}\mathbf{1}_{\{1<0\}}dx + \mathbf{C}\frac{e^{\mathbf{G}x}}{|x|^{1+\mathbf{Y}}}\mathbf{1}_{\{1<0\}}dx,$$

with $\mathbf{C} > 0, \mathbf{G} > 0, \mathbf{M} > 0$, and $\mathbf{Y} < 2$. The canonical decomposition of the process has the representation

$$X_t = t\mathbf{E}[X_1] + \int_0^t \int_{\mathbb{R}} x\left(\mu^X - \nu^{\mathbf{CGMY}}\right)(ds, dx),$$

while the Lévy triplet of the model is $(\mathbf{E}[X_1, 0, \nu^{\mathbf{CGMY}}])$ [93].

Chapter 4

Application and review of a Lévy model in a PIDE and its other resolution modes

Option problems under jump models [73] can be modelled by means of PIDEs. Due to inherent complexity in the modelling equations, one can rarely find closed-form analytical solutions to these models, and therefore one has to resort to numerical methods.

This chapter investigate the resolution of a PIDE under Lévy model and review other resolution modes.

4.1 Partial Integro-differential Equations approach

The above sections describe the Lévy processes under the expected value approach. Here, we consider the class of exponential Lévy model where $S_t = e^{rt+X_t}$ represents the risk-neutral of the underlying asset. The parameter X_t is a time-homogeneous jump-diffusion process. In this thesis we will apply this approach to determine the solutions of the PIDE.

4.1.1 Exponential Lévy models

In finance, one of the main purpose of exponential Lévy models is to price and hedge options. We assume that, $r \geq 0$ is a known constant riskless interest rate constant and $S_0 > 0$, the initial value. These models represent the price of a stock as the exponential of a Lévy process:

$$S_t = S_0 e^{rt+X_t}, \quad 0 \leq t \leq T, \tag{4.1}$$

where X is the Lévy process with characteristic triplet $(\sigma^2, \tilde{\Pi}, \tilde{\gamma})$ under measure $\mathbb{P}$ and satisfies some integrability condition. Under the assumption of no-arbitrage, the existence of an equivalent martingale measure $\mathbb{Q}$ to $\mathbb{P}$ must hold and $\mathbf{E}^{\mathbb{Q}}[e^{X_t}] = e^{rt}, t \geq 0$, provided that X has the characteristic triplet (σ^2, Π, γ). This translates that the expected return on stock S must be the same as that from the money account. Hence

$$\frac{\sigma^2}{2} + \gamma + \int_{\mathbb{R}} (e^x - 1 - x\mathbf{1}_{\{|x|\leq 1\}})\Pi(dx) = r \tag{4.2}$$

which is derived from the Lévy-Khintchine formula [28].
A multitude of different exponential Lévy models is accounted in the financial modelling literature. The reason of this diversity of choices is

based on the incomplete market observed in model with jumps. This gives a variety of choosing the equivalent martingale measure. The following definition amount to achieve the change of measure.

Definition 11. *Let X be a Lévy process on the probability space $(\Omega, \mathcal{F}, \mathbb{P})$.Then the Esscher transform is any change of $\mathbb{P}$ by the process X_t and a constant θ to an equivalent probability measure $\mathbb{Q}$ such that*

$$\frac{d\mathbb{Q}}{d\mathbb{P}}\bigg|\mathcal{F}_t = \frac{\exp(\theta X_t)}{\mathbf{E}[exp(\theta X_t)]}. \tag{4.3}$$

When the existence of Definition 11 holds, then

$$\gamma = \tilde{\gamma} + \theta\sigma^2 + \int_{-1}^{1} x(e^{\theta} - 1)\Pi(dx),$$

and $\Pi(dx) = e^{\theta x}\tilde{\Pi}(dx)$ should exist. This process is known as the Esscher transform of martingale measure and more about this transforms are detailed in [47].

4.1.2 Partial integro-differential equations for option prices

Let consider the value of a European option, $V(t,S)$, with the underlying asset S_t and terminal payoff Ψ. From the risk-adjusted measure (risk-neutral probability) $\mathbb{Q}$, we obtain

$$V(t,S) = e^{-r(T-t)}\mathbf{E}^{\mathbb{Q}}[\Psi\,(S_t)|\,S_t = S] = e^{-r(T-t)}\mathbf{E}^{\mathbb{Q}}[\Psi(Se^{X_{T-t}})]. \tag{4.4}$$

Introducing the change of variables $x = \ln S$ and $\tau = T - t$, and by defining $u(\tau,x) = V(t,S) = e^{-r\tau}\mathbf{E}^{\mathbb{Q}}[\Psi(e^{x+X_\tau})]$, we obtain a PIDE by differentiating $u(\tau,x)$ with respect to τ. The PIDE equation is written in a form of

$$\frac{\partial u}{\partial \tau} = \mathrm{L}u(x). \tag{4.5}$$

The operator L represents the infinitesimal generator of a Lévy process. it is defined as follows:

Proposition 1. *[28][**Infinitesimal generator of a Lévy process**] Let $(X)_{t\geq 0}$ be a Lévy process on $\mathbb{R}$ with characteristic triplet (σ^2, Π, γ). Then the infinitesimal generator of X is defined for any $f \in C_0^2(\mathbb{R})$ as*

$$\mathrm{L}f(x) = \frac{1}{2}\sigma^2 \frac{\partial^2 f}{\partial x^2}(x) + \gamma \frac{\partial f}{\partial x}(x) + \mathcal{J}', \tag{4.6}$$

where $\mathcal{J}' = \int_{\mathbb{R}} \Big(f(x+y) - f(x) - y\frac{\partial f}{\partial x}(x)\mathbf{1}_{\{|y|\leq 1\}} \Big)\Pi(dy)$ and $C_0^2(\mathbb{R})$ is the set of twice continuously differentiable functions, vanishing at infinity.

By further applying condition (4.2) in Equation (4.5), we obtain the following PIDE:

$$\frac{\partial u}{\partial \tau} = \frac{\sigma^2}{2}\frac{\partial^2 u}{\partial x^2}(\tau, x) + (r - \frac{\sigma^2}{2})\frac{\partial u}{\partial x}(\tau, x) - ru(\tau, x) + \tilde{\mathrm{J}}, \tag{4.7}$$

where

$$\tilde{\mathrm{J}} = \int_{\mathbb{R}} \left(u(\tau, x+y) - u(\tau, x) - (e^y - 1)\frac{\partial u}{\partial x}(\tau, x) \right)\Pi(dy).$$

The use of another change of variable, such as $S = e^x$ and $t = T - \tau$ will transform equation (4.7) to a similar equation for $V(t, S)$, as follow:

$$\frac{\partial V}{\partial t} + rS\frac{\partial V}{\partial S} + \frac{\sigma^2 S^2}{2}\frac{\partial^2 V}{\partial S^2} - rV(t, S) + \tilde{\mathbf{J}} = 0, \tag{4.8}$$

with $\tilde{\mathbf{J}} = \int_{\mathbb{R}} \Big(V(t, Se^y) - V(t, S) - S(e^y - 1)\frac{\partial V}{\partial S}(t, S) \Big)\Pi(dy)$.
Under the BS model, the Lévy process $\tilde{\mathbf{J}}$ is equal to 0, therefore, Equation (4.8) will be reduced to the BS PDE. But under a finite variation Lévy process, the second partial derivative term vanishes and the partial derivative term in the integral can be taken out. Hence, Equation (4.8) become a first order PIDE:

$$\frac{\partial V}{\partial t} + (r + \rho)S\frac{\partial V}{\partial S} - rV + \int_{\mathbb{R}} [V(t, Se^y) - V(t, S)]\Pi(dy) = 0, \tag{4.9}$$

with $\rho = \int (1 - e^y)\Pi(dy)$. This PIDE can be solve by using the exponential time integration method.

4.2 Exponential time integration methods

4.2.1 Background and motivation

As we mention in the introduction of this dissertation, most models in finance are represented by PDEs. Many financial problems are modelled under a form of these equations. The BS is the most important PDE in financial problems. It is a time dependent PDE with one space variable denoted by S and one time variable denoted by t. To solve time-dependent PDE numerically, one can discretize it in space by leaving the time variable continuous. This spatial discretization results to a system of ODEs. The conversion from PDEs to ODEs can be done by spectral, finite element, finite difference approaches [55]. The following example illustrates how to convert a PDE to a ODE by using a semi-discrete finite difference method. We consider the following heat equation

$$u_t = cu_{xx}, \quad 0 \leq x \leq 1, \quad t \geq 0,$$

with initial condition

$$u(0, x) = g(x), \quad 0 \leq x \leq 1,$$

and boundary conditions

$$u(t, 0) = 0, \quad u(t, 1) = 0, \quad t \geq 0.$$

By defining the spatial mesh points to be

$$x_i = i\Delta x, \quad i = 0, 1, ..., n+1,$$

with $\Delta x = \frac{1}{(n+1)}$. We then replace the derivative u_{xx} by the finite difference approximation

$$u_{xx}(t, x_i) \approx \frac{u(t, x_{i+1}) - 2u(t, x_i) + u(t, x_{i-1})}{(\Delta x)^2},$$

to obtain a system of ODEs

$$y_i^{'}(t) = \frac{c}{(\Delta x)^2}(y_{i+1}(t) - 2y_i(t) + y_{i-1}(t)), \quad i = 1, 2, ..., n,$$

and $y_i(t) \approx u(t, x_i)$. From the boundary conditions, $y_0(t)$ and $y_{n+1}(t)$ are identically zero, and from the initial conditions $y_0 = g(x_i), \quad i = 1, 2, ..., n$. The semi-discrete system of ODEs can be written in the matrix form

$$\mathbf{y}^{'} = \frac{c}{(\Delta x)^2}\begin{pmatrix} -2 & 1 & 0 & \cdots & 0 \\ 1 & -2 & 1 & \cdots & 0 \\ 0 & 1 & -2 & \cdots & 0 \\ \vdots & \ddots & \ddots & \ddots & \vdots \\ 0 & \cdots & 0 & 1 & -2 \end{pmatrix}\mathbf{y} = \mathbf{A}\mathbf{y}.$$

The matrix $\mathbf{A}$ is a Jacobian matrix with eigenvalues between $(\Delta x)^2$ and 0. This makes the ODE to be very stiff when the spatial mesh Δx becomes small [55]. When a problem or equation cannot be solve by using a explicit method, then it is called stiff. Therefore, to obtain an accurate solution of the above stiff ODEs we can use numerical method called ETI or exponential time difference (ETD) [66].

4.2.2 Historical background of the method

The introduction of the ETI as a suitable method to solve problems or equations with stiffness as been made back in the 1960's [80]. An historical overview made by [66] details the origin of this class of methods for efficiently solving large stiff problems. The references of the historical makers of this method will not be given since one can found all these references quoted in [66]. In its summary [66] mentions that the origin of the ETI method is found in the work of Hersch [57]. Hersch proved that, generally the numerical solution of differential equations never produce an exact solution even when we use an analytical approach of simple elementary methods. Then Certaine [21] used the variation of constants formula and the algebraical approximation of the non-linearity to develop the first multi-step ETD. The approach then became the beginning of a class of ETI which evaluate exactly the corresponding exponential by using the Jacobian approximation. The explicit exponential Adams methods was then developed through the same idea by Nørsett [90]. Through out the 60'S, 70'S and 90's the implementation and the development of the method was improved by other researchers such as Lawson [79], Edwards et al. [40], Hochbruck, Lubich, and Selhofer [60], Munthe-Kaas [87] and Krogstad [75].

Currently, to accurately solve large stiff problems, the use of methods such as ETI has been actively considered. But its application had been regarded to be computationally unattractive when the methods emerged. The non attraction was due to the fact that the method produced exponential functions with large matrices which could not be solved without an advanced computational programs. It was then considered to be a highly

costly method [80]. By using the Krylov projection techniques to accurately solve the exponential matrices in their works, [94] and [126] gave other researchers a way to development a number of ETI for general stiff systems. However, this did not make the method to be widely used. ETI still remain to be improved when its application is used for large scale problems compare to the Newton-Krylov implicit integrators [80].

4.2.3 Construction of the exponential time integrators

The simple definition of ETI is given by [66] as, *a method to solve differential equation which calculates the exponential or related function of the Jacobian.* For a general view of an exponential integrator, we take a look on the derivation of the exponential Euler method.
Let consider equation of the form

$$u^{'}(t) = F(t, u(t)), \quad u(0) = u_0. \tag{4.10}$$

Using the linearisation of (4.10) at time t by $J = -DF(t, u(t))$ as the Jacobian of F, with respect to u at t, and setting $k(t, u(t)) = F(t, u(t)) + Ju(t)$ as the remainder, we obtain the following semi-linear problem

$$u^{'}(t) + Ju(t) = k(t, u(t)), \quad u(0) = u_0. \tag{4.11}$$

The linear equation, $u^{'}(t) + Ju(t) = 0$, can be solved explicitly by

$$u(t) = e^{-tJ}u_0,$$

and applying the variation of constant formula, leads to the solution at time t represented by

$$u(t) = e^{-tJ}u_0 + \int_0^t e^{-(t-\theta)J}k(\theta, u(\theta))d\theta. \tag{4.12}$$

For simplicity, we approximate the non-linear function k over the interval $[0, t]$, by its value at the point $(0, u_0)$. Then we solve the rest of the integral explicitly by using the ETD or the exponential propagation iterative (EPI) methods.

4.2.4 Approach used to solve the exponential integral

For more clarity and generality, we can add the term cu to the right of equation (4.10), and multiply it through out by the integrating factor e^{-ct}, with c been a constant. We then integrate the equation over a single time step from $t = t_n$ to $t = t_{n+1} = t_n + h$ and obtain

$$u(t_{n+1}) = u(t_n)e^{ch} + e^{ch}\int_0^h e^{-c\tau}F(u(t_n+\tau), t_n+\tau)d\tau. \tag{4.13}$$

Therefore, to solve the integral in (4.13) we use the multi-steps ETD methods or ETD Runge-Kutta methods. We let $u(t_n) = u_n$ and $F_n = F(u_n, t_n)$. To simply approximate the integral in (4.13), we consider F as a constant, $F = F_n + O(h)$, between $t = t_n$ and $t = t_{n+1}$ to obtain the ETD1

$$u_{n+1} = u_n e^{ch} + \frac{F_n(e^{ch} - 1)}{c}, \tag{4.14}$$

with a local truncation error $h^2\dot{F}/2$. The application of (4.14) is mainly done in the field of computational electrodynamics [32]. In numerical analysis field, we assume that F is constant over $t_n \leq t \leq t_{n+1}$ and use the higher approximation

$$F = F_n + \frac{\tau(F_n - F_{n-1})}{h + O(h^2)}, \tag{4.15}$$

to obtain the numerical ETD2

$$u_{n+1} = u_n e^{ch} + \frac{F_n((1+hc)e^{ch} - 1 - 2hc)}{hc^2} + \frac{F_{n-1}(-e^{ch} + 1 + hc)}{hc^2}, \tag{4.16}$$

with a local truncation $5h^3\ddot{F}/12$. When $c \to 0$, (4.16) becomes the second-order Adams-Bashforth methods and when $|c|$ is large we obtain the first two terms of the basis of the non-linear Galerkin methods. For more comprehension on the practical and arbitrary order application of (4.16) one can refer to Section 2 in [32]. Solving the integral by using the multi-steps ETD can be inconvenient due to the availability of only one variable at initial condition. Since the exponential time differencing method of Runge-Kutta (ETDRK) has a smaller error constant and it is more stable than the multi-step methods, it can be used to avoid the problem faced in the use of multi-step methods. In this thesis, we will only give the second, third and forth order expressions of the ETDRK. One can consult [32] and the cited references for more details.

We first consider ETD1 as

$$a_n = u_n e^{ch} + \frac{F_n(e^{ch} - 1)}{c}.$$

Then the approximation

$$F = F(u_n, t_n) + (t - t_n)(F(a_n, t_n + h) - F(u_n, t_n))/h + O(h^2),$$

is used on the interval $t_n \leq t \leq t_{n+1}$ and substituted into (4.13) to obtain the second order of ETDRK (ETDRK2)

$$u_{n+1} = a_n + \frac{(F(a_n, t_n + h) - F_n)(e^{ch} - 1 - hc)}{hc^2}, \tag{4.17}$$

with a truncation error per step of $-h^3\ddot{F}/12$. This truncation error is smaller by a factor of 5 than that of ETD2. To obtain the third order ETDRK scheme, we use the same procedure that produced (4.17) [65]. Hence, ETDRK3 is given by

$$a_n = u_n e^{ch/2} + \frac{(e^{ch/2} - 1)F(u_n, t_n)}{c},$$

$$b_n = u_n e^{ch} + \frac{(e^{ch}-1)(2F(a_n, t_n + h/2) - F(u_n, t_n))}{c},$$

$$u_{n+1} = u_n e^{ch} + \frac{\epsilon_1 + \epsilon_2 + \epsilon_3}{h^2 c^3}, \tag{4.18}$$

with

$$\epsilon_1 = F(u_n, t_n)(-4 - hc + e^{ch}(4 - 3hc + h^2c^2)),$$

$$\epsilon_2 = 4F(a_n, t_n + h/2)(2 + hc + e^{ch}(-2 + hc)),$$

and

$$\epsilon_3 = F(b_n, t_n + h)(-4 - 3hc - h^2c^2 + e^{ch}(4 - hc)).$$

The values of u are approximated by a_n and b_n at respectively, $t_n + h/2$ and $t_n + h$. The equation (4.18) represents the quadrature formula of (4.13) derived using the points t_n, $t_n + h/2$ and $t_n + h$ from the quadratic interpolation [32]. Once again, we obtain fourth-order of ETDRK (ETDRK4) from the standard fourth order Runge-Kutta [65] by adding and changing some parameters. The process leads to the following expressions

$$a_n = u_n e^{ch/2} + \frac{(e^{ch/2}-1)F(u_n, t_n)}{c},$$

$$b_n = u_n e^{ch/2} + \frac{(e^{ch/2}-1)F(a_n, t_n + h/2)}{c},$$

$$d_n = a_n e^{ch/2} + \frac{(e^{ch/2}-1)(2F(b_n, t_n + h/2) - F(u_n, t_n))}{c},$$

and

$$u_{n+1} = u_n e^{ch} + \frac{v_1 + v_2 + v_3}{h^2 c^3}, \tag{4.19}$$

with

$$v_1 = F(u_n, t_n)(-4 - hc + e^{ch}(4 - 3hc + h^2c^2)),$$

$$v_2 = 2(F(a_n, t_n + h/2) + F(b_n, t_n + h/2))(2 + hc + e^{ch}(-2 + hc)),$$

$$v_3 = F(d_n, t_n + h)(-4 - 3hc - h^2c^2 + e^{ch}(4 - hc)).$$

All the steps used above are not the only way to solve the exponential integral. Hence we propose in the next Section an alternative method to complete the computation of such integral.

4.2.5 Alternative method to solve the exponential integral

A good choice of a time integrating scheme leads to a better resolution of stiff systems of non-linear differential equations. Then, the choice of the right methods, explicit or implicit, to solve stiff ODEs is sometimes challenging. Generally the implicit scheme is viewed as the better tool to use when solving (4.10) [32]. Cox gives a summary about the scheme on its Section 2.4, and reveals that the method has better stability properties than the explicit scheme. The disadvantage is that the method takes larger time steps which leads to more computation at each time iteration. Meanwhile, explicit schemes takes lower amount of computation per time step which is a limitation to the requirements of stability [122].

For efficient computation of stiff system over long time intervals, Tokman introduces a new class of exponential propagation techniques called EPI. In this dissertation, a summary of the scheme is given and one can consult [122] for more comprehension.

Tokman uses (4.10) and the same single time step used above this Section to construct the EPI. He found the integral form of the solution to (4.10) to be

$$u(t_n + h_n) = u_n + (e^{B_n h_n} - I)B_n^{-1} F_n + \int_{t_n}^{t_n+h_n} e^{B_n(t_n+h_n-t)} R(u(t))dt, \qquad (4.20)$$

where

$u_n \quad = \quad u(t_n) \in \mathbb{R}^N$ is the solution of (4.10) at t_n,

$F_n = F(u_n) \in \mathbb{R}^N$ is the right-hand side of (4.10) computed at t_n,
$B_n = \frac{DF(u_n)}{Du} \in \mathbb{R}^{N\times N}$ and $R(u(t)) = F(u(t)) - F_n - B_n(u(t)) - u_n \in \mathbb{R}^N$ is the non-linear remainder resulting from the expansion of $F(u)$ around u_n. The two last terms of (4.20) are computed by using a multiplication of large $N \times N$ matrix and a vector in $\mathbb{R}^N$. Tokman addresses the issue of this product in its Section 3.1 by using the Krylov subspace projections.

The construction of a time integrator is conditioned by the appropriate choice of a quadrature in order to evaluate the integral in (4.20). We either decide to use the polynomial approximation to the function $R(u(t))$ or the all integrand $e^{B_n(t_n+h_n-t)}R(u(t))$ [80, 122]. Choosing the first option leads to the construction of a multi-step type or Runge-Kutta-type scheme where the use of Krylov projection is required to approximate

$$g_k(B_n h_n)\nabla^k R(u(t_n)) = (-1)^k \int_0^1 e^{B_n h_n(1-s)} \binom{-s}{k} ds \nabla^k R(u(t)),$$

or

$$\phi_k(B_n h_n)\delta^k R(u(t)) = \int_0^1 e^{B_n h_n(1-s)} \binom{\gamma s}{k} ds \Delta^k R(u(t)),$$

with $k = 1, 2, ..., \gamma$ and γ representing the number of nodes used for the interpolation of the polynomial. The variable t has been replaced by s such that $t = t_n + sh_n$, and $\binom{s}{k} = s(s-1)....(s-k+1)/k!$ being the binomial coefficient. The Newton backward-and-forward-difference operators are respectively represented by ∇^k and Δ^k. Taking the second option, which has a low convergence rate than the first choice, leads to the application of Arnoldi iteration (see Section 3.1 of [122]) to estimate the all integrand term in (4.20). For better convergence, we will focus on the multi-step and Runge-Kutta-type schemes.

Multi-step type exponential propagation methods are constructed by using quadrature on equally spaced nodes to solve the integral in (4.20). The

process is to first discretize the time interval $t_i = t_0 + ih$, then over each interval $[t_n, t_n + h]$ we estimate $R(u(t))$ by using an interpolating polynomial with nodes γ and $t_n, t_{n-1}...., t_n - (\gamma - 1)$. If $t = t_n + sh, 0 < s < 1, R_i = R(u(t_i))$ and ∇^k is the kth Newton backwards difference operator, the integral in (4.20) can be estimated as

$$\begin{aligned}\int_{t_n}^{t_n+h_n} e^{B_n(t_n+h_n-t)}R(u(t))dt &\approx h\int_0^1 e^{B_nh(1-s)}\left(\sum_{k=0}^{\gamma-1}(-1)^k\binom{-s}{k}\nabla^k R_n\right)ds \\ &= h\sum_{k=0}^{\gamma-1}(-1)^k\left(\int_0^1 e^{B_nh(1-s)}\binom{-s}{k}\right)ds\nabla^k R_n.\end{aligned}$$

To obtain the multi-step type exponential propagation scheme of order $\mathbf{O}(h^\gamma)$, we must have

$$u(t_n + h_n) = u_n + (e^{B_nh_n} - I)B_n^{-1}F_n + \Theta, \tag{4.21}$$

where

$$\Theta = h\sum_{k=0}^{\gamma-1}(-1)^k\left(\int_0^1 e^{B_nh(1-s)}\binom{-s}{k}\right)ds\nabla^k R_n,$$

or

$$u(t_n + h_n) = u_n + (e^{B_nh_n} - I)B_n^{-1}F_n + h\sum_{k=0}^{\gamma-1}(-1)^k g_k(B_nh)\nabla^k R_n, \tag{4.22}$$

with

$$g_k(z) = \int_0^1 e^{z(1-s)}\binom{-s}{k}ds.$$

This scheme is very expensive when comes to the design of an adaptive method but has a simple derivation. The high cost of the implementation of an adaptive method is due to the fact that the solutions at previous time iterations must be re-computed when we change the time step size h. The cheaper way to obtain an adaptive time step method is to use the Runge-Kutta-type schemes [80, 122].

Following the above procedure, we start with the approximation of $R(u(t))$ in order to construct the Runge-Kutta EPI methods. This is done by using the interval $[t_n, t_n+h]$ and an interpolating polynomial defined on γ which has an equal spaced nodes $t_n, t_n+\frac{h}{\gamma}, t_n+\frac{2h}{\gamma}, ..., t_n+\frac{(\gamma-1)h}{\gamma}$. The process results to

$$\begin{aligned} R(u(t)) &= R(u(t_n+sh)) \approx R_n + \sum_{k=0}^{\gamma-1} \frac{(t-t_n)...(t-t_{n+\frac{k-1}{\gamma}})}{k!(\frac{h}{\gamma})^k} \Delta^k R_n, \\ &= R_n + \sum_{k=0}^{\gamma-1} \left(\frac{\gamma s}{k}\right) \Delta^k R_n, \end{aligned}$$

where $0 \leq s \leq 1$ and $R_n = R(u(t_n))$. When we combine this formula with Equation (4.20), we obtain

$$u(t_n+h) = u_n + h\frac{e^{B_n h} - I}{B_n h} F_n + h \sum_{k=0}^{\gamma-1} \left(\int_0^1 e^{B_n h(1-s)} \left(\frac{\gamma s}{k}\right) ds \right) \Delta^k R_n. \tag{4.23}$$

Equation (4.23) represents the general expression of Runge-Kutta EPI (RKEPI) methods. When we consider

$$g_{\gamma k}(z) = \int_0^1 e^{z(1-s)} \left(\frac{\gamma s}{k}\right) ds,$$

we can derive a two-stage RKEPI scheme as

$$r_1 = u_n + a_{11} g_{\gamma 0}\left(B_n \frac{h}{\gamma}\right) \frac{h}{\gamma} F_n, \tag{4.24}$$

$$u_{n+1} = u_n + g_{\gamma 0}(B_n h) h F_n + b_1 g_{\gamma 1}(B_n h) h R(r_1). \tag{4.25}$$

The same procedure is done to obtain the general formula of the third and fourth order RKEPI methods. The formulation is expressed as

$$r_1 = u_n + a_{11} g_{\gamma 0}\left(B_n \frac{h}{\gamma}\right) \frac{h}{\gamma} F_n, \tag{4.26}$$

$$r_2 = u_n + a_{21} g_{\gamma 0}\left(B_n \frac{2h}{\gamma}\right)\frac{2h}{\gamma} F_n + a_{22} g_{\gamma 1}\left(B_n \frac{2h}{\gamma}\right)\frac{2h}{\gamma} R_{r_1}, \tag{4.27}$$

$$\begin{cases} u_{n+1} &= u_n + g_{\gamma 0}(B_n h)hF_n + b_1 g_{\gamma 1}(B_n h)hR(r_1) \\ &+ b_2 g_{\gamma 2}(B_n h)h(-2R(r_1) + R(r_2)), \end{cases} \tag{4.28}$$

with $R_n = R(u_n) = 0$. More details are given by [80, 122] on how to obtain individual formulas of RKEPI order 3, 4 and more.

4.2.6 General solution of ETD

After applying various methods to compute the integral in (4.12), the exponential Euler method (4.12) is transformed to

$$u_1 = e^{-hJ}u_0 + h\phi_1(-hJ)k(0, u_0), \tag{4.29}$$

where $\phi_1(z) = \frac{e^z - 1}{z}$ is an analytic function. Its evaluation is a very important step when we use the EDT. The function is generally express as

$$\phi_\ell(z) = \frac{1}{(\ell - 1)!}\int_0^1 e^{(1-\theta)z}\theta^{\ell-1}d\theta, \quad \ell = 1, 2, ...$$

One can represents some values of this function when $\ell = 1, 2, 3$ and $z > 0$. These are

$$\phi_1(z) = \frac{e^z - 1}{z},$$
$$\phi_2(z) = \frac{e^z - z - 1}{z^2},$$
$$\phi_2(z) = \frac{e^z - z^2/2 - z - 1}{z^3}.$$

When $\phi_0(z) = e^z$, the function obey the recurrence

$$\phi_{\ell+1}(z) = \frac{\phi_\ell(z) - \frac{1}{\ell!}}{z}, \quad \ell = 0, 1, ...,$$

and when $z = 0$, the function is

$$\phi_\ell(0) = \frac{1}{\ell!}.$$

We can encounter some numericals issues when we evaluate this function. To overcome these difficulties, some possible approaches are made available. For small z, we use Taylor series and direct formula for non-small z [32]. Other approaches are the use of Krylov subspace approximation [60] and the contour integral method which works well for a suitable chosen radius of contour [67].

The idea behind exponential integrators is to split the differential equation into two part. One part must be linear, which can be computed exactly, and the second part must be non-linear, which need to be computed numerically. The computation of the non-linear part follows the same approach used above to obtain the implicit exponential Euler method or implicit ETD method. This will be represented by

$$u_1 = e^{-hJ}u_0 + h\phi_1(-hJ)k(t_1, u_1). \tag{4.30}$$

To compute these methods, we have to calculate the exponential or a related function of an operator or matrix together with the computation of a vector [66, 122].

4.3 Calibration of exponential Lévy models

4.3.1 An overview of calibration in finance

According to the general definition, calibration is the process of determining the relationship between the readings obtained by a measuring instrument or system and the applicable units of some defined system of measurement. The method have been applied for the last 5,000 years, according to the records uncovered by archaeologists [136]. The method is used in finance by tuning the parameters of a financial model to fit market data. The parameters of financial models describe the state of the economy or relate to the financial quantities. They can for example be associated to the volatility of a given market or reveal the state of the interest rate at a certain period of financial transactions. All fitting are not absolutely accurate. We may have for instance to perfectly fit the prices of bonds and end up with the volatility of the parameter in the formula being much greater than what it was supposed to be [3]. To avoid such abnormality, [3] developed an approach by using consistency hints in order to obtain plausible results. The technique is a valuable tool for complex models which have more parameters that can be used in the fit. Although fitting market data is the main propose of calibration in finance, it can also be used to help a specific application, such as relative-value trading, to predict the level of the current market value [3].

4.3.2 An example of calibration in a Lévy model

The example of calibration that can illustrate our study will be the one of exponential Lévy models. The process has been used in recent years to price and hedge options [116]. Let assume that the price of a stock has an initial value $S_0 > 0$ and a known interest rate $r \geq 0$. Therefore, the price of this stock will be represented by

$$S_t = S_0 e^{rt+X_t}, \quad t \geq 0, \tag{4.31}$$

where $(X_t)_{t\geq 0}$ is a Lévy process of characteristic triplet (σ^2, ν, γ). From (4.31), the jumps price process and the appropriate modelled returns represented by heavy tails will be taken into account. Its application in derivative pricing, for example, can be done by using the Lévy triplet (σ^2, ν, γ) under the risk neutral measure from the available data [116]. By using the characteristics estimation of the available data, we are applying the method called calibration. Usually, to obtain an accurate calibration, we encounter two types of errors, the deviation from and within the model. These errors can be corrected respectively by using the non-parametric models and assessing the means of confidence intervals.

The following example illustrates what we can encounter by using a Lévy model.

We consider the call option prices for Russell 2000 index (RUT) on 04/03/2008 as listed from the market watch website (www.marketwatch.com). The call option prices has 140 day to maturity. We then apply one of the popular Lévy model used in financial mathematics to calibrate the call options of RUT. Figure 4.3.1 represents the market and model prices for all strikes and maturities. The figure is obtain by using the Matlab codes in Appendix (Calibration of call option and the CGMY model prices). We

observe that the model does not fit completely the market prices. It is difficult to say if a model works better than other. One can test it by using other Lévy models and compare their fittings on the market prices. In general, we can have a model which works better on a dataset and worse on another. The next subsections explain how to avoid errors when we apply calibration by using Lévy models.

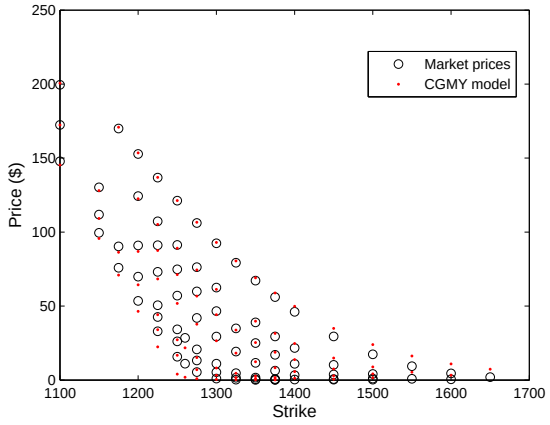

Figure 4.3.1: RUT call option and CGMY model prices on 04/03/2008 with $C = 0.026, G = 0.0765, M = 7.55, Y = 1.3$.

4.3.3 Given problem and theoretical solutions

An example of calibration in exponential Lévy models will be to consider the following problem proposed by [29].

Given prices of call options $C_0^*(T_i, K_i), i \in I$ at $t = 0$, construct a Lévy process X such that the discounted asset price $(S_t e^{-rt}) = \exp X_t$ is a martingale and the call option prices $C_0^*(T_i, K_i)$ observed at $t = 0$ are given by their

discounted risk neutral expectations:

$$C_0^*(T_i, K_i) = e^{(-rT_i)}\mathbf{E}[(S(T_i) - K_i)^+|S_0] = e^{(-rT)}\chi, \quad \forall i \in I, \tag{4.32}$$

and $\chi = \mathbf{E}[(S_0 \exp(rT_i + X_{T_i}) - K_i)^+]$.

Under the risk neutral probability $\mathbb{Q}$*, the price of an option is determine as a discounted expectation of its terminal payoff. Hence, the value of call option, by stationary and independence of increments of* X_t*, can be computed as :*

$$C(t, S; T = t + \tau, K) = e^{(-r\tau)}\mathbf{E}[(S_T - K)^+|S_t = S]$$

$$e^{(-r\tau)}\mathbf{E}[(Se^{r\tau + X_\tau} - K)^+] = Ke^{-r\tau}\mathbf{E}(e^{x + X_\tau} - 1)^+.$$

Taking the log forward moneyless variable

$$x = \ln\left(\frac{S}{K}\right) + r\tau,$$

the option price can be express through $g(\tau, x) = e^{r\tau}C(t, S; T = t + \tau, K)/K$*, and be simply in the form:*

$$g(\tau, x) = \mathbf{E}[(e^{x + X_\tau} - 1)^+] = \int \rho(t, dy)(e^{x+y} - 1)^+. \tag{4.33}$$

The variation of the call option prices will only depends on the initial level of the underlying and the Lévy triplet $(\sigma, \nu, \gamma(\sigma, \nu))$.

The aim of the calibration will be to identify the Lévy measure ν and the volatility σ from the available data of call option prices. The process requires that one must know the call option prices for one maturity and all the strikes price. Then, the volatility and the Lévy measure can be determine by following these steps:

1. Use the Breeden-Litzenberg formula, $q_T(\kappa) = e^{-\kappa}\{C''(\kappa) - C'(\kappa)\}$ and $\kappa = \ln K$ being the log strike, to compute the risk-neutral distribution of the log price in option prices.

2. Take the Fourier transform of q_T to determine the characteristic function (4.2) of the stock price.

3. Conclude by finding ν and σ from the characteristic function. The operation is easy to compute when we use the compound Poisson case. The reason behind is the fact that the bounded third term in the exponent of (4.2). This applies that:

$$\sigma = \lim_{g\to\infty} -\frac{2\ln\phi_T(g)}{Tg^2}, \quad \gamma = \lim_{g\to\infty} \frac{\frac{1}{T}\ln\phi_T(g) + \frac{1}{2}\sigma^2 g^2}{g}.$$

Therefore, the Lévy measure ν will be determine by Fourier inversion.

The precise knowledge of a call option prices for all strikes prices and a single maturity, allows one to determine all parameters in the exponential Lévy model and option prices of other maturities. This implies that, no further information on other maturities can be given by their data but only a contradiction on the previous maturity. Hence, the above enumerated process cannot have an application in practice. To justify the non application of the enumerated process in a practical problem, [29] and reference within give three reasons. One, call prices can have an infinite number of strike prices, which make the first and third enumerated point being extrapolated and the data interpolation being under-determined. Secondly, knowing the option prices for all strikes and maturities does not guarantee that the data generating process will be within the exponential Lévy class. Hence the proposed problem will not have a solution due to its equality constraints. Lastly, the presence of observational errors in the market data will make the derivatives in the first enumerated point to generate more errors which will make the computation more difficult.

In a view of all these reasons, the above given problem must be converted to an approximation problem.

4.3.4 Application of calibration to practical problem

To avoid errors observed in the given theoretical problem when we apply calibration using Lévy models. Research has been done to obtain accurate practical solution. This resulted to the work done in [10] and [4], for example, where they used minimization of the in-sample quadratic pricing error. The process is generally known as the non-linear least squares application. It is express as:

$$(\sigma, \nu) = \arg\inf_{\sigma,\nu} \sum_{i=1}^{N} \omega_i |C^{\sigma,\nu}(t=0, S_0, T_i, K_i) - C_0^*(T_i, K_i)|^2, \tag{4.34}$$

where $C_0^*(T_i, K_i)$ represents the call option price at $t = 0$. To obtain an optimal numerical solution of (4.34), the application of a gradient-based method is frequently used [4, 10]. Differently to (4.32), (4.34) can produce some solution since the minimization functional is non-convex. The location by a gradient descent of minimum may not be possible. This is due to the finite number of calibration constraints which is represented by the option prices. Hence the reproduction of call prices in equal precision may be obtain from many Lévy triplets. This will make the error landscape to have flat regions which produce the low sensitivity of the error on the model parameters variation. In conclusion, the numerical starting point of the minimization algorithm and the input prices are very sensitive to the calibrated Lévy measure [29]. To have more details on the mention sensitivity of the calibrated Lévy measure, one can refer to the examples made by [29] in his Subsection 3.1. A regulation method was introduced

by [42] to alleviate the sensitivity problem which affect the uniqueness and stability of the solution. The method uses a penalization term to obtain a unique and stable solution. It is express by the following equation:

$$(\sigma^*, \nu^*) = \arg\inf_{\sigma,\nu} \sum_{i=1}^{N} \omega_i |C^{\sigma,\nu}(t=0, S_0, T_i, K_i) - C_0^*(T_i, K_i)|^2 + B, \qquad (4.35)$$

where $B = \alpha F(\sigma, \nu)$. The term F is the measure of closeness of the model $\mathbb{Q}$ to a prior model $\mathbb{Q}_0$. It must be correctly chosen to make (4.35) well-posed [29].

The next Section is an application of the mentioned methods (spectral and ETD method) and model (Lévy model). We resume the application by presenting three different ways to approximate the spatial domain in the representation of discontinuous functions with polynomials:

1. a direct collocation method represented at the Chebyshev quadrature points;
2. a grid stretching (mesh refinement) in the neighbourhood of the discontinuities and;
3. a spatial discretization into elements placing the discontinuities at the edge of the elements of the domain.

Then we solve the PDE used to price vanilla option strategies for three different payoff functions; a European call option, a bull spread option and the butterfly strategy. In order to solve the PDE, a domain decomposition is used to discretize in space, and transform the original problem to an ODE. Finally we use a Krylov projection algorithm to numerically approximate the analytical solution of the ODE.

Chapter 5

Alleviating Gibbs phenomenon in pricing options under the spectral methods

In this chapter, we review some SCM convergence remedies including grid stretching (SCGSM), discontinuity inclusion (SCDIM) and SCDDM methods in pricing options. We first perform barycentric interpolations on European vanilla, bull spread and butterfly option payoffs, solve numerically the BS PDE with the proposed workarounds of barycentric spectral methods and then perform numerical comparisons. Spectral methods have been actively developed in the last decades. The main advantage of these methods is to yield exponential order accuracy when the function is smooth. However, for discontinuous functions, their accuracy deteriorates due to the Gibbs phenomenon. The main purpose of this Section is to show that high order accuracy can be recovered from spectral approxi-

mation contaminated with the Gibbs phenomenon if proper workarounds are applied.

5.1 Problem descriptions and applications

Let consider the BS PDE in Chapter 1, Section 1.3 such as,

$$\frac{1}{2}\sigma^2 S^2(t)\frac{\partial^2 V}{\partial S^2} + rS(t)\frac{\partial V}{\partial S} + \frac{\partial V}{\partial t} - rV = 0, \tag{5.1}$$

where V represents the call or put option price, with certain final payoff at maturity and (5.1) is valid if $S > 0$, $0 \leq t \leq T$. The general boundary values condition of (5.1) are

$$\begin{cases} V(S,0) &= V_0, \\ V(0,t) &= f(t) \text{ for all } t \geq 0, \\ V(S,t) &= g(t). \ S \to \infty, \end{cases} \tag{5.2}$$

where $f(t) = 0$ for a call, $f(t) = Ke^{-rt}$ for a put and $g(t) = S$ for both a call and put. The initial and boundary condition determine the type of financial option in consideration. The payoff function of a European call options has one discontinuity in the first derivative and is given by

$$f(S) = \max(S - K, 0), \tag{5.3}$$

where S is the stock price and K is the strike price.

A bull spread is a neutral strategy that is a combination of two call options. There are two strike prices (two discontinuities in the first derivative of the payoff) involved in the payoff function of a bull spread

option. The payoff function of a bull spread call option is given by

$$g(S) = \max(S - K_1, 0) - \max(S - K_2, 0), \quad K_1 < K_2. \tag{5.4}$$

where S is the stock price and K_1 and K_2 are strike prices.

A butterfly spread is a neutral strategy that has a combination of a bull spread and a bear spread. It is a limited profit, limited risk options strategy. There are three strike prices (three discontinuities) involved in a butterfly spread and it can be constructed using calls or puts. The payoff function of butterfly spread call options is expressed as

$$\begin{cases} h(S) &= \max(S - K_1, 0) - 2\max(S - K_2, 0) + \max(S - K_3, 0), \\ K_2 &= (K_1 + K_3)/2, \end{cases} \tag{5.5}$$

where S is the stock price K_1, K_2 and K_3 are three distinct strike prices such that $0 < K_1 < K_2 < K_3$. Figure 5.1.1 shows the payoffs of European call, bull spread call and butterfly spread options. For all tests that will be performed in this section, the parameters are chosen such that, $K = 50$ for the European call, $K_1 = 40$, $K_2 = 60$ for a bull spread call, and $K_1 = 30$, $K_2 = 50$, $K_3 = 70$ for a butterfly call options.

5.2 Numerical interpolations and applications

In practice, we are often confronted with situations where only limited amount of data is accessible and it is necessary to estimate values between two consecutive given data points. We can construct new points between known data points by interpolation or smoothing techniques. In finance, as only a finite set of securities are traded in financial markets, it is very

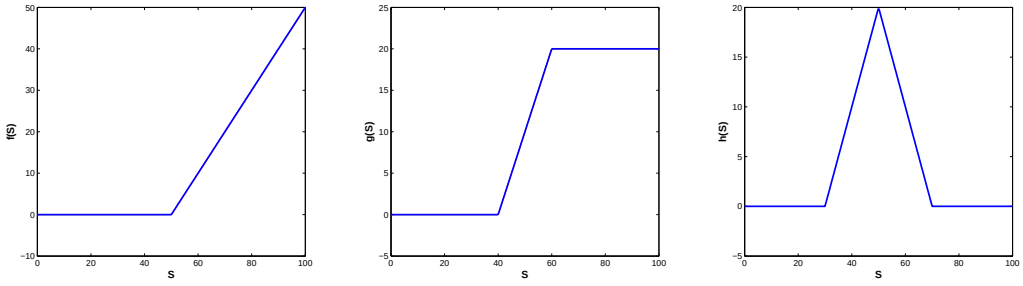

(a) European call option (b) Bull spread call option (c) Butterfly call option

Figure 5.1.1: Payoff of an European call, bull spread call, and a butterfly call options. Left: $K = 50$. Middle: $K_1 = 40$ and $K_2 = 60$. Right: $K_1 = 30$, $K_2 = 50$ and $K_3 = 70$.

important to construct a sensible curve or surface from discrete observable quantities using interpolation methods.

In this section, we describe spectral methods used to interpolate the payoffs of European call, bull spread call and butterfly spread options. These include reviews spectral collocation, grid stretching, discontinuity inclusion and domain decomposition interpolations in barycentric form.

To show the efficiency of the present methods in comparison with the exact solution we report maximum error which is defined by

$$L_\infty = \|u - U\|_\infty = \max_{1 \leqslant i \leqslant N} |u(x_i) - U(x_i)|, \tag{5.6}$$

where u and U represent the exact and approximate solutions of a payoff with different values of N, respectively. We refer by *error* the absolute value of the difference between the exact and the numerical solution.

5.2.1 Spectral barycentric interpolation

The review done by [96] on the Lagrange interpolation and the Barycentric formula shows the importance of the discretization in space with spectral methods. At first, a polynomial $u_N(x)$ is considered to be found among the vector space of all polynomials of degree N such that $u_N(x_j) = u_j$ with $j = 0, ..., N$. The result can be written in Lagrange form as ([78])

$$u_N(x) = \sum_{j=0}^{N} u_j \gamma_j(x), \quad \gamma_j = \prod_{k=0, k\neq j}^{N} \frac{x - x_k}{x_j - x_k}, \tag{5.7}$$

with Lagrange polynomial γ_j corresponding to the node x_j having the property

$$\gamma_j(x_k) = \begin{cases} 1 & \text{when} \quad j = k, \\ 0 & \text{otherwise.} \end{cases} . \tag{5.8}$$

The disadvantages of (5.7) are

1. The evaluation of each $u_N(x)$ needs an $\mathcal{O}(N^2)$ additions and multiplications.

2. The addition of a new pair of data (x_{N+1}, u_{N+1}) leads to a completely new computation.

3. The presence of inaccurate solution in the numerical computation is certain.

It is for that reason the modifications of (5.7) is required to overcomes those disadvantages. Hence, Berrut and Trefethen [12] modified (5.7) such that $u_N(x)$ can be computed in $\mathcal{O}(N)$ operation. This yields the barycentric formula $u_N(x)$ as

$$u_N(x) = \frac{\sum_{j=0}^{N} \frac{\omega_j}{x - x_j} u_j}{\sum_{j=0}^{N} \frac{\omega_j}{x - x_j}}. \tag{5.9}$$

where $w_0, w_1, \ldots, w_N$ are called barycentric weights. For every set of points $\{x_k\}$, there is a unique set of barycentric weights $\{w_k\}$. In this paper we only consider the Chebyshev points $x_k = cos(\frac{k\pi}{N})$, $k = 0, 1, 2, ..., N.$, with a set of barycentric weight $w_0 = c/2$, $w_k = (-1)^k c, k = 1, \ldots, N-1$, and $w_N = (-1)^N c/2$ for some non-zero constant c [8]. More details are given in [12] to obtain (5.9).

Barycentric interpolation method is used to approximate the solutions of differential equation by a polynomial which interpolates data $u_k = u(x_k)$ at the Chebyshev points $x_k = cos(\frac{k\pi}{N})$, $k = 0, 1, 2, ..., N$. The data u_k must be determined by the polynomial interpolants that satisfy the differential equation exactly at the points x_k. Depending of the smoothness of the solution, the error will decline at different rate as N increases [121].

To represent the payoff of an European call, bull spread call and a butterfly call option in the Chebyshev interpolation form, we transformed the Chebyshev domain $[-1, 1]$ to a physical domain $[S_{min}, S_{max}]$. We use, without loss of generality, $S = \frac{1}{2}(S_{max} - S_{min})x + \frac{1}{2}(S_{max} + S_{min})$, where x is the Chebyshev point. The graphs on Figure 5.2.1 are obtained for $S_{min} = 0$, $S_{max} = 100$ and $N = 200$. The *error* between the original payoff and the approximated Chebyshev interpolated payoff of the three call options is significantly lower away from the jump discontinuities points (K, K_1, K_2, K_3) while it is very high at discontinuity points. This confirm the problem of accuracy at these discontinuity points. To solve the problem of low accuracy at those points, one can use methods such that, the grid stretching, the discontinuity inclusion or the domain decomposition methods.

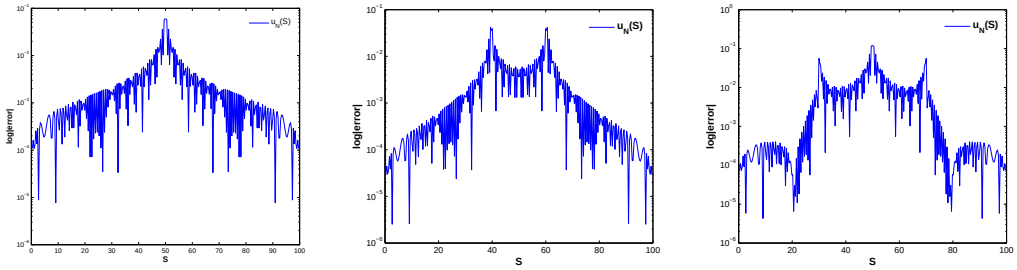

(a) European call option (b) Bull spread call option (c) Butterfly call option

Figure 5.2.1: Corresponding *error* between the numerical payoff and the Chebyshev interpolated payoff of an European call, bull spread call and a butterfly call options with $N = 200$.

5.2.2 Grid stretching

In the most common barycentric pseudo-spectral methods, the interpolation points in the interval $[-1,1]$ are the Chebyshev collocation points y_k, $k = 0,\ldots,N$. The Chebyshev points are clustered near the boundaries of $[-1,1]$. However, we need to accumulate these points in the vicinity of the region of rapid change. One way to do this is to use adaptive grids via coordinate transformations. In Pindza *et.al* [96], it is reported that to overcome the problem of discontinuity and differentiability in the payoff conditions at strike prices, the use of a grid refinement is one of the best tool to retain a satisfactory accuracy of the spectral method applied on those payoffs. The local grid refinement are known to improve the accuracy of numerical methods. In this paper, we use the conformal map g given in Pindza *et.al* [96] by

$$x = g(y) = \beta + \frac{1}{\alpha}\sinh\Big[\bar{\lambda}(y-\mu)\Big], \tag{5.10}$$

where

$$\bar{\lambda} = \frac{\gamma + \delta}{2}, \quad \mu = \frac{\gamma - \delta}{\gamma + \delta}, \tag{5.11}$$

with

$$\gamma = \sinh^{-1}[\alpha(1+\beta)], \quad \delta = \sinh^{-1}[\alpha(1-\beta)], \tag{5.12}$$

where α and β determine the location and the magnitude of the region of rapid change, respectively. The conformal map g is constructed from

$$y = g^{-1}(x) = \mu + \frac{1}{\bar{\lambda}} \sinh^{-1}[\alpha(x-\delta)]. \tag{5.13}$$

A significant advantage of the rational collocation method based on rational interpolation in barycentric form is that tedious transformations using the chain rule to approximate the derivatives of $u_N(x)$ are not required as it is usual in other spectral collocation methods.

The method shows a significant improvement of the approximation away and at the discontinuity points. From 5.2.2, the *error* between the numerical payoff and the Chebyshev interpolated payoff is represented in blue. Meanwhile, the function $\mathrm{v}_N^{\lambda,\theta}(S)$ in red represents the *error* between the numerical payoff and the interpolated payoff with the use of a grid stretching. As represented in Figure 5.2.2, the grid stretching method (SCGM) recovers the approximation very well at all levels. In all the three cases, the error obtained using the SCGM is of magnitude 10^{-14} as opposed to the error obtained using a naive spectral collocation method with order of magnitude 10^{-2}.

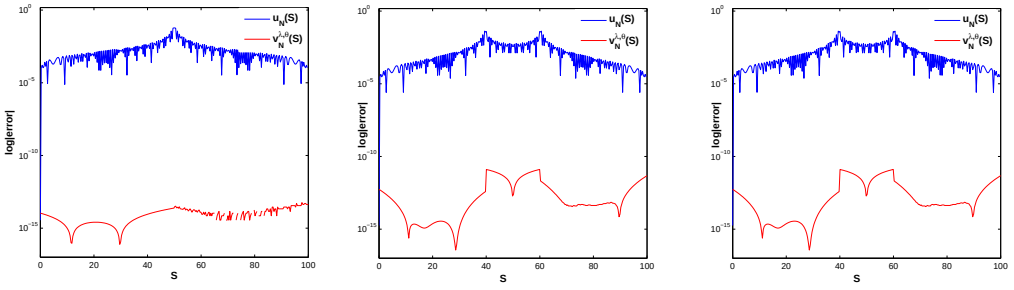

(a) European call option (b) Bull spread call option (c) Butterfly call option

Figure 5.2.2: Corresponding *error* between the original payoff and the interpolated payoff with the use of a grid stretching method with $N = 200$ and $\alpha = 10^8$.

5.2.3 Discontinuity inclusion

More often the computation of certain problems with jumps discontinuity involving piecewise analytic functions can be performed easily. Meanwhile, it is difficult to accurately approximate these functions with a single polynomial. A higher order of accuracy can be achieved by modifying the spatial discretization. One alternative is to use a spectral discretization based on discontinuity inclusion approach. Suppose the domain $\mathcal{D} = [a, b]$ is broken into M sub-domains $\mathcal{D}_1 = (x^{(0)}, x^{(1)}), \mathcal{D}_2 = (x^{(1)}, x^{(2)}), ..., \mathcal{D}_M = (x^{(M-1)}, x^{(M)})$ where $x^{(0)} = a$ and $x^{(M)} = b$. The domain $\mathcal{D}$ is covered by M sub-domains as $\mathcal{D} = \bigcup_{\mu=1}^{M} \mathcal{D}_\mu$. The collocation points $x_j^{(n)}$ on $\mathcal{D}_n$ are defined by

$$x_k^{(n)} = \begin{cases} \frac{x^{(n)} - x^{(n-1)}}{2} \cos\left(\frac{k\pi}{N}\right) + \frac{x^{(n)} + x^{(n-1)}}{2}, 0 \leqslant k \leqslant N, \ n = 1, \\ \frac{x^{(n)} - x^{(n-1)}}{2} \cos\left(\frac{k\pi}{N}\right) + \frac{x^{(n)} + x^{(n-1)}}{2}, 1 \leqslant k \leqslant N, \ 2 \leqslant n \leqslant M. \end{cases} \tag{5.14}$$

The approximation of u uses the formula (5.9) where the barycentric weights $\{w_k\}$ are evaluated numerically. This strategy will cluster grid nodes not only at the boundaries located at S_{min} and S_{max} but also at the singularity which is located at the strike price for European options. Such strategy is necessary to reduce the error caused by the non-smooth kink in the payoff function of most options. Note that this methodology is different from the domain decomposition method in a sense that the continuation condition is not needed here. In addition all the matrices are full matrices, whereas in the case of the domain decomposition method the matrices are bloc diagonal matrices.

The approximation of the different call options is also improved from the discontinuity points when we use the grid stretching method, but the method does not give an absolute accuracy of the solution. From 5.2.3, the *error* between the numerical payoff and the Chebyshev interpolated payoff is represented in blue. In the other hand, the function $p_N(S)$ in red represents the *error* between the numerical payoff and the interpolated payoff with the use of the discontinuity inclusion. Figure 5.2.3 shows the superiority of this method over the use of the Chebyshev interpolation method. The method is 10^4 more accurate than the original Chebyshev method.

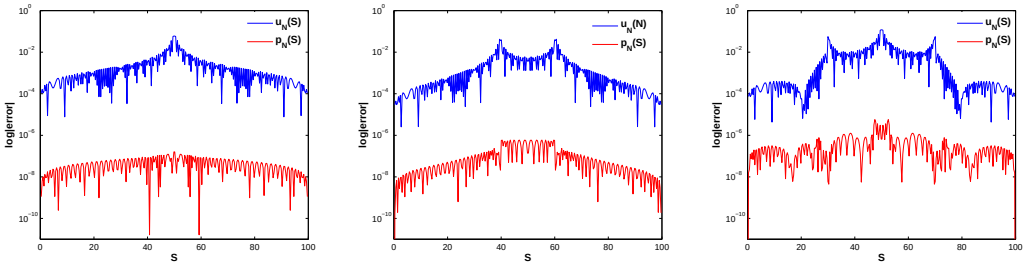

(a) European call option (b) Bull spread call option (c) Butterfly call option

Figure 5.2.3: Corresponding *error* between the original payoff and the interpolated payoff with the use of the discontinuity inclusion method with $N = 200$.

5.2.4 Interpolation with the domain decomposition

From Section 2.4, we apply the domain decomposition approach on the different call options and obtain the results shown in Figure 5.2.4. In 5.2.4, the *error* between the numerical payoff and the Chebyshev interpolated payoff is represented in blue. Meanwhile, in red we have the *error* between the numerical payoff and the interpolated payoff with the use of the domain decomposition method.

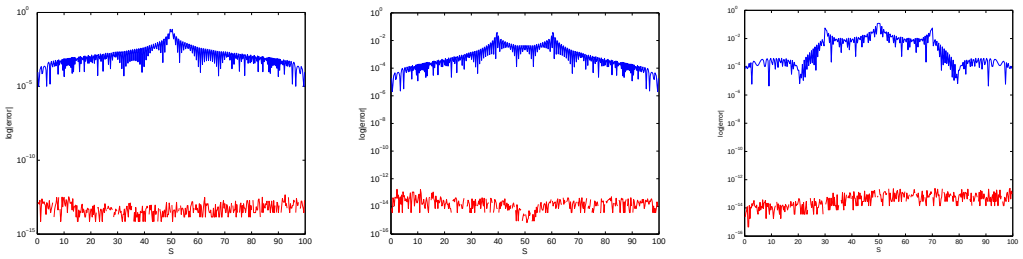

(a) European call option (b) Bull spread call option (c) Butterfly call option

Figure 5.2.4: Corresponding *error* when using the domain decomposition method on European call ($\mu = 3$, $\mathcal{D}_1 = 0, \mathcal{D}_2 = 50, \mathcal{D}_3 = 100$), bull spread call ($\mu = 4$, $\mathcal{D}_1 = 0, \mathcal{D}_2 = 40, \mathcal{D}_3 = 60, \mathcal{D}_4 = 100$), and butterfly spread call ($\mu = 5$, $\mathcal{D}_1 = 0, \mathcal{D}_2 = 30, \mathcal{D}_3 = 50, \mathcal{D}_4 = 70, \mathcal{D}_5 = 100$) options with $N = 200$.

We compare the result with the SCM and those obtained using the SCDDM. The results are shown in Figure 5.2.4. Clearly, in all the cases Figure 5.2.4 shows highly accurate results are obtained with the SCDDM while poor accuracy is recorded with SCM. It is noted that for $N = 200$, the magnitude of absolute error is 10^{-14} for SCDDM and 10^{-2} for SCM. The SCDDM allows the removal of Gibbs phenomenon and restores spectral accuracy for discontinuous problems.

We lastly investigate numerical convergence of the interpolation methods used in this section. We vary the number of grid points and recorded the maximal error. All the results are shown is Figure 5.2.5. It can be observed that SCM has very poor convergence. Other methods detain a very fast convergence as compared to the SCM. The SCDDM shows the best convergence as the number of grid points is increased.

In the next section, we use these methods to numerically solve

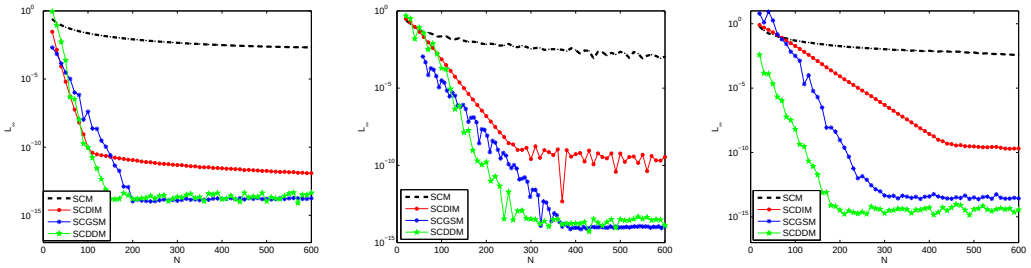

(a) European call option (b) Bull spread call option (c) Butterfly call option

Figure 5.2.5: Numerical convergence of SCM, SCDIM,SCGSM and SCDDM

the BS PDE.

5.3 Numerical discretization and application

In the next subsection, we show the space discretization of BS PDE by means of domain decomposition methods. Note that the domain decomposition method is a generalisation of other methods discussed in the above subsections. The Black-Scholes model has turned out to be very popular, but it is based on several crucial assumptions, such as no market friction, constraints on stock holdings, constant drift and volatility. Because empirical data shows that the log returns do not really behave according to a normal distribution many other models have been developed. Nonetheless, the Black-Scholes model serves as a good starting point. The availability of closed form solutions makes it easy to verify results generated with numerical pricing methods.

5.3.1 Barycentric spectral method

Suppose the domain $\mathcal{K} = [0, S_{\max}]$ of (5.1) is broken into M sub-domains $\mathcal{K}_1 = (S^{(0)}, S^{(1)}), \mathcal{K}_2 = (S^{(1)}, S^{(2)}), ..., \mathcal{K}_M = (S^{(M-1)}, S^{(M)})$ where $S^{(0)} = 0$ and $S^{(M)} = S_{\max}$. On the interval $\mathcal{K}$, the solution of (5.1) will be represented by V and on its decomposed domain $\tilde{\mathcal{K}_n} = [S^{n-1}, S^n]$ by V_n. All approximated solutions of $\mathcal{K}, \tilde{\mathcal{K}}$ will be respectively represented by V^N and V_n^N. Meanwhile, the collocation points on $\mathcal{K}_n$ are denoted by $S_j^{(n)}, 0 \leqslant j \leqslant N, 1 \leqslant n \leqslant M$, with N being a known integer. Hence we denote $S_j^{(n)}$ as $S_j^{(n)} = \frac{S^{(n)} - S^{(n-1)}}{2} \cos\left(\frac{j\pi}{N}\right) + \frac{S^{(n)} + S^{(n-1)}}{2}, 0 \leqslant j \leqslant N, 1 \leqslant n \leqslant M$.

A patching method for the (BS) equation is

$$\begin{cases} \left.\frac{\partial V_1^N}{\partial t}\right|_{S=S_j^1} + \frac{1}{2}\sigma^2 S^2 \left.\frac{\partial^2 V_1^N}{\partial S^2}\right|_{S=S_j^1} + rS \left.\frac{\partial V_1^N}{\partial S}\right|_{S=S_j^1} - rV_1^N\big|_{S=S_j^1} = 0 \\ \left.\frac{\partial V_2^N}{\partial t}\right|_{S=S_j^2} + \frac{1}{2}\sigma^2 S^2 \left.\frac{\partial^2 V_2^N}{\partial S^2}\right|_{S=S_j^2} + rS \left.\frac{\partial V_2^N}{\partial S}\right|_{S=S_j^2} - rV_2^N\big|_{S=S_j^2} = 0 \\ \vdots \\ \left.\frac{\partial V_M^N}{\partial t}\right|_{S=S_j^M} + \frac{1}{2}\sigma^2 S^2 \left.\frac{\partial^2 V_M^N}{\partial S^2}\right|_{S=S_j^M} + rS \left.\frac{\partial V_M^N}{\partial S}\right|_{S=S_j^M} - rV_M^N\big|_{S=S_j^M} = 0, \end{cases} \tag{5.15}$$

with $j = 0 : N$ and the boundary conditions

$$\begin{aligned} V_{n-1}^N\left(S^{(n-1)}, t\right) &= V_n^N\left(S^{(n-1)}, t\right), \ n = 2 : M, \\ \frac{\partial V_{n-1}^N}{\partial S}\left(S^{(n-1)}, t\right) &= \frac{\partial V_n^N}{\partial S}\left(S^{(n-1)}, t\right), \ n = 2 : M, \\ V_{n-1}^N(S^{(0)}, t) &= f(t), \\ V_{n-1}^N(S^{(M)}, t) &= g(t). \end{aligned}$$

To discretize Equation (5.15) in space, we replace $\left.\frac{\partial V_i^N}{\partial S}\right|_{S=S_j^i}$ and $\left.\frac{\partial^2 V_i^N}{\partial S^2}\right|_{S=S_j^i}$ by the following pseudo-spectral approximations

$$\left.\frac{\partial V_i^N}{\partial S}\right|_{S=S_j^i} = \frac{2}{S^{(i)} - S^{(i-1)}} \sum_{p=0}^{N} D_{jp}^{(m)} \left(V_i^N(S_p^{(i)}, t) - V_i^N(S_j^{(i)}, t)\right), \tag{5.16}$$

and

$$\left.\frac{\partial^2 V_i^N}{\partial S^2}\right|_{S=S_j^i} = \left(\frac{2}{S^{(i)}-S^{(i-1)}}\right)^2 \sum_{p=0}^{N} D_{jp}^{(m)}\left(V_i^N(S_p^{(i)},t) - V_i^N(S_j^{(i)},t)\right), \qquad (5.17)$$

with $p = 1,...,N-1$ and $D_{jp}^{(m)}$ being the entries of the differentiation matrix of order $m = 1,2$.

By setting $U_{ip}^N(t) = V_i^N(S_p^{(i)},t), U_{1N}^N(t) = f(t), U_{M0}^N(t) = g(t)$ and substituting (5.16), (5.17) into (5.15) we get

$$\begin{aligned}
&\frac{dU_{1j}^N(t)}{dt} + \mathcal{W}_1 = 0,\\
&\frac{dU_{2j}^N(t)}{dt} + \mathcal{W}_2 = 0,\\
&\qquad\vdots\\
&\frac{dU_{Mj}^N(t)}{dt} + \mathcal{W}_M = 0,
\end{aligned} \qquad (5.18)$$

where

$$\begin{aligned}
\mathcal{W}_1 &= \frac{2\sigma^2 S^2}{\left(S^{(1)}-S^{(0)}\right)^2}\sum_{p=0}^{N} D_{jp}^2\left(U_{1p}^N(t) - U_{1j}^N(t)\right)\\
&+ \frac{2rS}{\left(S^{(1)}-S^{(0)}\right)^2}\sum_{p=0}^{N} D_{jp}\left(U_{1p}^N(t) - U_{1j}^N(t)\right) - rU_{1j}^N(t),
\end{aligned}$$

$$\begin{aligned}
\mathcal{W}_2 &= \frac{2\sigma^2 S^2}{\left(S^{(2)}-S^{(1)}\right)^2}\sum_{p=0}^{N} D_{jp}^2\left(U_{2p}^N(t) - U_{2j}^N(t)\right)\\
&+ \frac{2rS}{\left(S^{(2)}-S^{(1)}\right)^2}\sum_{p=0}^{N} D_{jp}\left(U_{2p}^N(t) - U_{2j}^N(t)\right) - rU_{2j}^N(t)
\end{aligned}$$

$$\vdots$$

$$\mathcal{W}_M = 2\sigma^2 S^2\left(S^{(M)}-S^{(M-1)}\right)^{-2}\sum_{p=0}^{N} D_{jp}^2\left(U_{Mp}^N(t) - U_{Mj}^N(t)\right) + \beta,$$

$$\beta = 2rS\left(S^{(M)} - S^{(M-1)}\right)^{-2} \sum_{p=0}^{N} D_{jp}\left(U_{Mp}^{N}(t) - U_{Mj}^{N}(t)\right) - rU_{Mj}^{N}(t),$$

and

$$\begin{aligned}
U_{10}^{N}(t) &= U_{2N}^{N}(t),\\
U_{20}^{N}(t) &= U_{3N}^{N}(t),\\
&\vdots\\
U_{M-1,0}^{N}(t) &= U_{MN}^{N}(t), \qquad (5.19)\\
U_{1N}^{N}(t) = f(t), &\quad U_{M0}^{N}(t) = g(t).
\end{aligned}$$

$$\begin{aligned}
\frac{\partial V_1^N}{\partial S}\left(S_0^{(1)}, t\right) &= \frac{\partial V_2^N}{\partial S}\left(S_N^{(2)}, t\right),\\
\frac{\partial V_2^N}{\partial S}\left(S_0^{(2)}, t\right) &= \frac{\partial V_3^N}{\partial S}\left(S_N^{(3)}, t\right),\\
&\vdots\\
\frac{\partial V_{M-1}^N}{\partial S}\left(S_0^{(M-1)}, t\right) &= \frac{\partial V_M^N}{\partial S}\left(S_N^{(M)}, t\right). \qquad (5.20)
\end{aligned}$$

Equations (5.19) and (5.20) can be approximated by using (5.16) and (5.17) as

$$\begin{aligned}
\left(\frac{2}{S^{(1)} - S^{(0)}}\right)\sum_{p=0}^{N} D_{0p}^{(m)}\left(U_{1p}^{N}(t) - U_{10}^{N}(t)\right) &= \left(\frac{2}{S^{(2)} - S^{(1)}}\right)\sum_{p=0}^{N} D_{Np}^{(m)}\left(U_{2p}^{N}(t) - U_{2N}^{N}(t)\right),\\
\left(\frac{2}{S^{(2)} - S^{(2)}}\right)\sum_{p=0}^{N} D_{0p}^{(m)}\left(U_{2p}^{N}(t) - U_{20}^{N}(t)\right) &= \left(\frac{2}{S^{(3)} - S^{(2)}}\right)\sum_{p=0}^{N} D_{Np}^{(m)}\left(U_{3p}^{N}(t) - U_{3N}^{N}(t)\right),\\
&\vdots
\end{aligned}$$

$$\left(\frac{2}{S^{(M-1)} - S^{(M-2)}}\right)\sum_{p=0}^{N} D_{0p}^{(m)}\left(U_{M-1,p}^{N}(t) - U_{M-1,0}^{N}(t)\right) = K, \qquad (5.21)$$

with

$$K = \left(\frac{2}{S^{(M)} - S^{(M-1)}}\right) \sum_{p=0}^{N} D_{Np}^{(m)} \left(U_{Mp}^{N}(t) - U_{MN}^{N}(t)\right).$$

Therefore Equation (5.18) and (5.21) can be rewrite as a system of differential algebric equations (DAEs) of the form

$$\begin{cases} Y'(t) &= F(t, Y(t)), \\ Q_1(t, Y(t)) &= 0, \\ Q_2(t, Y(t)) &= 0, \\ Q_3(t, Y(t)) &= 0, \\ Y(0) &= Y_0, \end{cases} \tag{5.22}$$

with

$$Y(t) = [U_{10}^{N}(t), U_{11}^{N}(t), ..., U_{1N}^{N}(t), ..., U_{M0}^{N}(t), U_{M1}^{N}(t), ..., U_{MN}^{N}(t)]^T,$$

$$Y_0 = [V_0(S_0^1), V_0(S_1^1), ..., V_0(S_N^1), ..., V_0(S_0^M), V_0(S_1^M), ..., V_0(S_N^M)]^T,$$

$$Y'(t) = [U_{10}^{N'}(t), U_{11}^{N'}(t), ..., U_{1N}^{N'}(t), ..., U_{M0}^{N'}(t), U_{M1}^{N'}(t), ..., U_{MN}^{N'}(t)]^T,$$

$$F(t, Y(t)) = [F_{ij}(t, Y(t))]_{\{M\times(N+1)\}\times\{M\times(N+1)\}},$$

$$Q_1(t, Y(t)) = [Q_{11}(t, Y(t)), ..., Q_{1,M-1}(t, Y(t))],$$

$$Q_2(t, Y(t)) = [Q_{21}(t, Y(t)), ..., Q_{2,M-1}(t, Y(t))],$$

$$Q_3(t, Y(t)) = [Q_{31}(t, Y(t)), ..., Q_{3,2}(t, Y(t))],$$

and

$$F_{ij}(t, Y(t)) = -\Omega + rU_{ij}^{N}(t),$$

$$\Omega = \frac{2\sigma^2 S^2}{\left(S^{(i)} - S^{(i-1)}\right)^2} \sum_{p=0}^{N} D_{jp}^{2} \left(U_{ip}^{N}(t) - U_{ij}^{N}(t)\right) + \frac{2rS}{\left(S^{(1)} - S^{(0)}\right)^2} \sum_{p=0}^{N} D_{jp} \left(U_{ip}^{N}(t) - U_{ij}^{N}(t)\right),$$

$$Q_{1,i}(t, Y(t)) = [U_{i0}^{N}(t) - U_{i+1,N}^{N}(t)],$$

$$Q_{2,i}(t,Y(t)) = \sum_{p=0}^{N}(\alpha_1,-\alpha_2),$$

$$\alpha_1 = 2\left(S^{(i)}-S^{(i-1)}\right)^{-2} D_{0p}\left(U_{ip}^N(t)-U_{i0}^N(t)\right),$$

$$\alpha_2 = 2\left(S^{(i+1)}-S^{(i)}\right)^{-2} D_{Np}\left(U_{i+1,p}^N(t)-U_{i+1,N}^N(t)\right),$$

$$Q_{3,1}(t,Y(t)) = U_{0N}^N(t)-f(t),\quad Q_{3,2}(t,Y(t)) = U_{M0}^N(t)-g(t).$$

The above discretization (5.22) leads to the semi-discrete linear system

$$Y' = AY + b(t),\quad b(t) = \varepsilon_1 + \varepsilon_2 e^{-rt}, \tag{5.23}$$

where A is either a block dense diagonal matrix or a dense matrix depending on the number of domain in consideration. The parameters ε_1 and ε_2 are given by the boundary conditions.

5.3.2 Exponential time differencing schemes

Let consider Equation (5.23). Integrating the system of ODE (5.23) on the interval $[0,T]$ leads to the scheme

$$\begin{aligned} Y(T) &= e^{AT}Y(0) + e^{AT}\int_0^T e^{-At}b(t)dt, \\ &= e^{AT}Y(0) + A^{-1}\left(e^{AT}-I\right)\varepsilon_1 - (A-rI)^{-1}P, \end{aligned} \tag{5.24}$$

where $P = \left(e^{AT}-e^{-rT}I\right)\varepsilon_2$ and I is the identity matrix. Note that computation of the price of European options using (5.24) requires forming the matrix functions $f_1(A) = e^{AT}$, $f_2(A) = A^{-1}\left(e^{AT}-I\right)$ and $f_3(A) = (A-rI)^{-1}\left(e^{AT}-e^{-rT}I\right)$. In order to overcome the numerical difficulties encountered in computing matrix functions, we employ the Krylov projection algorithm [103]. The key idea behind this method, is to approximate the

product of a matrix function $\varphi(A)$ (A is a $N \times N$ matrix) and a vector v using projection of the matrix and the vector onto the Krylov subspace $K_m(A,v) = span\{v, Av, \ldots, A^{m-1}v\}$. The orthonormal basis $\{v_1, v_2, \ldots, v_m\}$ of $K_m(A,v)$ is constructed using the modified Arnoldi iteration [5, 103] which can be written in matrix form as

$$AV_m = V_m H_m + \bar{h}_{m+1,m} v_{m+1} e_m^T, \tag{5.25}$$

where $\bar{h}_{m+1,m}$ is an entry of the Hessenberg matrix H_m, $e_m = (0,\ldots,0,1,0,\ldots,0)^T$ is the unit vector with 1 as the m^{th} coordinate,
$\{v_1, v_2, \ldots, v_m, v_{m+1}\}$ is an orthonormal basis of $K_m(A,b)$, $V_m = [v_1 v_2 \ldots v_m] \in \mathbb{R}^{N\times m}$, and

$$H_m = V_m^T A V_m, \tag{5.26}$$

is an upper Hessenberg matrix calculated as a side product of the iteration. Matrix $P = V_m V_m^T$ is a projector into $K_m(A,v)$, thus $\varphi(A)v$ is approximated as a projection

$$\varphi(A)b \approx V_m V_m^T \varphi(A) V_m V_m^T b. \tag{5.27}$$

Recalling (5.26) and observing that $v_1 = v/\|v\|_2$, we make the final approximation through

$$\varphi(A)v \approx \|v\|_2 V_m \varphi(H_m) e_1. \tag{5.28}$$

The advantage of this formulation is that H_m is a $m \times m$ matrix of smaller size ($m \ll N$) and thus it is much cheaper to evaluate $\varphi(H_m)$ than $\varphi(A)$.

5.3.3 Numerical results

We apply the spectral approximation methods to value Black Scholes PDE (5.1) using the SCM, SCGSM, SCDIM and SCDDM. We use three different

payoff, European call (5.29) and bull spread (5.30) and butterfly spread (5.31) options. Hence, we have the following boundary values conditions express as, for a European call option

$$V(0,t) = 0, \text{ and } V(S_{\max},t) = S_{\max} - Ke^{-rt}, \tag{5.29}$$

for a European bull spread call option,

$$V(0,t) = 0, \text{ and } V(S_{\max},t) = S_{\max} - (K_2 - K_1)e^{-rt}, \ K_1 < K_2, \tag{5.30}$$

and for a European butterfly spread call option

$$V(0,t) = 0, \text{ and } V(S_{\max},t) = 0, \ K_1 < K_2 < K_3. \tag{5.31}$$

We solve the PDE (5.1) using the parameters $r = 0.05$, $\sigma = 0.2$, $K = 50$,

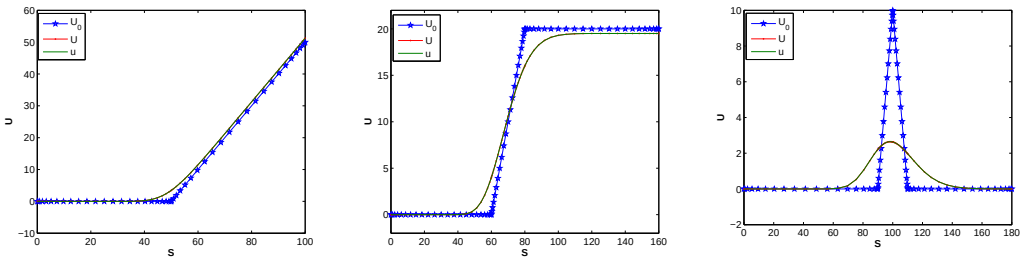

(a) European call option (b) Bull spread call option (c) Butterfly call option

Figure 5.3.1: Solutions of the analytical, numerical and domain decomposition of BS with $N = 100, r = 0.05, T = 0.5, \sigma = 0.2, S_{\max} = 200, S_{\min} = 0$ for all payoff options, $K = 50$ for a payoff of a European call, $K_1 = 30, K_2 = 70$ for a payoff of a bull spread call and $K_1 = 30, K_2 = 50, K_3 = 70$ for a payoff of a butterfly call option.

$S_{\min} = 0$, $S_{\max} = 4K$ for the European call option (5.29), $r = 0.05$, $\sigma = 0.2$, $K_1 = 60$, $K_2 = 80$ $S_{\min} = 0$, $S_{\max} = 4K_1$ for the European bull spread call option (5.30), and $r = 0.05$, $\sigma = 0.2$, $K_1 = 90$, $K_2 = (K_1 + K_3)/2$, $K_3 = 110$,

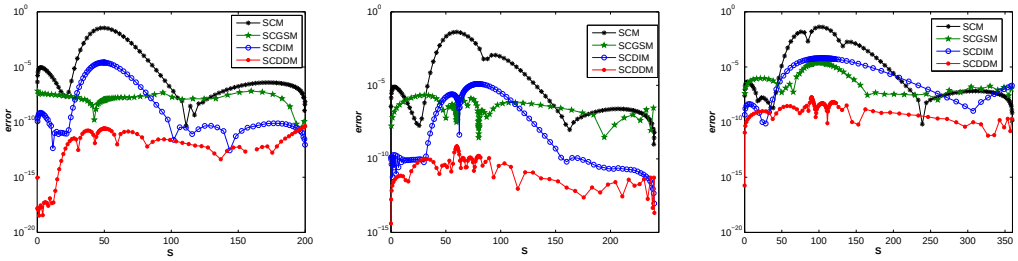

(a) European call option (b) Bull spread call option (c) Butterfly call option

Figure 5.3.2: Absolute difference error between the numerical and SCM, SCDIM, SCGSM, SCDDM solutions of the BS. $N = 150, r = 0.05, T = 0.5, \sigma = 0.2, S_{\max} = 200, S_{\min} = 0$ for all options, $K = 50$ for European call, $K_1 = 30, K_2 = 70$ for a bull spread call and $K_1 = 30, K_2 = 50, K_3 = 70$ for a butterfly call option.

$S_{\min} = 0$, $S_{\max} = 4K_1$ for the European butterfly spread call option (5.31). In all the cases, the number of grid points is chosen to be $N = 100$. We display the numerical and analytical solutions for the above mentioned payoff in Figure 5.3.1. From Figure 5.3.1, the blue line with stars represents the payoff's analytical solution of BS. The red line with dots represents the payoff's domain decomposition solution and the black line, the payoff's numerical solution of BS. Clearly, numerical solutions are in good agreement with analytical ones. However, we only show numerical results obtained with the domain decomposition method for clarity sake. Although numerical solutions are in good agreement with the analytical solutions, we would like to investigate how close these solutions are. We plot in Figure 5.3.2, the absolute difference between numerical and analytical solutions. To avoid a huge truncation error, we use $S_{\max} = 4K$ for call options and $S_{\max} = 4K_1$ for bull and butterfly spread options. For the SCGSM, an additional parameter, the grid stretching parameter, was cho-

sen such that $\beta = 10^4$. It is observed that the SCDDM has the smallest error of magnitude 10^{-11}, followed by the SCGSM with the error of magnitude 10^{-8}, the SCDIM with the error of magnitude 10^{-5} and finally SCM with the error of magnitude 10^{-2}.

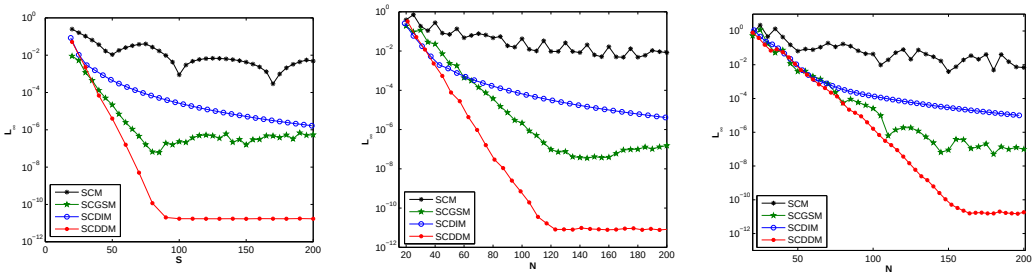

(a) European call option (b) Bull spread call option (c) Butterfly call option

Figure 5.3.3: Numerical convergence of SCM, SCDIM,SCGSM and SCDDM with $N = 150, r = 0.05, T = 0.5, \sigma = 0.2, S_{\max} = 200, S_{\min} = 0, \alpha = 10^4$ for all options, $K = 50$ for European call, $K_1 = 30, K_2 = 70$ for a bull spread call and $K_1 = 30, K_2 = 50, K_3 = 70$ for a butterfly call option.

In the last experiment, we investigate numerical convergence on these methods. We record the values of the maximal error while varying the number of grid points N. The results are shown in Figure 5.3.3. In all the cases, one can observe that SCMDD detains the best convergence compared to other methods. The convergence rate is exponential. The second best convergence is achieved by SCGSM. This convergence depends on the choice of the grid stretching parameter β. One can use this parameter adaptively in order to achieve exponential convergence [96]. The SCDIM is the third best performing method. This method only improves the convergence of spectral method without achieving exponential convergence. The SCM has a very bad convergence due Gibbs phenomenon at strike prices. In the presence of such phenomena the accuracy of high order

methods deteriorates [83, 108].

Chapter 6

Barycentric spectral domain decomposition methods for valuing a class of infinite activity Lévy models

In this chapter, we solve the semi-discrete equations obtained after the approximation of a financial PIDE. A barycentric spectral domain decomposition is used to solve these equations with an exponential time integrator scheme. Several numerical tests for the pricing of European and butterfly options are given to illustrate the efficiency and accuracy of this algorithm. We also show that the option Greeks such as the Delta and Gamma sensitivity measures are computed with no spurious oscillation.

6.1 Introduction and objective

As mention in the introduction of chapter 3, the constant volatility BS model is not consistent with market prices. Hence, the development of more models for stochastic dynamics of the risky assets. We have for example, the stochastic volatility models [58, 63], deterministic local volatility functions [25, 38], jump-diffusion models [73, 85], Lévy models [81] and infinite Lévy models [43, 100].
Under jump models, option problems can be modelled by means of PIDEs. Briani *et al.* [17] used the fully explicit schemes, although their approach required very restrictive conditions for stability. Cont and Volchkova [28] used implicit schemes to treat the differential part. The use of the Crank-Nicolson time stepping for the PDE portion and evaluation of the convolution integral term explicitly were tested by Tavella and Randall [119]. However, such an asymmetric treatment of PDE and integral part introduces biases in the viscosity solution. More specifically, the second order convergence is not achieved for long dated options. d'Halluin *et al.* [54] employed the Crank-Nicolson scheme with the Rannacher time smoothing to the PIDE. They used a fixed point iterative procedure as the system solver and obtained second order convergence even for long dated options.

In recent years, pure jump Lévy processes of infinite activity that governs stock market returns has been empirically and theoretically studied. The most successful process has been the pure Lévy process based on Brownian subordination. These models perfectly fit the market financial data, capture the excess kurtosis and skewness arising from the risk-neutral distribution returns. They are also analytically tractable. The work done by [20] generalizes the VG model to the Carr, German, Madan

and Yor (CGMY) model. The model has a jump component which follows dynamics that can represent either finite activity or infinite activity of infinite variation. They also demonstrated that a diffusion component is not needed if the jump process belongs to infinite activity or finite variation. In this dissertation, we propose a study of a barycentric spectral domain decomposition methods algorithm for solving partial integro-differential equation (PIDE) models related to European and butterfly option pricing problems under a class of infinite activity Lévy models. The method is based on the barycentric spectral domain decomposition methods, that allows the implementation of the boundary conditions in an efficient way. The semi-discrete equations obtained after approximation of the spatial derivatives, using barycentric spectral domain decomposition methods are solved, using an exponential time integration (ETI) scheme. Furthermore, various numerical results for the pricing of European and butterfly options are also given to illustrate the efficiency and accuracy of this algorithm. We show that the option Greeks such as the Delta and Gamma sensitivity measures are efficiently computed to high accuracy.

6.2 The jump-diffusion model

We assume an arbitrage-free market model with a single risky asset with price process $\{S_t\}_{t\in[0,T]}$ following an exponential Lévy model of the form

$$S_t = S_0 e^{X_t}, \tag{6.1}$$

on the filtered probability space $(\Omega, \mathcal{F}, \{\mathcal{F}_t\}_{t\in[0,T]}, \mathbb{P})$ where the Lévy process $\{X_t\}_{t\in[0,T]}$ has dynamics given by

$$X_t = \left(\mu - \frac{\sigma^2}{2} - \delta\right)t + \sigma W_t + \sum_{k=1}^{N_t} Y_k. \tag{6.2}$$

The jump process is represented by $J_t = \sum_{k=1}^{N_t} Y_k$ with $\{N_t\}_{t\in[0,T]}$ denoting a Poisson process with intensity $\lambda > 0$ and $\{Y_k\}_{k\geq 1}$ which are independent observations from a jump size variable Y.

Let consider $V(S,t)$ be the option value with the underlying asset S_t and T be the time to maturity. Under the equivalent risk neutral measure $\mathbb{Q} \sim \mathbb{P}$, the asset price $\{S_t\}_t \in [0,T]$ has the form (6.1), where X_t is now given by Equation (6.2), the value for a European option with strike price K is its discounted expected payoff

$$V(S,t) = e^{-r(T-t)}\mathbf{E}^{\mathbb{Q}}[\Psi(S_T)|S_t = S], \tag{6.3}$$

where $\Psi(S_T)$ is the payoff function. The value of a contingent claim $V(S,t)$ on the underlying asset S then solves the PIDE given by

$$V_t + \mathcal{L}V(S,t) = 0, \quad (S,t) \in \mathbb{R}_+ \times (0,T], \tag{6.4}$$

where the operator $\mathcal{L}$ is defined as

$$\begin{cases} \mathcal{L}V(S,t) &= \frac{\sigma^2}{2}S^2 V_{SS} + (r-q)S V_S - rV \\ &+ \int_{-\infty}^{+\infty} f(y)[V(Se^y,t) - V(S,t) - S(e^y - 1)V_S(S,t)]dy. \end{cases} \tag{6.5}$$

The function $f(y)$ is the Lévy density function given in Table 6.1. The boundary and the initial conditions make the difference between American and European style options as well as between put and call and other types of options.

For European vanilla call options, the initial and the boundary conditions are given by

$$\begin{cases} V(S,0) &= \max(S-K,0), \\ V(0,t) &= 0, \\ V(S,t) &= Se^{-qt} - Ke^{-rt}, \ \text{as} \ S \to \infty. \end{cases} \tag{6.6}$$

where K is the strike price.

A butterfly spread is a neutral strategy that has a combination of a bull spread and a bear spread. It is a limited profit, limited risk options strategy. There are three strike prices (discontinuities) involved in a butterfly spread and it can be constructed using calls or puts. The initial and boundary conditions of butterfly spread options is expressed as

$$\begin{cases} V(S,0) &= \max(S-K_1,0) - 2\max(S-K_2,0) + \max(S-K_3,0), \\ V(0,t) &= 0, \\ V(S,t) &= 0. \end{cases} \tag{6.7}$$

where S is the stock price K_1, K_2 and K_3 are three distinct strike prices such that $0 < K_1 < K_2 < K_3$, with $K_2 = (K_1 + K_3)/2$. In the *KoBoL model*

Model	Lévy density function
KoBol	$f(y) = \frac{C_- e^{-G\|y\|}}{\|y\|^{1+Y}}\mathbf{1}_{y<0} + \frac{C_+ e^{-M\|y\|}}{\|y\|^{1+Y}}\mathbf{1}_{y>0}$
Meixner	$f(y) = \frac{Ae^{-ay}}{y\sinh(by)}$
GH process	$f(y) = \frac{e^{\beta y}}{\|y\|}\left(\int_0^\infty \frac{e^{-\sqrt{2\zeta+\alpha^2}\|y\|}}{\pi^2\zeta\left(J^2_{\|\lambda\|}(\delta\sqrt{2\zeta})+Y^2_{\|\lambda\|}(\delta\sqrt{2\zeta})\right)}d\zeta + \max(0,\lambda)e^{-\alpha\|y\|}\right)$

Table 6.1: Density functions for Lévy Processes

[20], singularities are observed in the kernel of integration. This model is known as the Carr, German, Madan and Yor (CGMY) [20] when the parameters are set to be $C_- = C_+ = C > 0$, $G > 0, M > 0$ and $Y \in [0,2)$. The

parameter C indicates the overall level of activity. The parameters G and M are the measures depicting the skewness of the Lévy density such that $G = M$ yields a symmetric distribution. When choosing $G \neq M$ this leads to skewed distributions. The parameter Y describes the fine structure of the stochastic process. At $Y = -1$, the *KoBoL model* leads to a special case of Kou's double exponential model [43]. Furthermore, for $Y = 0$, we obtain the variance Gamma process. In a case of $Y \in (0,1)$, infinite activity models with finite variation are obtained and in a case of $Y \in [1,2]$, infinite activity models with infinite variation are depicted. There exist other singular kernel of integration Lévy processes. Meanwhile, the *hyperbolic and generalized hyperbolic* (GH) are used to obtain better estimation for the stock returns [112]. Here, the functions $J_\nu(\cdot)$ and $Y_\nu(\cdot)$ are the Bessel functions of first and second kind, respectively. The *Meixner* process was introduced in 1998, it is used when the environment is changing stochastically over the time showing a reliable valuation for some indices such as Nikkei 225 [82, 111].

6.3 Numerical interpolations and applications

In practice, we are often confronted with situations where only limited amount of data is accessible and it is necessary to estimate values between two consecutive given data points. We can construct new points between known data points by interpolation or smoothing techniques. In finance, as only a finite set of securities are traded in financial markets, it is very important to construct a sensible curve or surface from discrete observable quantities using interpolation methods.

In this section, one has to consult Chapter 2, Section 2.3 to review the concept of interpolation and differentiation matrix in barycentric spectral method framework. For the domain decomposition, section 2.4 has to be consulted. We only highlight the concept of quadrature rule in barycentric spectral method.

6.3.1 Spectral barycentric quadrature

Let consider the Equation (2.47) in Chapter 2, Section 2.3.3. There are two different ways to compute it:

- Firstly, one can use the direct rational quadrature. The technique consists of applying existing quadrature rules such as GaussLegendre or Clenshaw-Curtis [35, 124], which are known to perfectly approximate the integrals in (2.45).
- Secondly, we can apply the indirect rational quadrature. This may produce the integral $I = \int_a^b u(x)dx$ through the solution of an ordinary differential equation, see e.g. [70].

The Clenshaw-Curtis quadrature formula has the following convergence property.

Theorem 4 ([35, 124]). *Let f an analytic function in $[-1,1]$ and analytically continuable with $|f(z)| < M$ in the closed ellipse E_ρ. The error in $I_N(f)$, the Clenshaw-Curtis quadrature of degree N to $I(f)$, will decay geometrically with the bound*

$$|I - I_N| \leq \frac{64M}{15(\rho^2-1)(\rho^{N-1} - \rho^{-(N-1)})}, \quad N \geq 3 \text{ odd}. \tag{6.8}$$

In other words,

$$|I - I_N| = \mathcal{O}(\rho^{-N}). \tag{6.9}$$

Proof. See [35].

The main advantage with the Clenshaw-Curtis quadrature rule is that its weights and nodes can be computed efficiently via a fast Fourier transform (FFT) in only $(\mathcal{O}(N \ln N))$ operations.

In this dissertation, we restrict ourselves to the patching methods. The calculation of the integral part can be estimated in multi-domains as follows

$$\begin{aligned}
\int_{\mathcal{D}} u(x)dx &= \int_{\bigcup_{\mu=1}^{M} \mathcal{D}_\mu} u^{(\nu)}(x)dx = \sum_{\nu=1}^{M} \int_{\mathcal{D}_\nu} u^{(\nu)}(x)dx \\
&\approx \sum_{\nu=1}^{M} \int_{\mathcal{D}_\nu} p_N^{(\nu)}(x)dx, = \sum_{\nu=1}^{M} \int_{\mathcal{D}_\nu} \frac{\sum_{j=0}^{N} \frac{\omega_j^{(\nu)}}{x-x_j} u_j^{(\nu)}}{\sum_{j=0}^{N} \frac{\omega_j^{(nu)}}{x-x_j}} dx \\
&= \sum_{\nu=1}^{M} \sum_{j=0}^{N} \lambda_j^{(\nu)} u_j^{(\nu)}.
\end{aligned} \tag{6.10}$$

In the next section we discretize the PIDE (6.4) by means of spectral domain decomposition methods.

6.4 Numerical simulations

Let us begin this section by transforming the PIDE (6.4) into a simpler one. Since the kernel of the integral in (6.4) presents a singularity at $y = 0$, a useful technique is to split the real line, for an arbitrary small parameter $\varepsilon > 0$, into two regions $\Omega_1 = [-\varepsilon, \varepsilon]$ and $\Omega_2 = \mathbb{R}\backslash\Omega_1$ (the complementary

set of Ω_1 in the real line). The integral on Ω_1 is replaced by a suitable coefficient in the diffusion term of the differential part of (6.4) obtained by Taylor expansion of $V(Se^y,\tau)$ about S, see [26, 27].
This coefficient depending on ε is a convergent integral and takes the form

$$\breve{\sigma}^2(\varepsilon)=\int_{-\varepsilon}^{\varepsilon} f(y)(e^y-1)^2dy=\varepsilon\int_{-1}^{1} f(\varepsilon\phi)(e^{\varepsilon\phi}-1)^2d\phi,\ \ -1\leqslant\varepsilon\leqslant 1. \quad (6.11)$$

Letting $\tau=T-t$, the resulting approximating PIDE from (6.4) is given by

$$\frac{\partial V}{\partial\tau}=\frac{\hat{\sigma}^2}{2}S^2\frac{\partial^2 V}{\partial S^2}+(r-q-\gamma(\varepsilon))S\frac{\partial V}{\partial S}-(r+\chi(\varepsilon))V+\int_{\Omega_2} f(y)V(Se^y,\tau)dy, \quad (6.12)$$

where

$$\hat{\sigma}^2=\sigma^2+\breve{\sigma}^2(\varepsilon),\ \ \gamma(\varepsilon)=\int_{\Omega_2} f(y)(e^y-1)dy,\ \ \chi(\varepsilon)=\int_{\Omega_2} f(y)dy. \quad (6.13)$$

The approximation of $\breve{\sigma}^2$ in (6.11) is evaluated using the Clenshaw-Curtis quadrature and it is given by

$$\breve{\sigma}^2(\varepsilon)\approx\varepsilon\sum_{k=1}^{N}\lambda_k f(\varepsilon\phi_k)(e^{\varepsilon\phi_k}-1)^2, \quad (6.14)$$

where $\phi_k=cos\left(\frac{k\pi}{N}\right)$, and λ_k, $k=0,1,2,....,N$, are the Chebyshev-Gauss-Lobatto (CGL) nodes and the Clenshaw-Curtis weights [46, 123], respectively. The improper integrals $\chi(\varepsilon)$ and $\gamma(\varepsilon)$ in (6.13) are approximated using the shifted Laguerre-Gauss quadrature [45]. Under consideration of the change of variables $\eta=-y-\varepsilon$ for $y<0$ and $\eta=y-\varepsilon$ for $y>0$, the expressions $\chi(\varepsilon)$ and $\gamma(\varepsilon)$ have the following forms

$$\chi(\varepsilon)=\int_0^{\infty}(f(-\eta-\varepsilon)+f(\eta+\varepsilon))d\eta\approx\sum_{k=1}^{N}\bar{\lambda}_k F(\eta_k,\varepsilon), \quad (6.15)$$

and

$$\begin{aligned}\gamma(\varepsilon) &= \int_0^\infty [f(-\eta-\varepsilon)(e^{-(\eta+\varepsilon)}-1)+f(\eta+\varepsilon)(e^{\eta+\varepsilon}-1)]d\eta \\ &\approx \sum_{k=1}^{N} \bar{\lambda}_k G(\eta_k,\varepsilon), \end{aligned} \tag{6.16}$$

where

$$F(\eta,\varepsilon) = e^{\eta}(f(-\eta-\varepsilon)+f(\eta+\varepsilon)),$$

$$G(\eta,\varepsilon) = e^{\eta}\Big(f(-\eta-\varepsilon)(e^{-(\eta+\varepsilon)}-1)+f(\eta+\varepsilon)(e^{\eta+\varepsilon}-1)\Big).$$

Here η_k are the roots of the Laguerre polynomial $L_N(\eta)$ of degree N defined by

$$L_N(\eta) = \frac{e^{\eta}}{N!}\frac{d^N}{\eta^N}\left(\eta^N e^{-\eta}\right), \tag{6.17}$$

and the weights $\bar{\lambda}_k, k = 1,2,\ldots N$, are determined as in [45] by

$$\bar{\lambda}_k = \frac{1}{\eta_k\left(L_N'(\eta_k)\right)^2} = \frac{\eta_k}{(N+1)^2\left(L_{N+1}(\eta_k)\right)^2}. \tag{6.18}$$

6.4.1 Discretization of the PIDE on a single domain

We transform the PIDE (6.12) into a constant coefficient PIDE using the transformation $S = Ke^x$ and $u(x,\tau) = V(S,t)$. One obtains

$$u_\tau - \mathcal{L}u(x,\tau) = 0, \quad (x,\tau) \in \mathbb{R}\times(0,T], \tag{6.19}$$

where

$$\begin{aligned}\mathcal{L}u(x,\tau) &= \frac{1}{2}\hat{\sigma}^2 u_{xx} + \left(r-q-\frac{1}{2}\hat{\sigma}^2-\gamma(\varepsilon)\right)u_x - (r+\chi(\varepsilon))u \\ &+ \int_{\Omega_2} u(x+y,\tau)f(y)dy, \end{aligned} \tag{6.20}$$

We define the numerical domain by $\mathcal{D} = [y_M, y_m]$. The discretized version of (6.20) is given by

$$\dot{\mathbf{u}} = A\mathbf{u} + J\mathbf{u} + \zeta(\tau), \tag{6.21}$$

where $\mathbf{u} = [u_1, u_2, \ldots, u_N]$, $A = \frac{1}{2}\hat{\sigma}^2 D_2 + \left(r - q - \frac{1}{2}\hat{\sigma}^2 - \gamma(\varepsilon)\right) D_1 - (r + \chi(\varepsilon)) D_0$. The notations D_2 and D_1 are matrices with entries defined in Lemma 1 and D_0 is the identity matrix. J and ζ are defined in (6.25) and (6.26), respectively.

For the sake of convenience in the numerical treatment we rewrite the integral part of (6.19) as follows

$$\begin{aligned} J = \int_{\Omega_2} u(x+y,\tau) f(y) dy &= \int_{-\infty}^{+\infty} u(x+y,\tau)\hat{f}(y) dy \\ &= \int_{\mathcal{D}} u(x,\tau)\hat{f}(y-x) dy + \mathbb{k}, \end{aligned} \tag{6.22}$$

where

$$\mathbb{k} = \int_{\mathbb{R}\setminus\mathcal{D}} u(y,\tau)\hat{f}(y-x) dy$$

and

$$\hat{f}(y) = \begin{cases} f(y), & y \in \Omega_2, \\ 0, & y \in \Omega_1. \end{cases} \tag{6.23}$$

We use the Clenshaw-Curtis quadrature rule to compute the first integral over the interval $[y_m, y_M]$ to obtain

$$\begin{aligned} \int_{y_m}^{y_M} u(x,\tau)\hat{f}(y-x) dy &= \frac{1}{2}(y_M - y_m)\int_{-1}^{1} \hat{f}(y-x)u(x,\tau) d\phi, \\ &\approx \frac{1}{2}(y_M - y_m)\sum_{k=0}^{N} \lambda_k \hat{f}(x_k - x_j)u(x_k,\tau), \\ &= J\mathbf{u}(\tau), \end{aligned} \tag{6.24}$$

where $\mathbf{u} = [u_0, u_1, \ldots, u_N]^T$ and J is a $(N+1)\times(N+1)$ matrix with entries

$$\left(J_{jk}\right)_{0\leqslant j,k\leqslant N} = \frac{1}{2}(y_M - y_m)\left(\lambda_k \hat{f}(x_k - x_j)\right)_{0\leqslant j,k\leqslant N}. \tag{6.25}$$

Let $g_L(x,\tau)$ and $g_R(x,\tau)$ be the left and right boundary conditions of the PIDE (6.19). Therefore, the second integral over $\mathbb{R}\setminus[y_m,y_M]$ is approximated using the shifted Laguerre-Gauss quadrature [45] under consideration of the change of variables $\eta=-y+y_m$ for $y<y_m$ and $\eta=y+y_M$ for $y>y_M$. This leads to

$$\begin{aligned}
\zeta(x,\tau) &= \int_{-\infty}^{y_m} g_L(x,\tau)\hat{f}(y-x)dy+\int_{y_M}^{\infty} g_R(x,\tau)\hat{f}(y-x)dy,\\
&= -\int_{-y_m}^{\infty} g_L(x,\tau)\hat{f}(y-x)dy+\int_{y_M}^{\infty} g_R(x,\tau)\hat{f}(y-x)dy,\\
&= -\int_{-y_m}^{\infty} g_L(x,\tau)\hat{f}(-y-x)dy+\int_{y_M}^{\infty} g_R(x,\tau)\hat{f}(y-x)dy,\\
&= \int_{0}^{\infty} g_L(x,\tau)\hat{f}(\eta-y_m-x)d\eta+\int_{0}^{\infty} g_R(x,\tau)\hat{f}(\eta+y_M-x)d\eta,\\
&\approx g_L(x,\tau)\sum_{k=0}^{N}\bar{\lambda}_k e^{\eta_k}\hat{f}(\eta_k-y_m-x)+\mathcal{J}, \qquad (6.26)
\end{aligned}$$

where

$$\mathcal{J}=g_R(x,\tau)\sum_{k=0}^{N}\bar{\lambda}_k e^{\eta_k}\hat{f}(\eta_k+y_M-x).$$

6.4.2 Discretization of the PIDE on multi sub-domains

On each sub-domain $\mathcal{D}_\nu$, the PIDE can be written as

$$u_\tau^{(\nu)}=\mathcal{A}^{(\nu)}u+\mathcal{B}^{(\nu)}u+\zeta^{(\nu)}(\tau),\quad \nu=1,2,\ldots,M, \qquad (6.27)$$

where

$$\mathcal{A}^{(\nu)}u=\frac{1}{2}\hat{\sigma}^2u_{xx}^{(\nu)}+\left(r-q-\frac{1}{2}\hat{\sigma}^2-\gamma(\varepsilon)\right)u_x^{(\nu)}-(r+\chi(\varepsilon))u^{(\nu)}, \qquad (6.28)$$

$$\mathcal{B}^{(\nu)}u=\int_{\mathcal{D}_\nu}u^{(\nu)}(x,\tau)\hat{f}(y-x)dy, \qquad (6.29)$$

and

$$\zeta^{(\nu)}(\tau) = \int_{\mathbb{R}\setminus\mathcal{D}} u^{(\nu)}(y,\tau)\hat{f}(y-x)dy. \tag{6.30}$$

Next, we discretize the PIDE (6.19) in the numerical domain $\mathcal{D} = [x_{\min}, x_{\max}]$ by the means of the spectral domain decomposition method described in Section 2.4 . To this end, we divide the domain D into M sub-domains such that

$$\mathcal{D} = \bigcup_{\mu=1}^{M} \mathcal{D}_\mu. \tag{6.31}$$

The discretized version of (6.27) is given by

$$\dot{\mathbf{u}}^{(\nu)} = A^{(\nu)}\mathbf{u}^{(\nu)} + J^{(\nu)}\mathbf{u}^{(\nu)} + \zeta^{(\nu)}, \quad \nu = 1, 2, \ldots, M, \tag{6.32}$$

where

$$\mathbf{u}^{(\nu)} = [u_1^{(\nu)}, u_2^{(\nu)}, \ldots, u_{N_\nu}^{(\nu)}],$$

$$\begin{aligned} A^{(\nu)}\mathbf{u}^{(\nu)} &= \frac{1}{2}\hat{\sigma}^2\mathbf{u}^{(\nu)}D_2^{(\nu)} + \left(r - q - \frac{1}{2}\hat{\sigma}^2 - \gamma(\varepsilon)\right)D_1^{(\nu)}\mathbf{u}^{(\nu)} \\ &- (r + \chi(\varepsilon))D_0^{(\nu)}\mathbf{u}^{(\nu)}, \end{aligned} \tag{6.33}$$

$$J^{(\nu)}\mathbf{u}^{(\nu)} = \left[\left(J_{ij}\right)_{1\le i,j\le N_\nu}\right]\mathbf{u}^{(\nu)}, \quad J_{ij}^{(\nu)} = \lambda_j^{(\nu)}\hat{f}^{(\nu)}(x_i - x_j), \tag{6.34}$$

and $I^{(\nu)}u = \zeta(\tau)$ which incorporates the boundary conditions. Letting $L^\nu = A^\nu + B^\nu + I$, Equation (6.32) becomes

$$\dot{\mathbf{u}}^{(\nu)} = L^{(\nu)}\mathbf{u}^{(\nu)} + \zeta^{(\nu)}(\tau). \tag{6.35}$$

The solution on the whole domain $\mathcal{D}$ is given by

$$\dot{\mathbf{u}} = L\mathbf{u} + \zeta(\tau), \tag{6.36}$$

where

$$L = \begin{bmatrix} L^{(1)} & & \\ & \ddots & \\ & & L^{(M)} \end{bmatrix}, \quad \mathbf{u} = \begin{bmatrix} \mathbf{u}^{(1)} \\ \vdots \\ \mathbf{u}^{(M)} \end{bmatrix}, \quad \mathbf{u}^{(\nu)} = \begin{bmatrix} \mathbf{u}_1^{(\nu)} \\ \vdots \\ \mathbf{u}_{N_\nu}^{(\nu)} \end{bmatrix}, \quad \nu = 1, 2, \ldots M. \tag{6.37}$$

Note that when two sub-domains $\mathcal{D}_\nu$ and $\mathcal{D}_{\nu+1}$, touch each other, we apply the continuation conditions of the form

$$\begin{cases} u^{(\nu)}(x)\Big|_{x=x_{N_\nu}^{(\nu)}} = u^{(\nu+1)}(x)\Big|_{x=x_1^{(\nu+1)}} \\ \frac{\partial u^{(\nu)}}{\partial x}(x)\Big|_{x=x_{N_\nu}^{(\nu)}} = \frac{\partial u^{(\nu+1)}}{\partial x}(x)\Big|_{x=x_1^{(\nu+1)}} \end{cases}. \tag{6.38}$$

These last equations are reduced to ODEs when the boundary conditions of a call or put option are imposed in each sub-domains. The obtain ODEs are solved by using ETD scheme.

6.4.3 Exponential time differencing schemes

We consider to solve the system of ODEs (6.36)

$$u' = Lu + b(t), \quad u_0 = u(0), \tag{6.39}$$

where L is either a block dense diagonal matrix or a dense matrix depending on the number of domain in consideration, using exponential time differencing methods.

Exponential time differencing (ETD) schemes are known as an alternative to implicit methods for solving stiff systems of ODEs [67, 104, 110]. These methods rely on the a fast and stable computation of φ-functions

$$\varphi_0(z) = e^z, \quad \varphi_j(z) = \frac{1}{(j-1)!}\int_0^1 e^{(1-\theta)z}\theta^{j-1}d\theta, \quad j \geq 0, \tag{6.40}$$

i.e., functions of the form $(e^z-1)/z$. The computation of these functions depends significantly on the structure and the range of eigenvalues of the linear operator and the dimensionality of the semi-discretized PDE. Unfortunately, for spectral methods the linear part have eigenvalues approaching zero, which leads to complications in the computation of the coefficients. Saad [104], and Hochbruck and Lubich [61] introduced Krylov methods to compute φ-functions. Kassam and Trefethen [67] used Cauchy integral representation on a circle for a stable computation of φ-functions. Other evaluations of exponential and related φ-matrix functions follow the idea of Schmelzer and Trefethen [110]. This method is based on computing optimal rational approximations to the matrix functions on the negative real axis using the Carathéodory-Fejér procedure [125], closely.

The system of ODE (6.39) can be integrated explicitly on the interval $[0\ T]$ to give

$$Y(T) \quad = \quad e^{LT}Y(0) + e^{LT}\int_0^T e^{-Lt}b(t)dt. \tag{6.41}$$

The following lemma provides the background for the times stepping procedure for the evaluation of (6.41).

Lemma 2. *([89]) The solution of the non-autonomous linear initial value problem*

$$u' = Lu + \sum_{j=0}^{p-1} \frac{\tau^j}{j!} b_{j+1}, \quad u_{\tau_0} = u_0, \tag{6.42}$$

has the solution

$$u(\tau_0 + h) = \varphi(hL)u_0 + \sum_{j=0}^{p-1}\sum_{\ell=0}^{j} \frac{\tau_0^{j-\ell}}{(j-\ell)!} h^{\ell+1}\varphi_{\ell+1}(hL)b_{j+1}. \tag{6.43}$$

The proof of the above lemma can be found in Niesen and Wright [89]. The computation of the matrix functions φ is obtained by means of the Krylov projection algorithm [89].

6.5 Numerical results

In this section, we numerically solve the PIDE discretized in Section 5.4 . Two options are used to compare the accuracy of the KoBoL, Meixner and GH models on the financial PIDE. We refer as **Example 1**, the case of European call options and as **Example 2**, the case of butterfly call options.

Example 1. We consider a European call option with $K = 50, T = 0.5, r = 0.05, q = 0, \sigma = 0.2, \varepsilon = 0.1, x_{\min} = -3$ and $x_{\max} = 1$. The parameters K, T, r, q, σ respectively represent the strike price, the time of maturation, the interest rate, the dividend and the volatility of the option. The parameters for Lévy models used in this example are given in Table 6.2. Next, we discretize the PIDE (6.19) in the numerical domain $\mathcal{D} = [x_{\min}, x_{\max}]$ by the means of the spectral domain decomposition method described in Section 2.4, 5.41 and 5.4.2 such that

$$\mathcal{D} = \mathcal{D}_1 \cup \mathcal{D}_2 \cup \mathcal{D}_3 \cup \mathcal{D}_4, \tag{6.44}$$

where $\mathcal{D}_1 = [x_{\min}, -\varepsilon]$, $\mathcal{D}_2 = [-\varepsilon, 0]$, $\mathcal{D}_3 = [0, \varepsilon]$ and $\mathcal{D}_4 = [\varepsilon, x_{\max}]$. Note that the domain $\mathcal{D}$ is divided into four sub-domains. In Figure 6.5.1, we show the representation of the spectral differentiation matrices of the spectral method.

Figure 6.5.1(a) represents the case of naive applications of the spectral method in one domain, Figure 6.5.1(b) depicts the matrix rep-

Model	Parameters
CGMY	$C_- = 0.3,\ C_+ = 0.1\ \ G = 15,\ M = 25$ and $Y = 20.$
Meixner	$A = 15,\ a = -1.5$ and $b = 50.$
GH	$\alpha = 4,\ \beta = -3.2,\ \delta = 1.4775$ and $\lambda = -3$

Table 6.2: The parameters for Lévy models used in both examples.

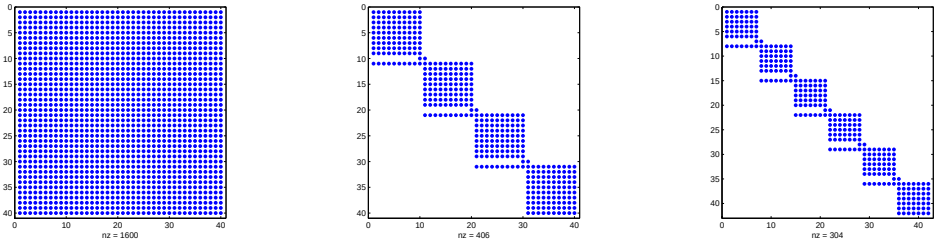

(a) 1 domain (b) 4 sub-domains (c) 6 sub-domains

Figure 6.5.1: Spectral domain decomposition method matrix structures.

resentation in the case of European call options with four sub-domains, while Figure 6.5.1(c) illustrates the case of butterfly spread options with six sub-domains. Note that the domain decomposition reduces the number of unknowns and the computational time in solving the linear system (6.39). Figure 6.5.2 represents numerical solutions of European call options and their Greeks ($\Delta = \frac{\partial V}{\partial S}$ and $\Gamma = \frac{\partial^2 V}{\partial S^2}$) under KoBoL, Meixner and GH Lévy models. The Greeks measure the sensitivity of the option value with respect to the variations in the asset price and the parameters associ-

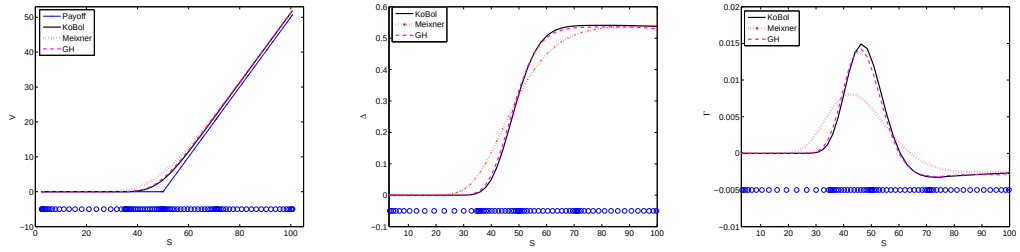

(a) European call (b) Delta (c) Gamma

Figure 6.5.2: Numerical valuation of European call options for the KoBoL, Meixner and GH model with their Greeks for $N = 25, K = 50$.

ated with the model [119]. In practice, accurate approximations to Greeks are needed for hedging purposes.

We report the accuracy of our numerical scheme by means of absolute error $\mathbf{AE} = |U_{Benchmark} - U_{Numerical}|$ where $U_{Benchmark}$ and $U_{Numerical}$ represents the benchmark solution computed with $N = 150$ (the number of grid points in each sub-domain) and the numerical solution, respectively. Table 6.3 shows the benchmark solution values at $S = \{40, 50, 60\}$ for different Lévy models. We vary the number of grid points N and compute the absolute errors (**AE**) for each Lévy model. Table 6.4 represents all the computed **AE** values for each Lévy model with different values of N and S.

We observe a very rapid decrease of the **AE** as the number of grid points N increases. Note that the approximations of order 10^{-4}, 10^{-5}, 10^{-7} and 10^{-10} in Table 6.4 are in general difficult to attain with standard finite difference, finite element and finite volume methods.

Example 2. In this subsection, we investigate the performance of our proposed method for valuing European butterfly options under Lévy mod-

Model	S		
	40	50	60
KoBoL	0.2210443864	3.3785900783	11.3681462140
Meixner	1.3420365535	5.4934725848	12.7780678851
GH processes	0.3237597911	3.8485639686	11.9164490861

Table 6.3: The benchmark European call option values under Lévy processes with different values of S and $N = 150$.

els at the strike prices $K_1 = 40$, $K_2 = 50$ and $K_3 = 60$ using the parameters presented in Table 6.2 and in **Example 1**. In this particular case, we need to divide the domain at five different points, three different strike prices (K_1, K_2 and K_3), and at two singularities ($-\varepsilon$ and ε) present in the kernel of the integral (6.23). Figure 6.5.3 represents numerical solutions of European butterfly call options and their Greeks ($\Delta = \frac{\partial V}{\partial S}$ and $\Gamma = \frac{\partial^2 V}{\partial S^2}$) under KoBoL, Meixner and GH Lévy models. Table 6.5 shows the benchmark

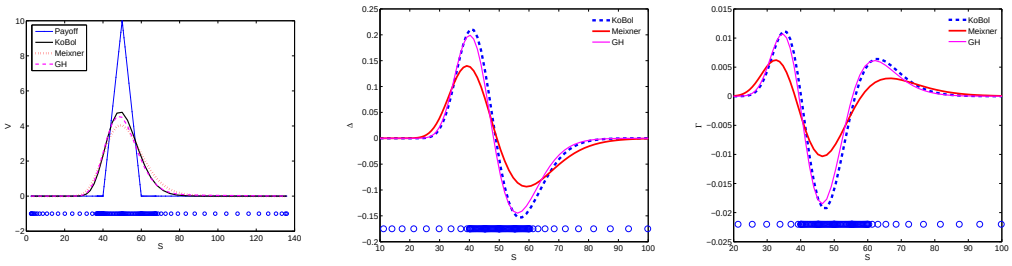

(a) European butterfly call (b) Delta (c) Gamma

Figure 6.5.3: Numerical valuation of European butterfly call options for the KoBoL, Meixner and GH model with $N = 16, K_1 = 40, K_2 = 50, K_3 = 60$.

prices of butterfly call options. Table 6.6 depicts the **AE** between bench-

	S	40	50	60
	N	**AE**	**AE**	**AE**
KoBoL	10	$1.15e^{-4}$	$1.28e^{-4}$	$1.35e^{-4}$
	15	$1.23e^{-5}$	$1.73e^{-5}$	$1.45e^{-5}$
	20	$2.75e^{-7}$	$2.13e^{-7}$	$2.34e^{-7}$
	25	$3.33e^{-10}$	$3.15e^{-10}$	$3.24e^{-10}$
Meixner	10	$2.12e^{-4}$	$2.45e^{-4}$	$2.35e^{-4}$
	15	$2.78e^{-5}$	$2.65e^{-5}$	$2.67e^{-5}$
	20	$3.40e^{-7}$	$3.23e^{-7}$	$3.14e^{-7}$
	25	$4.77e^{-10}$	$4.65e^{-10}$	$4.33e^{-10}$
GH processes	10	$3.33e^{-4}$	$3.29e^{-4}$	$3.17e^{-4}$
	15	$4.55e^{-5}$	$4.370e^{-5}$	$4.14e^{-5}$
	20	$5.14e^{-7}$	$5.21e^{-7}$	$5.14e^{-7}$
	25	$7.11e^{-10}$	$7.25e^{-10}$	$7.33e^{-10}$

Table 6.4: Absolute errors (**AE**) of the benchmark and the European call option apply to the KoBoL, Meixner and GH processes models with different values of N and S.

mark prices and numerical solutions of each model with different values of N and S. We observe a very rapid convergence in the case of European butterfly spread option which has five regions of singularity. Our approach allows a high resolution of grids around the strike prices K_1, K_2 and K_3, and at two singularities $-\varepsilon$ and ε present in the kernel of the integral (6.23). Once again, we obtain approximations of order 10^{-4}, 10^{-5}, 10^{-7} and 10^{-10} in Table 6.6. They are in general difficult to attain with standard finite difference, finite element and finite volume methods.

Model	S		
	40	50	60
KoBoL	2.2845953002	4.6814621409	2.1592689295
Meixner	2.2689295039	3.7101827676	2.3159268929
GH processes	2.3942558746	4.2898172323	1.7989556135

Table 6.5: The benchmark values of the European butterfly call option values under Lévy processes with different values of S and $N = 100$.

	S	40	50	60
	N	**AE**	**AE**	**AE**
KoBoL	07	$1.88e^{-4}$	$1.76e^{-4}$	$1.76e^{-4}$
	10	$1.45e^{-5}$	$1.81e^{-5}$	$1.71e^{-5}$
	13	$2.91e^{-7}$	$2.33e^{-7}$	$2.25e^{-7}$
	16	$3.72e^{-10}$	$3.34e^{-10}$	$3.81e^{-10}$
Meixner	07	$2.45e^{-4}$	$3.32e^{-4}$	$3.22e^{-4}$
	10	$2.72e^{-5}$	$2.75e^{-5}$	$2.46e^{-5}$
	13	$3.54e^{-7}$	$3.28e^{-7}$	$3.69e^{-7}$
	16	$5.68e^{-10}$	$5.55e^{-10}$	$5.88e^{-10}$
GH processes	07	$3.12e^{-4}$	$3.02e^{-4}$	$3.45e^{-4}$
	10	$5.51e^{-5}$	$6.1e^{-5}$	$5.92e^{-5}$
	15	$7.11e^{-7}$	$7.25e^{-7}$	$7.33e^{-7}$
	20	$8.25e^{-10}$	$9.12e^{-10}$	$9.23e^{-10}$

Table 6.6: Absolute errors (**AE**) between the benchmark and European butterfly call options under KoBoL, Meixner and GH processes models with different values of N and S.

Chapter 7

Conclusion

The verification of the numerical methods applied in this dissertation was achieved by using numerical experiments and comparisons. A number of techniques to remove Gibbs phenomenon encountered in interpolating non-smooth functions with spectral methods were proposed. Numerical tests performed on different payoffs options has shown that the spectral workarounds provide an efficient way to remove Gibbs phenomenon. In the case of SCDDM, the exponential convergence was achieved in pricing financial options. Hence, when representing a discontinuous function with polynomials at the Chebyshev points, a domain decomposition in elements, placing the points of discontinuity at the edge of elements, is the method with the smallest truncation error. Likewise, when solving the BS PDE using the domain decomposition and a Krylov projection, the exponential convergence of the approximate solution to the exact solution is only retained if the discontinuities in the initial condition are placed at the edge of elements. Furthermore, a spectral domain decomposition

method for pricing call options for a class of infinite activity Lévy models, including KoBoL, Meixner and GH models was presented. The method is coupled with the exponential time integrator (6.41) to approximate a system of ordinary differential equations (6.39). The method produce accurate results in both examples and the computation of the Greeks was free of spurious oscillations. All approximations used in this dissertation alleviate the problem encountered in getting accurate solutions of financial PDEs and PIDEs.

For future research one can reference our approach to solve multi-asset Lévy models problem.

Chapter 8

Appendix

In this chapter, we provides the main Matlab codes used to represent the simulations and the application of the spectral methods and Lévy models on pricing option.

8.1 The first five Chebyshev polynomials

```
%The first five Chebyshev polynomials
x = -1:1;
T_0 = 1;
T_1 = x;
T_2 = 2*x^2-1;
T_3 = 4*x^3-3*x;
T_4 = 8*x^4-8*x^2+1;
plot(x, T_0, x, T_1, x, T_2, x, T_3, x, T_4)
```

8.2 Brownian motion simple path

```
%function Brownian_Motion(mu,sigma)
mu = 0.20;
sigma = 0.15;
T = 1;
N = 5000;
h = T/N; t = (0:h:T);
X(1) = 0;
for i=1:N
X(i+1) = X(i) + mu*h + sigma*sqrt(h)*randn;
end
plot(t,X);
```

8.3 Calibration of call option and the CGMY model prices

```
%function CGMYcalibration
%clear;
%format compact;
%Definition of the global variable
global ma strike t S_0 size_S size_T lstrike
   pmarchenorm r q a N...
eta b lambda alpha0 u x T B pma sma tma maturg strikeg
    A
%matrix of the prices of european call options
```

```
ma = [ 147.80 0 0 172.4 0 199.5 0; 99.45 0 111.8 130.2
    0 0 0 ;
75.9 0 90.3 0 0 0 170.0 ; 53.5 0 69.9 91.0 0 124.3
   152.8 ;33.0 ...
42.6 50.6 73.1 91.1 107.3 136.8 ...
;15.8 26.2 34.3 57.05 74.8 91.3 121.2; 11.1 0 28.5 0 0
    0 0;
5.4 13.3 20.7 42 59.9 76.3 106.1; ...
1.0 5.3 11.05 29.4 46.6 62.5 92.4; 0.25 1.6 4.65 19.3
   34.9 0 79.3...
; 0.15 0.575 1.675 11.6 25.0 39.0 67.2;
0.1 0.25 0.65 6.4 17.1 29.5 56.1; 0 0 0.35 3.275 11.0
   21.7 46.1;...
0 0 0.3 0.725 3.8 10.25 29.5 ; 0 0 0 0.275 1 4.1 17.4;
    ...
0 0 0 0 0 0.85 9.35;0 0 0 0 0 0.55 4.5;0 0 0 0 0 0 2];
%Strikes
strike= [ 1100 1150 1175 1200 1225 1250 1260 1275 1300
    1325 1350 ...
1375 1400 1450 1500 1550 1600 1650];
%Maturity of the considered options
T = [0.023904 0.10757 0.19522 0.4502 0.6932 0.9442
   1.45817];
% Market price of the risky underlying a time 0
S_0= 1243.73;
% parameters of the model
%risk free rate
```

```
r=0.05;
%dividends
%q=0.0165;
%preliminary calculus (normed by S_0)
size_S=length(strike);
size_T=length(T);
%log-strike normalize
lstrike= log(strike/S_0);
%normalized matrix of prices
pmarchenorm=ma'/S_0;
%integration grid - log strike grid
%sommecarre=[];
a = 600*2; % integration between 0
%and a for the inverse Fourier transform
N = 4096*2; % number of strike pour for FFT
A=zeros(size_T,N); B=zeros(size_T,size_S);
eta = a/N; % integration grid
b = pi/eta; % limits of the log-strike (-b,+b)
lambda = 2*pi/a; % step of the log strike
% Carr and Madan parmater (to avoid integration
   problem in 0)
alpha0 = 0.75;
%alpha0=1.25;
% integration grid
u = (0:N-1) * eta;
% log strike grid
x = -b + (0:N-1) * lambda;
```

```
53 %initialization of the C,G,M,Y parameters
54 v0=[0.026 0.0765 7.55 1.3];
55 %Activate the following lines may improve precision
   for the minima search
56 %options=optimset( LargeScale , on ,
     display , iter , TolFun ,1e-8,
     TolX ,1e-8);
57 %search for the minima. The two vectors represents the
    range of the search
58 sigma_m=fmincon(@sommecarre,v0,[],[],[],[],[0 0 0
   0],[15 15 15 15]);
59 %root mean square error
60 sc=sommecarre(sigma_m); Az=zeros(size_T,size_S);
61 nboptions=sum(sum(not(Az==pmarchenorm)));
62 roomsq=S_0*sqrt(sc/nboptions);
63 maturg=[]; strikeg=[]; marcheg=[]; calculg=[];
64 for compteur8=1:size_S
65 for compteur7=1:size_T
66 if ma(compteur8,compteur7)~=0
67 strikeg=[ strikeg, strike(compteur8)];
68 marcheg=[ marcheg, ma(compteur8,compteur7)];
69 calculg=[calculg , S_0*B(compteur7,compteur8)];
70 maturg=[maturg,T(compteur7)];
71 end;
72 end;
73 end;
74 plot(strikeg,marcheg,'o',strikeg,calculg,'+');
```

```
xlabel('Strike','FontSize',12);
ylabel('Price ($)','FontSize',12);
bbb=[]; sizegg=size(strikeg);
%for compteur9=1:sizegg(2)
% pma=marcheg(compteur9);tma=maturg(compteur9);sma=
    strikeg(compteur9);
% aaa=fzero(@bsm,0.2);
%bbb=[bbb aaa];
%end;
%model implied volatility surface;
ccc=[];
for compteur9=1:sizegg(2)
pma=calculg(compteur9);tma=maturg(compteur9);sma=
    strikeg(compteur9);
aaa=fzero(@bsm,0.2);
ccc=[ccc aaa];
end;
```

8.4 Major codes used in Chapter 4

```
%Spectral Methods and workarounds
%clear, home, close all
%kind='european_call';
%
kind='bull_spread_call';
%kind='butterfly_spread_call';
```

```
switch kind
case 'european_call'
% N =100;E=50;a=0;b=100;
% h=@(x) 0*(x<=E) + 1.*(E<x);% digital options
% xel = [a,E,b];  % any ordered vector of length M+1
    will give the same result
% xnh = 200;   % interpolation vector, determines
    number of C-rows

N =200;xE=0;a=0;b=100;E=50;
h=@(x) max(x-E,0);% digital options
xel = [a,E,b];  % any ordered vector of length M+1
    will give the same result
xnh = 298;   % interpolation vector, determines number
     of C-rows

% choose between Chebyshev (0) and Legendre (1) points
xflag = 0;
% how to compute derivatives at internal element
    boundaries (mortars).
% This is usually irrelevant - mortar BCs take
    precedence.
% DFLAG=0 mimics the effect of mortar BCs.
dflag = 1;
mflag =  1;

```

```
[x,xp,C,D,D2,m,MM] = pcheb(N,xel,xnh,xflag,dflag,mflag);
%[x,xx,C,~,D2,m,M] = pcheb(N,xel,nh);
%A=C';
%A(m,:) = 0;  A = A + MM;
f = h(x);
fp = h(xp);
ud=C*f;
% ud = interp1(x,f,xp,'spline');
%up = barychebeval(w,x,f,xp);
%uc=  barychebeval(w,y,f,xp);
figure (1)
%up = filterChebyshev(ak,xp,filterChoice,filterOrder);
plot(xp,fp,'r',xp,ud,'g')
xlabel 'S', ylabel 'f(S)';
figure(2);
semilogy(xp,abs( fp - ud ),'r');hold on
xlabel 'S', ylabel 'log|error|'
case 'bull_spread_call'
N =200;a=0;b=100;Q=20;E1=40;E2=60;
h=@(x) max(x-E1,0) - max(x-E2,0);% Suppershare Option
xel = [a,E1,E2,b];  % any ordered vector of length M+1 will give the same result
xnh = 298;   % interpolation vector, determines number of C-rows
% choose between Chebyshev (0) and Legendre (1) points
xflag = 0;
```

```
% how to compute derivatives at internal element boundaries (mortars).
% This is usually irrelevant - mortar BCs take precedence.
% DFLAG=0 mimics the effect of mortar BCs.
dflag = 1;
mflag =  0;

[x,xp,C,D,D2,m,MM] = pcheb(N,xel,xnh,xflag,dflag,mflag);
f = h(x);
fp = h(xp);
ud=C*f;
figure (1)
%up = filterChebyshev(ak,xp,filterChoice,filterOrder);
plot(xp,fp,'r',xp,ud,'b')
xlabel 'S', ylabel 'f(S)';
figure(2);
semilogy(xp,abs( fp - ud ),'r');hold on
xlabel 'S', ylabel 'log|error|'
case 'butterfly_spread_call'
N =200;E1=30;E3=70;a=0;b=100;E2=(E1+E3)/2;
%h= @(x) max(x-xE1,0)-2*max(x-xE2,0)+ max(x-xE3,0);% butterfly spread options
h= @(x) max(x-E1,0)-2*max(x-E2,0) + max(x-E3,0);% butterfly spread options
```

```
xel = [a,E1,E2,E3,b];  % any ordered vector of length M+1 will give the same result
xnh = 298;   % interpolation vector, determines number of C-rows
% choose between Chebyshev (0) and Legendre (1) points
xflag = 0;
% how to compute derivatives at internal element boundaries (mortars).
% This is usually irrelevant - mortar BCs take precedence.
% DFLAG=0 mimics the effect of mortar BCs.
dflag = 1;
mflag =  0;

[x,xp,C,D,D2,m,MM] = pcheb(N,xel,xnh,xflag,dflag,mflag);
f = h(x);
fp = h(xp);
ud=C*f;
figure (1)
%up = filterChebyshev(ak,xp,filterChoice,filterOrder);
plot(xp,fp,'r',xp,ud,'b')
xlabel 'S', ylabel 'f(S)';
figure(2);
semilogy(xp,abs( fp - ud ),'r');hold on
xlabel 'S', ylabel 'log|error|'
end
```

```
clear all
%for T=[0.5 1 2]
% NN1=[];NN=[];NN2=[];MM=[];
%  for n=5:1:50;
% NN=[NN N];
%MM=[MM M];
n=20;
K1=90;K3=110;K2=(K1+K3)/2;r = 0.05; T = 0.5;
sigma = 0.2;delta = 0.0; Smax = 2*K1;Smin =0;
ws = (-1).^(0:n-1)'.*[0.5;ones(n-2,1);0.5];
xs = -cos((0:n-1)'*pi/(n-1));
%dom=[0 K1/2 K1 K2 3*K2/2 Smax];
dom=[0 K1 K2 K3 Smax];
%dom=[0 K 1.5*K 2*K 2.5*K 3*K];
m=length(dom);
A=spalloc(n*(m-1),n*(m-1),100*n*(m-1));xx=[];
M=eye(n*(m-1),n*(m-1));
for k=1:m-1
pdom=[dom(k),dom(k+1)];l=(pdom(2)-pdom(1))/2;med=(pdom
    (2)+pdom(1))/2;
x=l*xs+med;xx=[xx;x];I = eye(length(x));
[D1(:,:,k),D2(:,:,k)] = barychebdiff(ws,x);
AA=1/2*sigma^2*diag(x.^2)*D2(:,:,k)+(r-delta)*diag(x)*
    D1(:,:,k)-r*I;
E=zeros(m-1);E(k,k)=1;
BB=kron(E,AA);
A=A+BB;
```

```
%EE=zeros(m-1,1);EE(k)=1;b=b+kron(EE,bb);
end
for k=1:m-2
A(k*n,(k-1)*n+1:k*n)=[zeros(1,n-1) 1];
A(k*n,k*n+1:(k+1)*n)=[-1 zeros(1,n-1)];
%A(k*n,(k-1)*n+1:k*n)=1/2*A(k*n,(k-1)*n+1:k*n);
%A(k*n,k*n+1:(k+1)*n)=3/2*A(k*n+1,k*n+1:(k+1)*n);
A(k*n+1,(k-1)*n+1:k*n)=D1(end,:,k);
A(k*n+1,k*n+1:(k+1)*n)=-D1(1,:,k+1);
M(k*n,(k-1)*n+1:k*n)=[zeros(1,n-1) 0];
M(k*n,k*n+1:(k+1)*n)=[zeros(1,n-1) 0];
M(k*n+1,(k-1)*n+1:k*n)=[zeros(1,n-1) 0];
M(k*n+1,k*n+1:(k+1)*n)=[zeros(1,n-1) 0];
end
i=2:length(xx)-1;II = eye(length(xx));
N=length(xx);%NN=[NN N];
%AA(1,:)=[1 zeros(1,n*(m-1)-1)];A(end,:)=[zeros(1,n*(m
    -1)-1) -1];
AA=[II(1,:);A(i,:);-II(end,:)];
M(1,1)=0; M(end,end)=0;
y0=max(xx-K1,0) - 2*max(xx-K2,0)+ max(xx-K3,0);%
    butterfly spread options
mm=10^3;h=T/mm; t=0:h:T;
b=@(t)0*II(:,end);
[y,yy]=ivpsolver_alex(t,y0,M,AA,b);
%[y,yy]=ivpsolver_cn(t,y0,M,AA,b);
Y=blackscholescall(xx,K1,T,r,delta,sigma)-...
```

```
144 2*blackscholescall(xx,K2,T,r,delta,sigma)+...
145 blackscholescall(xx,K3,T,r,delta,sigma);%analytic
    solution of Euopean call
146 %nL2=norm(Y-y);
147 %nMax=max(abs(Y-y));
148 %NN1=[NN1 nL2];
149 %NN2=[NN2 nMax];
150 %----------------------plot figures
    ---------------------------------------
151 figure(1);plot(xx,y0,xx,y,'r.-',xx,Y);
152 %figure(2);semilogy(xx,abs(Y-y),'b.-');hold on
153 % clear D1 D2
154 %  end
155 %  figure(6);semilogy(NN,NN2,'r.-');hold on
```

8.5 Major codes used in Chapter 5

```
1 clear all
2 time=cputime;tic;
3 NN1=[];NN=[];NN2=[];MM=[];elaps=[];
4 %kind='KoBol';
5 %kind='Meixner';
6 kind='GH';
7 Cplus=0.1;Cminus=0.3;G=25;Mk=15;Y=20;% KoBol
    parameters
8 Am=4;a=-2.5;b=20;% Meixner parameters
```

```
alpha=4;beta=-3.2;delta=0.4775;lambda=-3; % GH process
    parameters
nl=10;% degree of Laguerre polynomial
ncc=50;% number of integration points in Clenshaw-
    Curtis quadrature
n=25; % number of grid points in each subdomain
sigma=0.2;q=0.00;r=0.05;K1=40;K3=60;K2=(K1+K3)/2;T
    =0.5; %PIDE parameters
xmin=-3;xmax=1;epsilon=0.1;% discretisation domain
gammaLL=gammaL(kind,epsilon,Cplus,Cminus,G,Mk,Y,Am,a,b
    ,alpha,beta,delta,lambda,nl);
xiL=xi(kind,epsilon,Cplus,Cminus,G,Mk,Y,Am,a,b,alpha,
    beta,delta,lambda,nl);
sigma_h=sigma_hat(kind,epsilon,Cplus,Cminus,G,Mk,Y,Am,
    a,b,alpha,beta,delta,lambda,nl,ncc);
sigma_hatL=sigma^2+sigma_h;
ws = (-1).^(0:n-1)'.*[0.5;ones(n-2,1);0.5];
xs = -cos((0:n-1)'*pi/(n-1));
%=====subdomains======================
d1=min(log(K1/K2),-epsilon);d2=max(log(K1/K2),-epsilon
    );
d3=min(log(K3/K2),epsilon);d4=max(log(K3/K2),epsilon);
dom=[xmin d1 d2 0 d3 d4 xmax];
%dom=[xmin log(K1/K2) 0 log(K3/K2) xmax];
m=length(dom);
%========Matrices==========
```

```
A=spalloc(n*(m-1),n*(m-1),100*n*(m-1)); JJ=spalloc(n*(m-1),n*(m-1),100*n*(m-1)); xx=[];ww=[];
M=eye(n*(m-1),n*(m-1));
for k=1:m-1
pdom=[dom(k),dom(k+1)]; l=(pdom(2)-pdom(1))/2;med=(pdom(2)+pdom(1))/2;
x=l*xs+med; xx=[xx;x]; I = eye(length(x));ww=[ww;ws];
[D1(:,:,k),D2(:,:,k)] = barychebdiff(ws,x);
J(:,:,k)=integral_matrix_IF(kind,epsilon,xx(1),xx(end),Cplus,Cminus,G,Mk,Y,Am,a,b,alpha,beta,delta,lambda,nl,n);
% JI(:,:)=integral_matrix_IF(kind,epsilon,xx(1),xx(end),Cplus,Cminus,G,Mk,Y,Am,a,b,alpha,beta,delta,lambda,nl,n);
AA=1/2*sigma_hatL*D2(:,:,k)+(r-q-1/2*sigma_hatL-gammaLL)*D1(:,:,k)-(r+xiL)*I+J(:,:,k);
%AA=1/2*sigma_hatL*D2(:,:,k)+(r-q-1/2*sigma_hatL-gammaLL)*D1(:,:,k)-(r+xiL)*I;
E=zeros(m-1);E(k,k)=1;
BB=kron(E,AA);
%JJJ=kron(E,JI);
A=A+BB;%JJ=JJ+JJJ;
%EE=zeros(m-1,1);EE(k)=1;b=b+kron(EE,bb);
end
for k=1:m-2
A(k*n,(k-1)*n+1:k*n)=[zeros(1,n-1) 1];
A(k*n,k*n+1:(k+1)*n)=[-1 zeros(1,n-1)];
```

```
%A(k*n,(k-1)*n+1:k*n)=1/2*A(k*n,(k-1)*n+1:k*n);
%A(k*n,k*n+1:(k+1)*n)=3/2*A(k*n+1,k*n+1:(k+1)*n);
A(k*n+1,(k-1)*n+1:k*n)=D1(end,:,k);
A(k*n+1,k*n+1:(k+1)*n)=-D1(1,:,k+1);
M(k*n,(k-1)*n+1:k*n)=[zeros(1,n-1) 0];
M(k*n,k*n+1:(k+1)*n)=[zeros(1,n-1) 0];
M(k*n+1,(k-1)*n+1:k*n)=[zeros(1,n-1) 0];
M(k*n+1,k*n+1:(k+1)*n)=[zeros(1,n-1) 0];
end
%clear n
i=2:length(xx)-1;II = eye(length(xx));
N=length(xx);NN=[NN N];
%AA(1,:)=[1 zeros(1,n*(m-1)-1)];A(end,:)=[zeros(1,n*(m
    -1)-1) -1];
AA=[II(1,:);A(i,:);-II(end,:)];
M(1,1)=0; M(end,end)=0;
y0 = max(K2*exp(xx)-K1,0)-2*max(K2*exp(xx)-K2,0)+max(
    K2*exp(xx)-K3,0);
mm=5*10^2;h=T/mm; t=0:h:T;%time stepping size
%bb=@(t) ((K*exp(xmax-q*t)-K*exp(-r*t))*II(:,end) + M*
    ell_european(kind,xx,t,K,q,r,epsilon,xmax,Cplus,
    Cminus,G,M,Y,A,a,b,alpha,beta,delta,lambda,nl));
bb=@(t)(0)*II(:,end);
%[y,yy]=ivpsolver_alex(t,y0,M,AA,bb);
[y,yy]=ivpsolver_cn(t,y0,M,AA,bb);
%Y=blackscholescall(xx,K,T,r,delta,sigma);%analytic
    solution of Euopean call
```

```
% [l,u]=lu(M-h*AA); % LU decomposition
% y = max(xx-K,0);
%nL2=norm(Y-y);
%nMax=max(abs(Y-y));
%NN1=[NN1 nL2];
%NN2=[NN2 nMax];
% e=cputime-time;
% elaps=[elaps e];
%e=toc;
%elaps=[elaps e];
% for it=2:length(tau) % timestepping
% b=(Smax-K*exp(-r*tau(it)))*II(:,end);
% w=u\(l\(AA*y+b));
% y=y+h*w;
nn=length(xx);
WW=(-1).^(0:nn-1)'.*[0.5;ones(nn-2,1);0.5];
S=K2*exp(xx);
SS=[40 50 60]';
U25= barychebeval(ww,S,y,SS);
%V5=interp1(S,y,SS,'spline');
figure(1);plot(S,y0,'b.-',S,y,'g.-');hold on
%figure(1);plot(xx,y0,xx,y,'r.-',xx,Y);
%figure(5);semilogy(xx,abs(Y-y),'r.-');hold on
%clear D1 D2
%end
%figure(6);semilogy(NN,NN2,'b.-');hold on
%figure(7);semilogy(elaps,NN2,'r.-');hold on
```

```
%%%%%%%%%%%%%%%%%%%%%%%%%%%%%%%%%%%%%%%%
% differentiation matrix
%    S0         Initial asset price
%    E          Strike Price
%    r          Interest rate
%    T          Time to maturity of option
%    sigma      Volatility of underlying asset
%    delta      Continuous dividend yield
%    Smax       Maximum stock price
%    Smin       Minimum stock price
%    M          Number of points in time grid to use
%    N          Number of points in asset price grid to use
% t = values of time at which solution is obtained (time nodes)
% V = matrix of solutions: V(:,j) is U(S) at t = t(j)
%%%%%%%%%%%%%%%%%%%%%%%%%%%%%%%%%%%%%%%%
%tic
%for T=[0.5 1 2]
%NN1=[];NN=[];NN2=[];MM=[];
%for N=20:10:300;
% NN=[NN N];
%MM=[MM M];
K = 50;r = 0.05; T = 0.5;
 sigma = 0.2;delta = 0.00; Smax = 4*K;Smin =0;N =50;
% --- Compute mesh spacing and time step
 L=Smax-Smin;
```

```
%------------
kind='sc';
epsilon=10^4;
del=1/(Smax-Smin)*(2*K-(Smax-Smin));
%[x,D1,D2]=get_diffmatrix('tee',N,epsilon,del);
[w,x,D1,D2]=diff_matrix(kind,N,epsilon,del);
%x=legslb(N);D1=legslbdiff(N,x);D2=D1^2;
j=2:length(x)-1;
S=0.5*(Smax-Smin)*x + 0.5*(Smax+Smin);
% % ---------------------Initial conditions
    ---------------------------------
V0=max(S(j)-K,0);%payoff call options
u1=max(S-K,0);%call
% %%----------------------Spectral Space
    Discretization------------------
I=eye(length(x));
P=diag(0.5*sigma^2*(2/L)^2*S.^2);
Q=diag((r-delta)*(2/L)*S);
B=P*D2 + Q*D1 - r*I;
%----------------------call boundary conditions
    --------------------
A=B(j,j);b=B(j,end);II=I(j,j);
%%------------------------demo2
    --------------------------------
F=@(t,u) B*u +  b*(Smax*exp(-delta*t)-E*exp(-r*t));%
    call
```

```
142 f=@(t,u) B2*u + b*(Smax*exp(-delta*t)-E*exp(-r*t));%
    call
143 %=========================================
144 epsilon1=Smax*b; epsilon2=K*b;ExpA = expm(A*T);
145 H = (A\(ExpA-II))*epsilon1 - ((A+r*II)\(ExpA-II*exp(-r
    *T)))*epsilon2;
146 V = ExpA*V0 + H;
147 %%----------IMEX time integration--------
148 U=[0;u;bc(T,delta,r,Smax,E)];
149 SS=E;
150 V8=interp1(S,U,SS,'spline');
151 Y=blackscholescall(S,K,T,r,delta,sigma);%analytic
    solution of Euopean call
152 YE=interp1(S,Y,SS,'spline');
153 %r8=abs(V8-YE)/abs(YE);
154 %figure(1);plot(S(j),Y,'r-',S(j),u,'b.',S(j),u0,'k-',S
    (j),-10,'k.');hold on
155 %figure(1);plot(S(j),u,'b.-',S(j),u0,'g.-');hold on
156 %figure(2);semilogy(S(j),abs(Y-u),'r-');hold on
157 %nL2=norm(Y-u)/sqrt(length(Y));
158 %nMax=max(abs(Y-u));
159 %DELTA=(2/Smax)*D1*U; GAMMA=(2/Smax)^2*D2*U;
160 %subplot(2,2,1);
161 figure(1);plot(S(j),V0,'b-',S(j),Y(j),'go-',S(j),V,'r
    .-'); grid on;hold on
162 %subplot(2,2,2);
163 figure(2);plot(S(j),DELTA(j),'b+-'); grid on
```

```
164 subplot(2,2,3);
165 figure(3);plot(S(j),GAMMA(j),'b+-'); grid on
166 subplot(2,2,4);
167 figure(5);semilogy(S(j),abs(V-Y(j)),'b+-');grid on;
      hold on
168 %-----------------------------------------------
169 %nL24=norm(Y-U)/sqrt(length(Y));
170 %nMax4=max(abs(Y-U));
171 %NN1=[NN1 nL2];
172 %NN2=[NN2 nMax];
173 %DELTA=D1*u(:,end)/E; GAMMA= D2*u(:,end)/E^2;
174 %end
175 %figure(1);semilogy(NN,NN2,'r.-');hold on
176 %[X Y]=meshgrid(t,S(j));
177 %mesh(X,Y,u); colormap(1e-6*[1 1 1]);
178 %end
179 %figure(1);semilogy(NN,NN2,'c.-');hold on
```

Bibliography

[1] M. Abramowitz and I. Stegun (Eds.), *Handbook of Mathematical Functions*, 5th edition, Dover, 1968.

[2] M. Abramowitz and I. A. Stegun,*Handbook of mathematical functions with formulas, graphs, and mathematical tables*, Dover, New York, USA, 1972.

[3] Y. S. Abu-Mostafa, Financial model calibration using consistency hints, *IEEE Transactions on neural networks*, **12(4)**, 2001.

[4] L. Andersen and J. Andreasen, Jump diffusion models: volatility smile fitting and numerical methods for pricing, *Review of Derivatives Research*, **4**, 231262, 2000.

[5] W. Arnoldi, The principle of minimized iteration in the solution of the matrix eigenvalue problem, *Quarterly of Applied Mathematics*, **9**, 17-29, 1951.

[6] L. J. B. A. Bachelier, Théorie de la spéculation, *Annales Scientifiques de l'École Normale Supérieure*, **3(17)** , 21-86, 1900.

[7] R. Baltensperger and M. R. Trummer, Spectral differencing with a twist, *SIAM Journal on Scientific Computing*, **24**, 1465-1487, 2003.

[8] R. Baltensperger, J. P. Berrut, and B. Noël, Exponential convergence of a linear rational interpolant between transformed Chebyshev points, *Mathematics of Computation*, **68**, 1109-1120, 1999.

[9] O. E. Barndorff-Nielsen, T. Mikosch, and S. Resnick, *Lévy Processes: Theory and Applications*, Birkhäuser Editions, 2001.

[10] D. S. Bates, Jumps and stochastic volatility: the exchange rate processes implicit in Deutschemark options, *Review of financial studies*, **9(1)**, 69107, 1996.

[11] J.-P. Berrut, R. Baltensperger, and H. D. Mittelmann, Recent developments in barycentric rational interpolation in Trends and Applications in Constructive Approximation, *ISNM*, **151**, 27-51, 2005.

[12] J. P. Berrut and L. N. Trefethen, Barycentric Lagrange Interpolation, *SIAM Review*, **46 (3)**, 501-517, 2004.

[13] J. Bertoin, *Lévy Processes*, Cambridge University Press, Cambridge, UK, 1996.

[14] F. Black and M. Scholes, Pricing of options and corporate liabilities, *Journal of Political Economy*, **81(3)**, 637-654, 1973.

[15] T. Björk, *Arbitrage theory in continuous time*, 3rd edition, Oxford Finance University Press, New York, 2009.

[16] J. P. Boyd, *Chebyshev and Fourier Spectral Methods*, 2nd edition, Dover Publication, Mineola, New York, 2001.

[17] M. Briani, C. La Chioma and R. Natalini, Convergence of numerical schemes for viscosiy solutions to integro-differential degenerate

parabolic problems arising in financial theory, *Journal of Numerical Mathematics* **98(4)** (2004), 607-646.

[18] C. Canuto, M. Y. Hussaini, A. Quarteroni, and T. A. Zang, *Spectral methods in fluid dynamics*, Springer, Berlin, Germany, 1988.

[19] C. Canuto and *et al.*, *Spectral Methods: Fundamentals in Single Domains*, Scientific Computation, Springer, 2007.

[20] P. Carr, H. German, D. B. Madan and M. Yor, The fine structure of asset returns : An empirical investigation, *Journal of Business*, **75**, 305-332, 2002.

[21] J. Certaine, The solution of ordinary differential equations with large time constants, *In Mathematical methods for digital computers, Wiley, New-York*, 128-132, 1960.

[22] E. W. Cheney, *Introduction to Approximation Theory*, McGraw-Hill, New York, 1966.

[23] C. W. Clenshaw, The numerical solution of linear differential equation in Chebyshev series, *Proc. Cambridge Phil. Soc.*, **53**, 134-149, 1957.

[24] C. W. Clenshaw and A. R. Curtis, A method for numerical integration on an automatic computer, *Numerical Mathematics* **2**, 197-205, 1960.

[25] T. F. Coleman, Y. Li and A Verma, Reconstructing the unknown local volatility function, *Journal of Computational Finance* **2**, 77-100, 1999.

[26] R. Company, L. Jódar, M. Fakharany, Positive solutions of European option pricing with CGMY process models using double discretization difference schemes, *Abstr. Appl. Anal. 2013*, 111, 2013.

[27] R. Cont, Model uncertainty and its impact on the pricing of derivative instruments, *Journal of Computational Finance*, **16(3)**, 519-547, 2006.

[28] R. Cont and E. Voltchkova, A finite difference scheme for option pricing in jump diffusion and exponential Lévy models, *SIAM Journal of Numerical Analysis* **43(4)**, 1596-1626, 2005.

[29] R. Cont and P. Tankov, *Calibration of jump-diffusion option-pricing models: a robust non-parametric approach*, Internal report, Centre de Mathémathiques Appliquées (CMAP) No. 490, Ecole Polytechnique, Palaiseau, France, 2002.

[30] J. M. Corcuera *et al*, Completion of Lévy market by power jump assets, *Finance Stochastic*, **9**, 109-127, 2005.

[31] J. M. Courtault, Y. Kabanov, B. Bru, P. Crépel, I. Lebon, and A. Le Marchand, Louis Bachelier on the centenary of Théorie de la Spéculation, *Mathematical Finance*, **10(3)** , 339-353, 2000.

[32] S. M. Cox and P. C. Matthews, Exponential time differencing for stiff systems, *Journal of Computational Physics*, **176(2)**, 430-455, 2002.

[33] J. C. Cox, S. A. Ross and M. Rubinstein, Option pricing: A simplified approach, *Journal of Financial Economics*, **7(3)**, 229-263, 1979.

[34] G. Dahlquist and A. Björck, Numerical Methods in Scientific Computing, *Volume I. SIAM*, Philadelphia, 2007.

[35] P.J. Davis and P. Rabinowitz, *Methods of numerical integration*, Academic Press Inc., Orlando, FL, 2nd edition, 1984.

[36] P. J. Davis, *Interpolation and Approximation*, Dover Publications Inc., New York, 1975.

[37] P. J. Davis and P. Rabinowitz, *Methods of Numerical Integration*, Second Edition, Academic Press, 1984.

[38] B. Dupire, Pricing with a smile, *RISK Magazine* **1**, 18-20, 1994.

[39] E. Eberlein and J. Jacob, On the range of options prices, *Finance Stochastic*, **1**, 131-140, 1997.

[40] W. S. Edward, Krylov methods for the incompressible Navier-Stokes equations, *Journal of Computational Physics*, **110(1)**, 82-102, 1994.

[41] M. El-Daou , E. Ortiz, The tau method, *SIAM Journal, Numerical Analysis*, **6(3)**, 480-492, 1998.

[42] H. W. Engl, M. Hanke and A. Neubauer, *Regularization of inverse problems*, Kluwer Academic Publishers, Dordrecht/London/Boston, 1996.

[43] M. Fakharany, R. Company, L. Jódar, Solving partial integro-option pricing problems for a wide class of infinite activity Lévy processes, *Journal of Computational and applied Mathematics*, **296**, 739-752, 2016.

[44] B. Fornberg, *A practical guide to pseudo-spectral methods*, Cambridge University Press, Cambridge, UK, 1996.

[45] R. Frontczak and R. Söchbel, On modified Mellin transforms, GaussLaguerre quadrature, and the valuation of American call options, *Journal of Computational and Applied Mathematics* **234**, 1559-1571, 2010.

[46] D. Funaro, *Polynomial Approximation of Differential Equations*, Springer, Berlin, 1992.

[47] H. U. Gerber and E.S.W. Shiu, Option pricing by Esscher transforms, *Transactions of the Society of Actuaries* **46**, 99-191, 1994.

[48] T. Goll and J. Kallen, Optimal portfolios for logarithmic utility, *Stochastic Process. Appl.*, **89**, 31-48, 2000.

[49] T. Goll and L. Rüschendorf, Minimax and minimal distance martingale measures and their relationship to portfolio optimization, *Finance Stochastic*, **5**, 557-581, 2001.

[50] D. Gottlieb and S. A. Orszag, *Numerical analysis of spectral methods: theory and applications*, SIAM, Philadelphia, USA, 1977.

[51] D. Gottlieb and C. -W. Shu, On the Gibbs phenomenon IV: Recovering exponential accuracy in a subinterval from a Gegenbauer partial sum of a piecewise analytic function, *Journal of Computational and Applied Mathematics*, **64(211)**, 1081-1095, 1995.

[52] D. Gottlieb and C. -W. Shu, On the Gibbs phenomenon and resolution, *SIAM Review*, **39(4)**, 644-668, 1995.

[53] P. Grandclément, *Introduction to spectral methods*, Laboratoire Univers et ses Théories, Observatoire de Paris, 5 place J. Jansen, 92195 Meudon Cedex, France, 2006.

[54] Y. d'Halluin, P.A. Forsyth and K.R. Vetzal, Robust numerical methods for contigent claims under jump-diffusion processs, *IMA Journal of Numerical Analysis* **25(1)**, 87-112, 2005.

[55] M. T. Heath, *Scientific computation: An introduction survey (Chap.11: PDE)*, Lecture Notes, University of Illinois, 2002.

[56] P. Henrici, *Essentials of Numerical Analysis with Pocket Calculator Demonstrations*, Wiley, New York, 1982.

[57] J. Hersch, Contribution á la méthode des équations aux diifences, *Z. Angew. Math. Phys.*, **9a**, 129-180, 1958.

[58] S. L. Heston, A close-form solution for options with stochastic volatility with applications ton bond and currency options, *The Review of Financial Studies*, **6(2)**, 327-343, 1993.

[59] N.J. Higham, The numerical stability of the barycentric Lagrange interpolalion, *IAM Journal of Numerical Analysis* **24** , 547-556, 2004.

[60] M. Hochbruck *et al*, Exponential integrator for large systems of differential equations, *SIAM Journal on Scientific Computing*, **19(5)**, 1552-1574, 1998.

[61] M. Hochbruck and C. Lubich, On Krylov subspace approximations to the matrix exponential operator, *SIAM Journal of Numerical Analysis* **34** , 1911-1925, 1997.

[62] J. C. Hull, *Options, futures and other derivatives*, 7th edition, Pearson Prentice-Hall International Limited, London, 1997.

[63] J. Hull and A White, The pricing of options with stochastic volatilities, *Journal of Finance* **42** , 281-300, 1987.

[64] M. Y. Hussaini and T. A. Zang, Spectral methods in fluid dynamics, *Annual Review of Fluid Mechanics*, **19(1)**, 339-367, 1987.

[65] A. Iserles, *A First Course in the Numerical Analysis of Differential Equations*, Cambridge University Press, Cambridge, UK, 1996.

[66] P. Kandolf, *Exponential integrators*, Lecture Notes, McMaster University Hamilton, 2011.

[67] A. K. Kassam and L. N. Trefethen, Fourth-order time-stepping for stiff PDEs, *SIAM Journal on Scientific Computing* , **26(4)**, 1214-1233, 2005.

[68] L. E. Kidder and L. S. Finn, Spectral methods for numerical relativity: the initial problem data, *Physics Review D*, **62(8)**:084026, 2000.

[69] G. Klein, Applications of linear barycentric rational interpolation, PhD Thesis, department of Mathematics, Faculty of Science, University of Fribourg, Switzerland, 2012.

[70] G. Klein and J.P. Berrut, Linear barycentric rational quadrature, *BIT Numerical Mathematics* **52**, 407-424, 2012.

[71] P. E. Kloeden, G. J. Neuenkirch and T. Shardlow, The exponential integrator scheme for stochastic partial differential equations: Pathwise error bounds, *Journal of Computational and Applied Mathematics*, **235(5)**, 1245-1260, 2011.

[72] D. A. Kopriva, *Implementing Spectral Methods for Partial Differential Equations: Algorithms for Scientists and Engineers*, Scientific Computation, Springer, New York, 2009.

[73] S. G. Kou, A Jump-Diffusion Model for Option Pricing, *Management Science* **8(48)**, 1086-1101, 2001.

[74] J. G. Kristoffer, The analysis of PDEs arising in non-linear and non-standard option pricing, PhD Thesis, School of Mathematics, Faculty of Engineering and Physical Science, University of Manchester, 2008.

[75] S. Krogstad, Generalized integrating factor methods for stiff PDEs, *Journal of computational Physics*, **203(1)**, 72-88, 2005.

[76] A. E. Kyprianou, *Introductory Lectures on Fluctuations of Lévy Processes with Applications*, Springer Editions, 2006.

[77] A. E. Kyprianou, W. Schoutens, and P. Wilmott, *Exotic Option Pricing and Advanced Lévy Models*, Wiley Editions, 2005.

[78] J. L. Lagrange, Leçons élémentaires sur les mathématiques, *données à l'Ecole Normal en 1795*, *in Oeuvres VII*, *Gauthier-Villars*, *Paris*, **7**, 183-287, 1877.

[79] J. D. Lawson, Generalized Runge-kutta processes for stable systems with large Lipschitz constants, *SIAM Journal of Numerical Analysis*, **4**, 372-380, 1967.

[80] J. Loffeld and M. Tokman, Comparative performance of exponential, implicit, and explicit integrators for stiff systems of ODEs, *Journal of Computational and Applied Mathematics*, **241**, 45-67, 2013.

[81] D.B. Madan and E. Seneta, The variance gamma model for share market returns, *Journal of Business* **63**, 511-524, 1990.

[82] D. Madan and M. Yor, Representing the CGMY and Meixner Lvy processes as time changed Brownian motions, *Journal of Computational Finance* **12 (1)**, 27-47, 2008.

[83] C. Markakis, and L. Barack, High-order difference and pseudospectral methods for discontinuous problems, *Cornell University library, arXiv: 1406.4865v1 [maths.NA]*, 1-9, 2014.

[84] J. C. Mason and D. C. Handscomb, *Chebyshev Polynomial*, CRC Press, New York, 2003.

[85] R.C. Merton, Option pricing when the underlying stocks are discontinuous, *Journal of Financial Economics* **5** , 125-144, 1976.

[86] R. C. Merton, Theory of rational option pricing, *The Bell Journal of Economics and Management Science*, **4(1)**, 141-183, 1973.

[87] H. Munthe-Kaas, High order Runge-Kutta methods on manifolds, *In proceeding of the NSF/CBMS Regional Conference on Numerical Analysis of Hamiltonian differential equation*, **29**, 115-127, 1999.

[88] E. Ngounda, K. C. Patidar, and E. Pindza, Contour Integral Method for European Options with Jumps, *Communications in Nonlinear Science and Numerical Simulation*, **18(3)**, 478-492, 2013.

[89] J. Niesen and W. M. Wright, A Krylov subspace method for option pricing, Technical report SSRN 1799124, 2011.

[90] S. P. Nørsett, An A-stable modification of the Adams-Bashforth methods, *In Conference on Numerical Solution of Differential Equations, Springer, Berlin*, 214-219, 1969.

[91] S. A. Orszag, Spectral methods for problems in complex geometries, *Journal of Computational Physics*, 37-70, 1980.

[92] H. K. Pang and H. W. Sun, Fast exponential time integration for pricing options in stochastic volatility jump diffusion models, *East Asian Journal on Applied Mathematics*, **4(1)**, 52-68, 2014.

[93] A. Papapantoleon, *An introduction to Lévy processes with applications in finance*, Lecture Notes, University of Freiburg, 2008.

[94] T. J. Park and J. C. Light, Unitary quantum time evolution by iterative Lanczos reduction, *Journal of Chemical Physics*, **85**, 5870-5876, 1986.

[95] H. P. Pfeiffer, L. E. Kidder, M. A. Scheel, and S. A. Teukolsky, A multi-domain spectral method for solving elliptic equations, *Computer Physics Communications* **152**, 253-273, 2003.

[96] E. Pindza, K. C. Patidar and E. Ngounda, Implicit-Explicit Predictor-Corrector Methods Combined With Improved Spectral Methods For Pricing European Style Vanilla And Exotic Options, *Electronic Transaction on Numerical Analysis*, **40**, 268-293, 2013.

[97] N. U. Prabhu, *Stochastic Storage Processes* , 2nd edition, Springer, 1998.

[98] R. Raible, Lévy Processes in Finance: Theory, Numerics and Empiral Facts, PhD thesis, University of Freiburg, 2000.

[99] E. D. Rainville, *Special Functions*, Macmillan, New York, 1960.

[100] N. Rambeerich, D. Y. Tangaman, M. Bhuruth, Numerical Pricing Of American Option Under Infinite Activity Lévy Processes, *Journal of Futures Markets*, **31(9)**, 809-829, 2011.

[101] M. Richardson, *Chebyshev interpolation for functions with endpoint singularities via exponential and double-exponential transforms*, Oxford University, Mathematical Institute, UK, 2012.

[102] M. J. Ruijter, M. Versteegh, C. W. Oosterlee, On the application of spectral filters in a Fourier option pricing technique, *Journal of Computational Finance*, **19(1)**, 1-24, 20015 .

[103] Y. Saad, *Iterative Methods for Sparse Linear Systems*, PWS Publishing Company, USA, 1996.

[104] Y. SAAD, Analysis of some Krylov subspace approximations to the matrix exponential operator, *SIAM Journal of Numerical Analysis* **29**, 209-228, 1992.

[105] P. A. Samuelson, Mathematics of speculative price, *SIAM Review*, **15(1)** , 1-42, 1973.

[106] P. Samuelson, Rational theory of warrant pricing, *Industrial Management Review*, **6**, 13-31, 1965.

[107] S. A. Sarra, *Chebyshev Super Spectral Viscosity Solution of a Two-Dimensional Fluidized Bed Model*, Department of Mathematics, Marshall University, One John Marshall Drive, Huntington, 2000.

[108] S. A. Sarra, *Algorithm: The Matlab Postprocessing Toolkit*, ACM Transaction on Mathematical Software, Marshall University, Huntington, 2009.

[109] K. Sato, *Lévy Processes and infinitely divisible distribution*, Cambridge University Press, Cambridge, UK, 1999.

[110] T. Schmelzer and L. N. Trefethen, Evaluating Matrix Functions for Exponential Integrators via Carathéodory-Fejér Approximation and Contour Integrals, *Electronic Transactions on Numerical Analysis* **29**, 1-18, 2007.

[111] W. Schoutens and J.L. Teugels, Lévy processes, polynomials and martingales, *Communications in Statistics. Stochastic Models* **14 (1-2)**, 335-349, 1998.

[112] W. Schoutens, *Lévy processes in Finance: pricing financial derivatives*, Wiley series in probability and statistics, 2003.

[113] A. V. Selivanov, On martingale measures in exponential Lévy models, *Theory Probab. Appl.*, **49**, 261-274, 2005.

[114] J. Shen, T. Tang, L.L. Wang, *Spectral methods: Algorithms, Analysis and Applications*, Springer Series in Computational Mathematics 41, 2011.

[115] R. Seydel, *Tools for computational finance*, Springer Verlag, 2009.

[116] J. Söhl and M. Trabs, *Option calibration of exponential Lévy process models: Implementation and empiral results*, SFB 649 Discussion Paper 2012-017, Humboldt-Universität zu Berlin, Germany. Available at http://hdl.handle.net/10419/56624.

[117] E. Süli and D. Mayers, *An Introduction to Numerical Analysis*, Cambridge University Press, 2003.

[118] D. Y. Tangman, A. Gopaul and M. Bhuruth, Exponential time integration and Chebyshev discretisation schemes for fast pricing options, *Applied Numerical Mathematics*, **58(9)**, 1309-1319, 2008.

[119] D. Tavella and C. Randall, *Pricing Financial Instruments: The Finite Difference Method*, Wiley, New York, 2000.

[120] W. J. Taylor, Method of Lagrangian curvilinear interpolation, *Journal of Research of the National Bureau of Standards*, **35**, 151-155, 1945.

[121] T. W. Tee and L. N. Trefethen, A Rational Spectral Collocation Method With Adaptively Transformed Chebyshev Grid Points, *SIAM Journal of Scientific Computing*, United Kingdom, **28(5)**, 1798-1811, 2006.

[122] M. Tokman, Efficient integration of large stiff systems of ODEs with exponential propagation iterative (EPI)methods, *Journal of Computational Physics*, **213**, 748-776, 2006.

[123] L. N. Trefethen, *Spectral methods in MATLAB*, SIAM, Philadelphia, USA, 2000.

[124] L.N. Trefethen, Is Gauss quadrature better than Clenshaw-Curtis? *SIAM Review* **50 (1)**, 67-87, 2008.

[125] L.N. Trefethen and H.M. Gutknecht, The Carathéodory-Fejér method for real rational approximation, *SIAM Journal on Numerical Analysis* **20**, 420-436, 1983.

[126] H. A. van der Vorst, An iterative solution method for solving $f(A)x = b$ using Krylov subspace information obtained for the symmetric positive definite matrix A, *Journal of Computational and Applied Mathematics*, **18**, 249-263, 1987.

[127] H. Vandeven, Family of Spectral Filters for Discontinuous Problems, *SIAM Journal of Scientific Computing*, **6 (2)**, 159-192, 1991.

[128] M. Versteegh, The Gibbs phenomenon in option pricing methods: Filtering and other techniques applied to the COS method, MSc thesis, Department of Applied Mathematics, Faculty of Engineering, Mathematics and Computer Science, Delft, Netherlands, 2012.

[129] R. G. Voigt, D. Gottlieb, and M. Y. Hussaini, *Spectral methods for partial differential equations*, SIAM, Philadelphia, USA, 1984.

[130] H. Wang and S. Xiang, On The Convergence Rates Of Legendre Approximation, *Mathematics Of Computation*, **81(278)**, 2012.

[131] M. Webb, L.N. Trefethen and P. Gonnet, Stability of the barycentric interpolation formulas, *SIAM Journal on Scientific Computing* **24(4)** , 547-556, 2010.

[132] W. Werner, Polynomial interpolation: Lagrange versus Newton, *Mathematics of Computation* **43 (167)**, 205-217, 1984.

[133] M. Winkel, *Lévy processes and Finance*, Lecture notes, Oxford University, 2010.

[134] X. Wu and Y. Shen, Differential Quadrature Domain Decomposition Method for a Class of Parabolic Equation, *Computer and Mathematics with Applications* **48**, 1819-1832, 2004.

[135] T. Yue, Spectral element method for pricing European options and their Greeks, PhD Thesis, Department of Electrical and Computer Engineering, Duke University, 2012.

[136] http://asq.org/quality-progress/2005/05/measure-for-measure/calibration-what-is-it.html, Access on 01/10/2015, 12:45pm.